Abstracts of the Annual Meeting of Planetary Geologic Mappers

Edited By Tracy K.P. Gregg,[1] Kenneth L. Tanaka,[2] *and* R. Stephen Saunders,[3]

Open-File Report 2004-1100

2004

U.S. DEPARTMENT OF THE INTERIOR
U.S. GEOLOGICAL SURVEY

[1] The State University of New York at Buffalo, Department of Geology, 710 Natural Sciences Complex, Buffalo, NY 14260-3050.

[2] U.S. Geological Survey, 2255 North Gemini Drive, Flagstaff, AZ 86001.

[3] NASA Headquarters, Office of Space Science, 300 E. Street SW, Washington, DC 20546.

June 19–22, 2003
Brown University
Providence, Rhode Island

Introduction

The annual Planetary Geologic Mappers Meeting was hosted by Jim Head and the Department of Geological Sciences at Brown University in Providence, Rhode Island. Presentations (both formal oral presentations and informal poster presentations) were conducted on June 19 and 20. Terry Tullis (Brown U.), Geoff Collins (Wheaton College) and Jim Head led optional field trips on Saturday and Sunday to examine the bedrock and glacial geology of Rhode Island.

Approximately 40 people attended the meeting. Encouragingly, among the attendees were many students (high-school through graduate) as well as researchers who wish to learn more about the mapping process. Mappers submitted a total of 22 abstracts, which make up the body of this report.

On Thursday, we heard eight presentations from researchers mapping different areas of Mars. An emphasis was made that Thermal Emission Imaging System (THEMIS) images, in spite of being somewhat sparse at the moment, were proving to be vital mapping data sets. Different mappers demonstrated that THEMIS images were able to locally fill the data gap in image resolution left between Viking Orbiter and Mars Orbiter Camera (MOC) Narrow Angle (NA) images. In addition, THEMIS data are sufficiently sensitive to reveal subtle topographic features that are not apparent in Mars Orbiter Laser Altimeter (MOLA) digital elevation models. The MOLA data are providing useful, controlled bases for regional to global scale geologic mapping and various topical studies. MOC NA images are useful for analyzing local surfaces, but have limited value in geologic mapping in most cases because they only cover a few percent of the planet's surface.

Ken Tanaka presented a paradigm for mapping methods that may prove to be particularly useful for Mars: the concept of "allostratigraphic" (also known as "unconformity bounded") units and how they may be used in place of and in addition to more traditional lithostratigraphic units. He also discussed how geographic names, as used in terrestrial mapping, may be helpful in defining unit names and how unit colors can be chosen to help show relative age. Trent Hare gave us a brief update on the Planetary Interactive GIS on-the-Web Analyzable Database (PIGWAD) and its capabilities. He reminded the mappers that his job is to help them create better maps and do science more easily through the use of Geographic Information Systems (GIS).

The Geologic Mapping Subcommittee (GEMS) met during lunch, and during that relatively short meeting, we addressed the issue of acceptable format for Venus correlation charts (CC) and sequence of map unit (SOMU) charts that was raised last year. Specifically, we produced a working document that presented guidelines for

presenting such charts on geologic maps, based on terrestrial and martian precedents, as well as on our collective experience in mapping Venus. This document was distributed to the mappers on June 20th for discussion.

On Friday, June 20, we heard 7 presentations from researchers mapping Venus and 4 from those mapping the outer satellites. Dave Williams indicated that his global Io map is not yet funded to generate an official USGS cartographic project. In contrast, groups mapping Europa (presented by Ken Tanaka) and those mapping Ganymede (presented by Geoff Collins and Wes Patterson) do have intentions to publish USGS-sponsored maps.

Vicki Hansen showed us the methods she has been using for mapping Venus. Her methods include the mapping of primary vs. secondary structures, and she encouraged other Venus mappers to adopt them. Her presentation naturally led into a group discussion regarding mapping methods and goals. Steve Saunders, in his role as NASA Planetary Geology and Geophysics program manager, stood up to remind the mappers that although the most important thing is to separate one's observations from one's interpretations, the interpretations are what tell the scientists' story. He would prefer to see more creative interpretations (as long as they are clearly indicated to be such) rather than dry maps that don't leave the reader with any idea as to the author's beliefs.

The present members of the mapping community approved the Venus CC/SOMU guidelines, which are attached below. We also reached a consensus that both descriptive and geographic unit names should be used as appropriate, and acknowledged that care should be applied in avoiding the use of secondary features in defining and naming map units.

Friday evening the GEMS panel met again to discuss which Mars quadrangles should be used as "test cases" for incorporating THEMIS data into the mapping program. Maps currently being created by Tracy Gregg (Tyrrhena Patera region), Jim Zimbelman (Medusae Fossae formation) and Ken Tanaka (South Polar region) will be used.

VENUS SOMU's

There have been various styles of venusian correlation charts submitted, and the GEMS panel feels that the community as a whole would benefit from written guidelines re standardization of these correlation charts. However, we don't wish to stifle the science that a researcher or group of researchers may want to present. With those thoughts in mind, GEMS offers the following standards for venusian correlation charts.

1. Rather than vertical contacts being marked by a question mark ("?") where the precise stratigraphic boundaries are uncertain, a jagged line should be used.

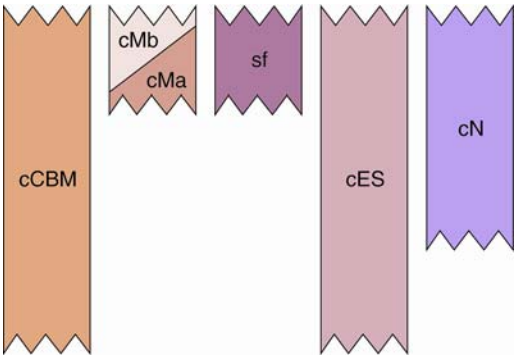

Figure 1a. Jagged vertical contacts are are **preferred** when boundaries are uncertain. The depth (or length) of the teeth is considered to be meaningless.

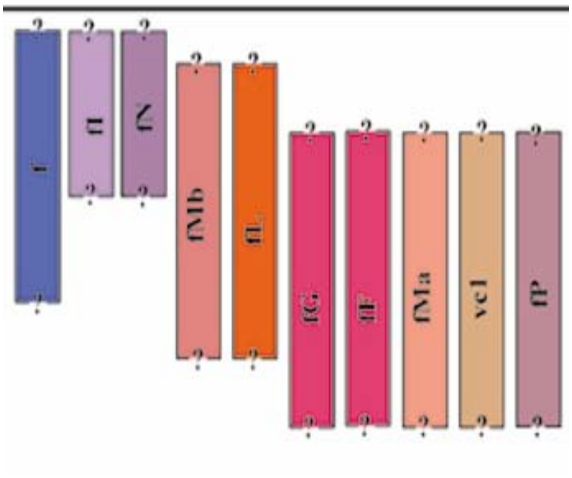

Figure 1b. Queried vertical boundaries **not preferred**.

2. A diagonal line separating units (Fig. 1a) indicates that locally, the lower unit may actually be younger than the upper unit, and vice-versa. However, the great majority of the lower unit is older than the great majority of the upper unit.

3. The formation of structures, and other processes, does have a place on a correlation chart, and that place is off to one side, in a separate (but adjacent) column or box—not interspersed throughout the chart.

4. Explanations for a non-traditional chart (a graphical legend appearing adjacent to the chart; see Figure 2) are encouraged.

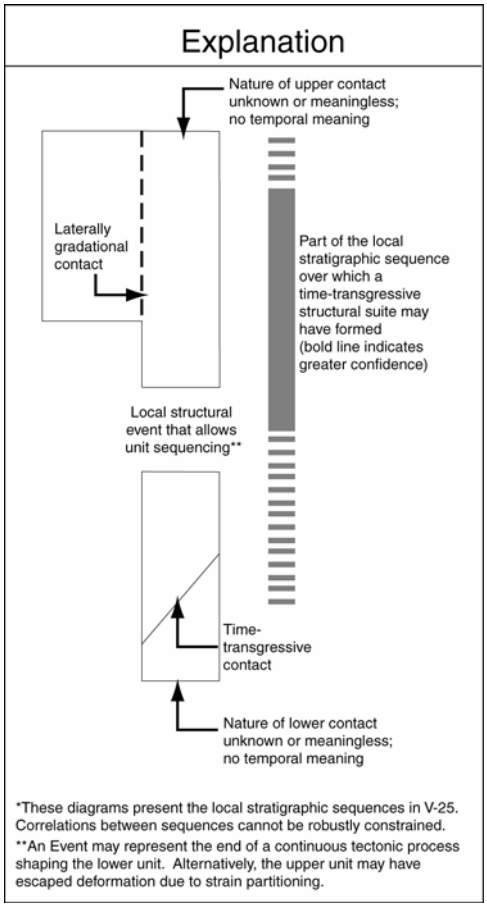

Figure 2. Example of an explanation for correlation chart.

5. Dashed vertical contacts are discouraged in the correlation chart. If the contact is gradational or uncertain on the map, this should be reflected in a dashed contact on the map, and/or explained in the map text. Although there may be a precedent for these on terrestrial geologic maps, there is no precedent on published extraterrestrial maps.

6. Having adjacent units touching in the correlation chart should be reserved for units sharing a geologic intimacy. Touching indicates that the units are always found together or are always in the same context. Groups of intimately associated units should be spatially separated on the correlation chart from units that are not closely associated.

Some folks have obviously put a lot of effort into creating a correlation chart to convey as much information as possible. Unfortunately, this has resulted in a confusing array of graphics—not all of which can be accurately described as correlation charts. We invite all mappers to create FIGURES to display information graphically, and on the published map sheet. These figures can be shown immediately above, below or beside the actual correlation chart.

ABSTRACTS CONTENTS

Mars

Geologic mapping of the martian highlands: Eastern Promethei Terra/southeast Hesperia Planum
D.A. Crown and S.C. Mest

MTM quadrangle –20257: Western Hesperia Planum, Mars
M. A. Farley, T.K.P. Gregg, and D.A. Crown

Geologic map of the MTM 85080 quadrangle, Planum Boreum region of Mars
K.E. Herkenhoff

Results of geologic mapping of the south polar region of Mars at 1:3,000,000 scale and future 1:1,500,000-scale polar mapping
E.J. Kolb and Kenneth L. Tanaka

Geologic map of MTM –20272 and –25272 quadrangles, Tyrrhena Terra region of Mars
S.C. Mest and D.A. Crown

Results of Mars northern plains geologic mapping
K.L. Tanaka, J.A. Skinner, Jr., T.M. Hare, T. Joyal, and A. Wenker

Geologic evolution in Margaritifer Sinus, Mars, as revealed by 1:500,000 geomorphic mapping
K.K. Williams and J.A. Grant

Mars and Venus

Geologic mapping of Mars (eastern portion of the Medusae Fossae Formation) and Venus (V15 quadrangle, Bellona Fossae)
J.R. Zimbelman

Venus

Characterization of Venus midlands (V57 Fredegonde, and V3 Meskhent Tessera quadrangles) and developing criteria to test geological history models
J.W. Head and M.A. Ivanov

Lakshmi Planum quadrangle (V-7) Venus
M.A. Ivanov and J.W. Head

Results from ongoing mapping of the Nemesis Tesserae (V14) quadrangle, Venus
E.B. Grosfils

Geologic map of the Greenaway quadrangle (V-24), Venus
N.P. Lang and V.L. Hansen

The geology of the V39 Taussig quadrangle
A.W. Brian and E.R. Stofan

Preliminary geologic mapping of Helen Planitia quadrangle (V52), Venus
I. Lopez and V.L. Hansen

Coronae and rifting in V53 and V28: Insights from geologic mapping
E.R. Stofan and J.E. Guest

Geologic history of Lada Terra, Venus: Mapping of Mylitta Fluctus, and preliminary mapping of V-56, Lada Terra, quadrangles
M.A. Ivanov and J.W. Head

Geologic map of the Mylitta Fluctus quadrangle (V-61), Venus
M.A. Ivanov and J.W. Head

Galilean satellites

Global geological mapping of Europa: Strategy and update
P.H. Figueredo, K. Tanaka, D. Senske, T. Hare, R. Greeley, and T. Becker

Global mapping of bright terrain on Ganymede: A post-Galileo view of units and structures
G.C. Collins, J.W. Head, G.W. Patterson, R.T. Pappalardo, and L.M. Prockter

Global mapping of Ganymede at 1:15M scale: Defining dark terrain
G.W. Patterson, J.W. Head, G.C. Collins, R.T. Pappalardo, and L.M. Prockter

Regional geologic mapping of Io using *Galileo* spacecraft data
D.A. Williams, L.P. Keszthelyi, E.P. Turtle, J. Radebaugh, W.L. Jaeger, M.P. Milazzo, A.S. McEwen, J.M. Moore, P.M. Schenk, R.M.C. Lopes, and R. Greeley

Other

Mapping tectonomagmatic planets
V.L. Hansen

GEOLOGIC MAPPING OF THE MARTIAN HIGHLANDS: EASTERN PROMETHEI TERRA/SOUTHEAST HESPERIA PLANUM. *David A. Crown[1] and Scott C. Mest[2]*, [1]Planetary Science Institute, 620 N. Sixth Avenue, Tucson, AZ, 85705, [2]Department of Geology and Planetary Science, University of Pittsburgh, Pittsburgh, PA 15260, crown@psi.edu and smest@kasei.gsfc.nasa.gov

Introduction

Viking Orbiter, Mars Global Surveyor (MOC and MOLA), and Mars Odyssey (THEMIS) data sets are being used for geologic mapping studies and geomorphic analyses of highland terrains surrounding the Hellas impact basin. Scientific objectives include identifying sequences and styles of highland degradation, documenting erosional and depositional histories, and providing constraints on volatile inventories and climatic conditions. The present work focuses on three Mars Transverse Mercator (MTM) quadrangles, -35237, -40237, and –45237, in the eastern Promethei Terra/southeast Hesperia Planum region [1]. This area exhibits large expanses of ridged and knobby plains that cover low-lying regions adjacent to degraded, heavily cratered highlands to the east of the Hellas basin.

The spatial and temporal variability of highland geologic evolution is being investigated through comparative analyses of different circum-Hellas regions. A parallel geologic mapping study of the Tyrrhena Terra region of Mars examines two MTM quadrangles (-20272 and –25272) north of the Hellas basin [2]. These two current mapping studies build on recent analyses of the Reull Vallis region [3-6] and complement earlier investigations of the eastern Hellas region [7-9], volcanic studies of Tyrrhena and Hadriaca Paterae [10-13], and mapping of highland outflow channels [14]. Documentation of the geologic history of the eastern Promethei Terra/southeast Hesperia Planum map area will provide new constraints on the styles and timing of volcanic, tectonic, fluvial, mass-wasting, cratering, and potential lacustrine and glacial processes that have shaped the complex geologic record that is preserved in the southern highlands of Mars.

Geologic Mapping of Eastern Promethei Terra/Southeast Hesperia Planum

MTM quadrangles –35237, -40237, and –45237 include the eastern part of the highlands of Promethei Terra, the ridged plains of southeast Hesperia Planum, the crater Arrhenius, and knobby plains [15]. Key scientific issues for this investigation of highland geology include: a) the origin and modification of ridged plains, including potential sedimentary components, b) use of ridged plains as a stratigraphic referent, c) the resurfacing and erosional histories of cratered terrains, including styles of impact crater degradation, d) the stratigraphic position and origin of knobby plains, with specific comparisons to large depositional events adjacent to Reull Vallis, and e) small-scale morphologic evidence for water/ice and geologically recent activity. Statistical analyses of impact crater populations will be employed to evaluate age constraints on geologic events.

A preliminary geologic map of MTM quadrangles –35237, -40237, and –45237 has been completed that shows structural features and geologic units. Mapped structures include scarps, ridges, channels, and crater rim crests. Geologic units can be divided into four major categories: highland materials (mountainous material, cratered-plateau material, basin-rim unit), plains materials (ridged plains material, knobby plains material), crater materials (well preserved, moderately degraded, and highly degraded material and crater floor material), and surficial materials (debris apron material). The major geologic units mapped for the MTM quadrangles are derived from those identified and mapped by Greeley and Guest [15] but their distribution has been reevaluated and the 1:500,000-scale allows significantly greater detail to be represented.

The highland terrains and the map area as a whole contain numerous large impact craters that display a range of preservation states. MTM mapping allows the crater materials to be mapped in detail to help derive the geologic history of the region. Many craters have prominent rims, well-defined ejecta blankets and rugged floors, whereas others are extensively degraded and exhibit low-relief morphologies, gullied rims, and filled interiors. Many craters have complex interiors; crater floors contain smooth, lineated, and pitted regions, as well as display central peaks, mounds, and lobate features. Many craters in the region show well-developed gullies on their interior rims along with associated debris forming aprons/fans that extend to the crater floor. Gullies are observed to start at different heights along crater rims and are typically, but not exclusively, found on pole-facing slopes. Intercrater regions of the cratered plateau and basin-rim units exhibit small channels and gullies. Lobate debris aprons extend from some highland massifs [16].

Large expanses of ridged and knobby plains cover low-lying regions adjacent to cratered highlands. Ridged plains exhibit prominent orthogonal ridge trends characteristic of Hesperia Planum as well as numerous ridge rings. Ridged plains occur primarily in two exposures, at elevations of ~700 and ~1100 m. Ridged plains display smooth and pitted surfaces, rampart craters, channels, and scarps, some of which appear to be structural and others that

appear to be lobe margins. In Viking images, it is not clear whether the channels observed are volcanic or fluvial in nature. Parts of the channels are bounded by lateral zones that have a slightly darker albedo. From Viking images, the topography is uncertain so it is difficult to assess whether these zones are constructional lobes or levees bounding a central volcanic channel or "floodplains" adjacent to a fluvial channel. In MOC images, it is clear that these are fluvial channels dissecting the surface surrounded by lateral zones of surface erosion.

Knobby plains adjacent to the crater Arrhenius were identified by Greeley and Guest [15] and the knobs were interpreted to be erosional remnants of a more extensive unit, although a volcanic origin for some of the knobs was not ruled out. In MTM quadrangles -35237, -40237, and –45237, knobby plains are more extensive than mapped previously. Knobby plains are concentrated in low-lying regions but are not found in all low areas. Knobby surfaces are found superposed on ridged plains, within crater ejecta, and in crater interiors, and a gradational contact between knobby and ridged plains is evident. A complex local stratigraphy is suggested by relationships between knobs, pedestal craters, and layering within plains units. Individual knobs vary in size, shape, and spacing. Most knobs are equant to irregular with flat, rounded, or pitted upper surfaces. Knobs occur in clusters, some of which exhibit linear to curvilinear patterns, and are associated with pedestal craters, buried craters, and buried wrinkle ridges.

In areas of knobby plains, on the cratered plateau, and on the rim of crater Arrhenius, MOC images show repeated sequences of textures consistent with mid-latitude mantling deposits described by other investigators [16-18]. Smooth, typically featureless upper surfaces are observed in association with hummocky textures. The hummocky textures appear to be exposed upon removal of the smooth texture by erosion. The smooth texture is preferentially preserved on equator-facing slopes. Other investigators [16-18] have described the smooth texture as typically uncratered, suggesting a very young geological age. In the map area, there appear to be two types of mantling deposits, one that is uncratered and another that contains a significant population of small craters. The uncratered mantle is found in association with knobby plains, and the cratered mantle is observed on and adjacent to the cratered plateau.

In the southern part of the map area, dark and mottled albedo areas, some with lobate margins, are observed within the heavily cratered basin-rim unit. This is similar to that observed by Mest and Crown [3] further to the west to the south of Reull Vallis. In MOC images, these deposits appear to be some type of blocky lag deposit [19] that may indicate a distinct style of surface degradation that is geographically concentrated. This may or may not be related to the proposed ice-cemented mantle described by others [16-18].

Ongoing analyses as part of geologic mapping of MTM quadrangles -35237, -40237, and –45237 include morphologic and statistical analyses of knobs, examination of layering within and thicknesses of plains units, studies of crater modification, and use of crater populations to constrain stratigraphic ages and assess elevation- or age-dependencies. In addition, as THEMIS data becomes available for the region of interest, it will be utilized to refine and further characterize the mapped geologic units.

References: [1] Crown, DA and SC Mest, Geologic map of MTM -35237, -40237, and –45237 quadrangles, *US Geol Surv*, in prep, 2003. [2] Mest, SC and DA Crown, Geologic map of MTM –20272 and –25272 quadrangles, *US Geol Surv*, in review, 2003. [3] Mest, SC and DA Crown, *Icarus*, 153, 2001. [4] Mest, SC and DA Crown, *US Geol Surv Geol Inv Ser Map I-2730*, 2002. [5] Mest, SC and DA Crown, *US Geol Surv Geol Inv Ser Map I-2763*, 2003. [6] Crown, DA and SC Mest, Geologic map of MTM –30247, -35247, and –40247 quadrangles, *US Geol Surv*, in prep, 2003. [7] Crown, DA et al., *Icarus*, 100, 1-25, 1992. [8] Tanaka, KL and GJ Leonard, *J Geophys Res*, 100, 5407-5432, 1995. [9] Mest, SC, *Geologic History of the Reull Vallis Region, Mars*, MS Thesis, University of Pittsburgh, 217 pp., 1998. [10] Greeley, R and DA Crown, *J Geophys Res*, 95, 7133-7149, 1990. [11] Crown, DA and R Greeley, *J Geophys Res*, 98, 3431-3451, 1993. [12] Gregg, TKP et al., *US Geol Surv Misc Inv Ser Map I-2556*, 1998. [13] Crown, DA and R Greeley, Geologic map of MTM –30262 and –30267 quadrangles, *US Geol Surv*, in review, 2002. [14] Price, KH, *US Geol Surv Misc Inv Ser Map I-2557*, 1998. [15] Greeley, R and JE Guest, *US Geol Surv Misc Inv Ser Map I-1802B*, 1987. [16] Pierce, TL and DA Crown, *Icarus*, doi:10.1016/S0019-1035(03)00046-0, in press, 2003. [17] Mustard, JF et al., *Nature,* 412, 411-414, 2001. [18] Mangold, N, *J Geophys Res*, 108, doi: 10.1029/2002JE001885, 2003. [19] Crown, DA et al., *Lun Planet Sci Conf XXXIV*, Abstract 1126, 2003.

MTM Quadrangle –20257: Western Hesperia Planum, Mars. M. A. Farley[1], T. K. P. Gregg[1], and D. A. Crown[2], [1]The State University of New York at Buffalo, Department of Geology, 876 Natural Sciences Complex, Buffalo, NY 14260-3050 (mafarley@buffalo.edu), [2]Planetary Science Institute, Tucson, AZ.

Tyrrhena Patera, (~22 S, 253.5 W), is a broad, low relief, central-vent volcano located in the western portion of Hesperia Planum, Mars. The extant crater statistics for the base of the Hesperian Epoch [1] were collected from Hesperia Planum as defined by Greeley and Guest [2]. Mapping the Tyrrhena Patera summit region (MTM Quadrangle –20252) revealed that a portion of what had originally been mapped as Hesperia Planum deposits [2] is actually composed of Tyrrhena Patera materials [3, 4]. Therefore, existing crater statistics for Hesperia Planum, and the base of the Hesperian Epoch globally on Mars, may be erroneous. We are mapping MTM quadrangles –20257 and –15257 (Figure 1) to determine the precise nature of the boundary between Western Hesperia Planum, Tyrrhena Patera, and the surrounding Noachian-aged highlands. Our first step in mapping MTM Quadrangles –20257 and –15257 is to determine if units identified in adjacent MTM quadrangle –20252 can be confidently extended.

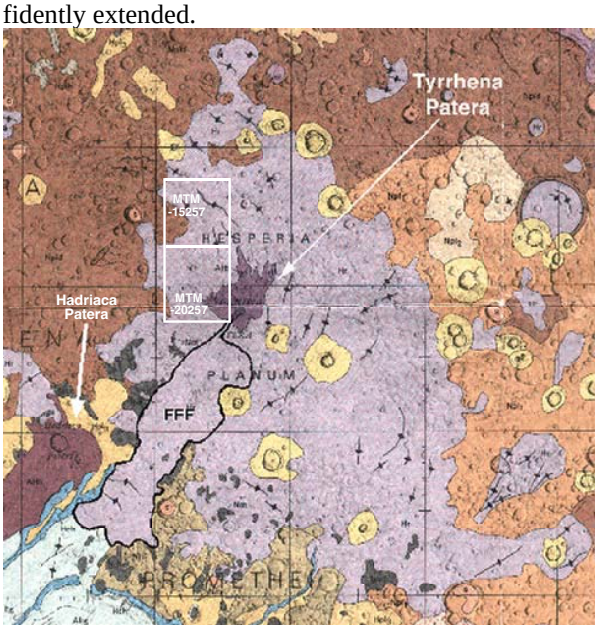

Figure 1: Location map of MTM Quadrangles –20257 and –17257. Geologic map of Hesperia Planum region NE from Hellas basin. MTM Quadrangles –20257 and –17257 are highlighted in white and are located northwest of Tyrrhena Patera.

Previous photogeologic mapping of MTM Quadrangle –20252 using Viking Orbiter images suggests that this volcano is composed of four or possibly five principle units [4]: basal shield material, lower summit shield material, upper summit shield material, rille-floor material, and channel-fill material [3]. Based on morphology and erosional characteristics, the oldest and most areally extensive deposits are most likely pyroclastic deposits, which comprise the three shield units [4, 5].

The central caldera complex of Tyrrhena Patera contains two elliptical depressions, surrounded by dissected shield materials of the volcano (Figure 2). Three major channels extend radially from the summit area; one to the northwest, one to the northeast, and the most prominent channel originates in the summit caldera and extends to the southwest. These channels are interpreted to be volcano-tectonic rilles modified by erosion and may have been conduits for volcanic materials extruded onto the plains and southwest flank flow unit [4].

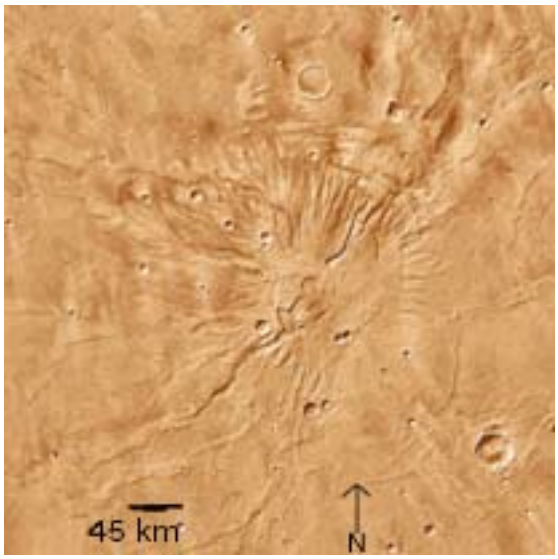

Figure 2: Tyrrhena Patera. False color image of Tyrrhena Patera volcano located at ~22 S, 253.5 W. The central caldera complex, three volcano-tectonic channels, and heavily dissected flanks are clearly visible.

The channels dissecting Tyrrhena Patera shield materials were mapped as containing "channel-floor material" in an adjacent quadrangle [3]. This unit was originally characterized by a mottled surface albedo dissected by small, v-shaped channels, and was interpreted to be reworked summit and basal shield materials transported downslope by both fluvial and mass-wasting processes [3] (Figure 3). Close examination of high resolution (40-60 m/pixel) Viking Orbiter images in MTM –20257 (VO445A20 and VO445A48)

do not unequivocally reveal the presence of channel-floor material. MOC narrow-angle images are also incapable of revealing distinctions between the surface characteristics of channel floor material and adjacent units. This suggests that at Viking Orbiter and MOC image resolutions, channel-floor material is indistinguishable from the surrounding plains and shield materials. However, both MOLA and THEMIS data appear to confirm the presence of a deposit on the channel floors. High resolution THEMIS daytime infrared image #I00821002N crosses a large basin and its tributaries where channel-fill material is suspected to exist, approximately 115 km NW from the summit caldera (Figure 4). The channel and basin floors are characterized by a high spectral reflectance relative to the surrounding landscape consistent with the presence of fine-grained, channel-fill material.

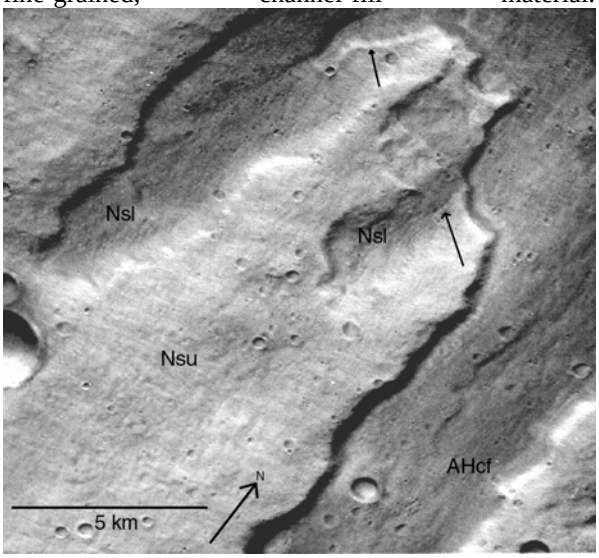

Figure 3: Channel-fill material. Nested channels (arrows) within lower and upper summit shield materials (Nsl and Nsu, respectively) ~15 km northwest of Tyrrhena summit. Note the fine texture of channel-fill material (AHcf), oriented downstream, within nested channels. Viking Orbiter image 794A04.

The position of the northern channel-fill material contact mapped in MTM –20252 is not detectable in Viking Orbiter images and cannot be traced into and through the MTM quadrangle –20257. The use of individual MOLA tracks provides an accurate topographic profile of key regions within the map area. MOLA is useful in interpreting contacts between units, such as the channel-fill and surrounding plains materials. In addition, MOLA topography detects subtle structures such as channels and ridges that cannot be resolved by Viking Orbiter images. Two MOLA cross-sectional profiles have been examined to date, which cross a large basin within the basal shield material, approximately 115 km northwest of the Tyrrhena Patera summit. The topography of this basin, interpreted from Viking Orbiter images and gridded MOLA data, appears to be a broad, flat floored basin bound by steep sided walls with subtle changes in slope along the basin floor. However, MOLA cross-sectional topography reveals that the basin floor has an undulating profile with sharp changes in slope and structures interpreted to be nested channels.

After the extent of channel-fill material has been constrained using MOLA and THEMIS (as available) data, we will continue to examine the continuation of other units originally identified in the adjacent quadrangle (MTM –20252) [2].

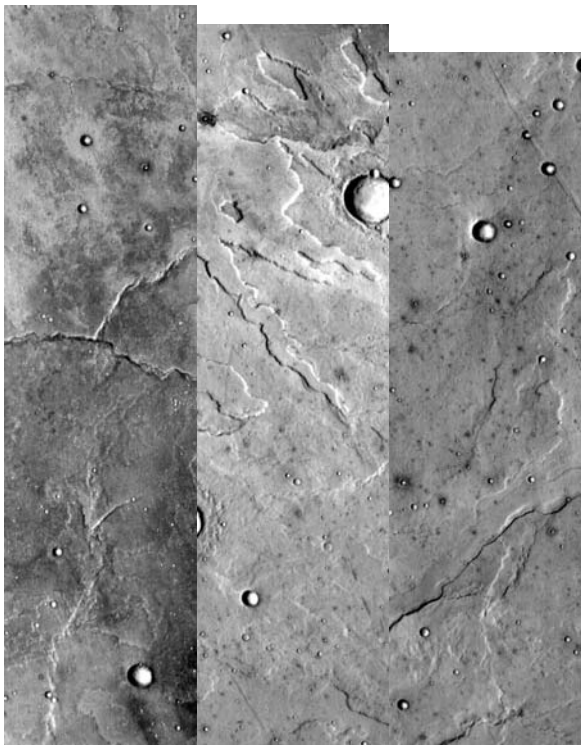

Figure 4: Tiled THEMIS daytime infrared image #I100821002N. Left tile is northern most section. North is up. Image center is approximately 115 km NW from the summit caldera of Tyrrhena Patera. Northern section of image is part of the plains material of Hesperia Planum. Southern section covers the shield material of Tyrrhena Patera. Center section is significantly brighter relative to surrounding area, and is consistent with a fine-grained, channel-fill material present on the floor of the basin and tributary channels.

References: [1] Tanaka K. L. (1986) *JGR, 91*, E139-E158. [2] Greeley R. and Guest J. E. (1987) *U.S. Geol. Surv. Misc Investigation Series I-1802B.* [3] Gregg T. K. P. et al. (1998) *U.S. Geol. Surv. Misc.*

Investigation Series I-2556. [4] Greeley R. and Crown D. A. (1990) *JGR, 95*, 7133-7149. [5] Greeley R. and Spudis P. D. (1981) *JGR, 19*, 13-41.

GEOLOGIC MAP OF THE MTM 85080 QUADRANGLE, PLANUM BOREUM REGION OF MARS.

K. E. Herkenhoff, U. S. Geological Survey, 2255 N. Gemini Dr., Flagstaff, AZ 86001 (kherkenhoff@usgs.gov).

Introduction: The polar deposits on Mars probably record martian climate history over the last 10^7 to 10^9 years [1]. The area shown on this 1:500,000-scale map includes polar layered deposits and polar ice, as well as some exposures of older terrain. This quadrangle was mapped in order to study the relations among erosional and depositional processes on the north polar layered deposits and to compare them with the results of previous 1:500,000-scale mapping of the south polar layered deposits [2,3].

The polar ice cap, areas of partial frost cover, the layered deposits, and two nonvolatile surface units--the dust mantle and the dark material--were mapped in the south polar region [4] at 1:2,000,000 scale using a color mosaic of Viking Orbiter images. We constructed Viking Orbiter rev 726, 768 and 771 color mosaics (taken during the northern summer of 1978; Fig. 1) and used them to identify similar color/albedo units in the north polar region, including the dark, saltating material that appears to have sources within the layered deposits [5]. However, no dark material has been recognized in this map area. There is no significant difference in color between the layered deposits and the mantle material mapped by Dial and Dohm [6], indicating that they are either composed of the same materials or are both covered by aeolian debris [3,4]. Therefore, in this map area the color mosaics are most useful for identifying areas of partial frost cover. Because the resolution of the color mosaics is not sufficient to map the color/albedo units in detail at 1:500,000 scale, contacts between them were recognized and mapped using higher resolution black-and-white Viking Orbiter images.

No craters have been found in the north polar layered deposits or polar ice cap [7,8]. The observed lack of craters larger than 300 m implies that the surfaces of these units are no more than 100,000 years old or that they have been resurfaced at a rate of at least 2.3 mm/yr [8]. The recent cratering flux on Mars is poorly constrained, so inferred resurfacing rates and ages of surface units are uncertain by at least a factor of 2.

Stratigraphy and structure: The oldest mapped unit, mantle material (unit Am), is distinguished by its rough, sometimes knobby surface texture. The knobs and mesas of mantle material that crop out within areas of smooth layered deposits suggest that the mantle material was partly eroded before the layered deposits were laid down over them. The layered deposits appear to cover the mantle material except on steep scarps that expose the mantle material. The layered deposits may be more resistant to erosion than the mantle material, so that the steep scarps formed by more rapid erosion of mantle material beneath layered deposits. Therefore, the mantle material in this area does not appear to have been derived from erosion of the polar layered deposits.

The layered deposits (unit Al) are recognized by their distinct bedded appearance, red color and lower albedo relative to the polar ice cap and frost deposits; they appear to be the youngest bedrock unit in this area. In both polar regions, layers are apparent at least partly because of their terraced topography, especially where accented by differential frost retention [13,14]. MOC images show that layered deposit exposures are commonly rough, with evidence for deformed beds and unconformities [16]. No definite angular unconformities have been found within the south polar layered deposits [2,3], unlike the north polar layered deposits, where truncated layers have been recognized in higher resolution images [7,13]. Angular unconformities have been found in various locations within this map area, including lat 85.7 N., long 61 W., lat 82.6 N., long 82 W., and lat 83.6 N., long 90 W. The unconformities are mapped using hachures on the side of the contact where layers are truncated.

The partial frost cover (unit Af) is interpreted as a mixture of seasonal frost and defrosted ground on the basis of its albedo, color, and temporal variability. Bass and others [17] found that frost albedo reaches a minimum early in the northern summer, then *increases* during the rest of the summer season. This behavior is illustrated in Figure 1, where frost appears darker because it is less red. The increase in albedo is interpreted as resulting from condensation of H_2O from the atmosphere onto cold traps in the north polar region [17]. Because the images used for the base and for mapping were taken in mid-summer, the extent of the high-albedo units shown on this map is greater than during early summer.

The albedo of the residual polar ice cap (unit Ac) is higher than all other units on this map. The contact with the partial frost cover (unit Af) is gradational in many areas, most likely because unit Af represents incomplete cover of the same material (H_2O frost) that comprises unit Ac. The summer extent of the north polar cap was the same during the Mariner 9 and Viking Missions [17], which suggests that it is controlled by underlying topography. Albedo patterns in these summertime images are correlated with topographic

features seen in springtime images. Areas of the highest albedos must be covered by nearly pure coarse-grained ice or dusty fine-grained frost [18,19]. The presence of perennial frost is thought to aid in the long-term retention of dust deposits [20], so areas covered by frost all year are the most likely sites of layered-deposit formation.

The MTM 85080 geologic map has been reviewed and accepted for publication in the USGS Miscellaneous Investigations Series. Unfortunately, map production has been delayed because the linework was completed on an old version of the Viking MDIM photomosaic base. The offset between the old and new (MDIM 2.0) base is significant, so that the linework must be shifted manually and mapping extended in some areas. This process is time-consuming, but publication is expected late in 2003.

References:

[1] Thomas P. *et al.* (1992) Polar deposits on Mars, in *Mars*, University of Arizona Press, 767-795.

[2] Herkenhoff K. E. and Murray B. C. (1992) *USGS Misc. Inv. Series Map I-2304*; Herkenhoff K. E. and Murray B. C. (1994) *USGS Misc. Inv. Series Map I-2391*; Herkenhoff K. E. (2001) *USGS Misc. Inv. Series Map I-2686*.

[3] Herkenhoff K. E. (1998) *USGS Misc. Inv. Series Map I-2595*.

[4] Herkenhoff K. E., and Murray B. C. (1990) *JGR, 95*, 1343-1358.

[5] Thomas P. C. and Weitz C. (1989) *Icarus, 81*, 185-215.

[6] Dial A. L. Jr. and Dohm J. M. (1994) *USGS Misc. Inv. Series Map I-2357*.

[7] Cutts J. A. *et al.* (1976) *Science, 194*, 1329-1337.

[8] Herkenhoff K. E. and Plaut J. J. (2000) *Icarus, 144*, 243-253.

[9] Zuber M. T. *et al.* (1998) *Science, 282*, 2053-2060.

[10] Smith D. E. *et al.* (1999) *Science, 284*, 1495-1503.

[11] Murray B. C. *et al.* (1972) *Icarus, 17*, 328-345.

[12] Cutts J. A. (1973) *JGR, 78*, 4231-4249.

[13] Howard A. D. *et al.* (1982) *Icarus, 50*, 161-215.

[14] Herkenhoff K. E. and Murray B. C. (1990) *JGR, 95*, 14,511-14,529.

[15] Blasius K. R. *et al.* (1982) *Icarus, 50*, 140-160.

[16] Edgett K. S. and Malin M. C. (1999) *LPS XXX*, Abstract #1029; Malin M. C. and Edgett K. S. (2001) *JGR, 106*, 23,429-23,570.

[17] Bass D. S. *et al.* (2000) *Icarus, 144*, 382.

[18] Clark R. N. and Lucey P. G. (1984) *JGR, 89*, 6341-6348.

[19] Kieffer H. H. (1990) *JGR, 95*, 1481-1493.

[20] James P. B. *et al.* (1979) *Icarus, 68*, 422-461.

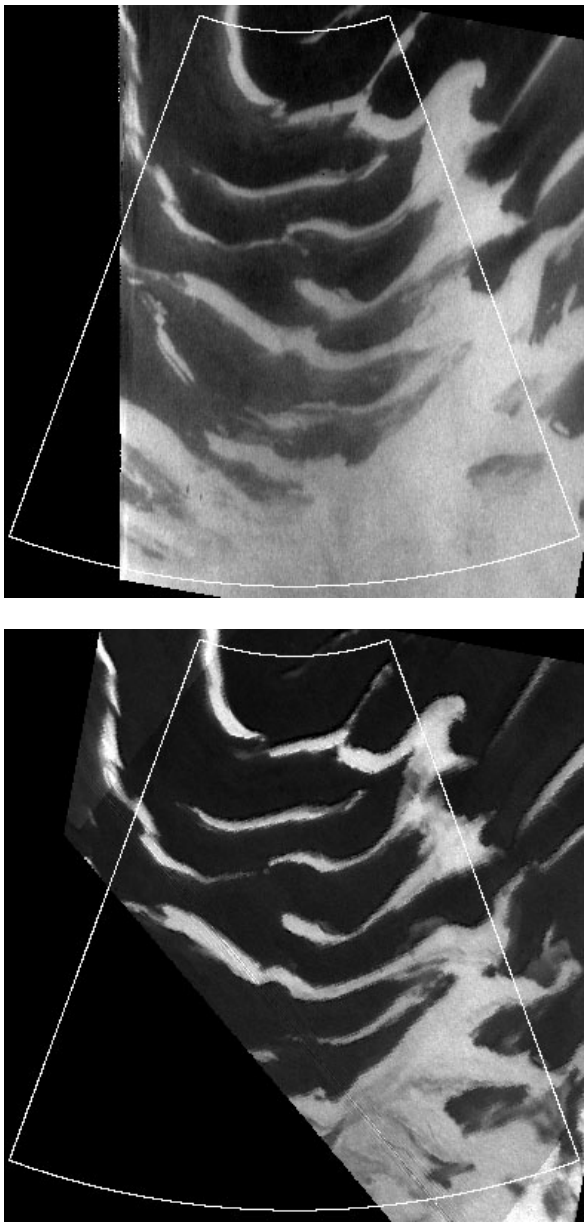

Figure 1. Red/violet ratio mosaics of Viking Orbiter 1 images of the map area, taken almost a Mars year after the images used to create the photomosaic base map. White corresponds to red/violet = 2.2, totally black regions indicate no image coverage or red/violet < 1.5. Polar stereographic projection (same as map base; map outline shown), north is up. Area shown in each mosaic ~310 km across. (top) Rev 726 mosaic (L_s = 100), taken during a period of hazy atmospheric conditions. (bottom) Rev 768 mosaic (L_s = 119), showing much clearer atmospheric conditions and changes in frost distribution.

RESULTS OF GEOLOGIC MAPPING OF THE SOUTH POLAR REGION OF MARS AT 1:3,000,000 SCALE AND FUTURE 1:1,500,000 SCALE POLAR MAPPING. E.J. Kolb[1] and K.L. Tanaka[2], [1]Arizona State University, Dept. of Geological Sciences, Tempe, AZ 85287, eric.kolb@asu.edu, [2]Astrogeology Team, U.S. Geological Survey, 2255 N. Gemini Dr., Flagstaff, AZ 86001, ktanaka@usgs.gov.

South Polar Mapping at 1:3,000,000 Scale

Status. We have completed our 1:3,000,000-scale geologic mapping of the south polar region of Mars from 60°S to 90°S. Geologic mapping was largely based on data provided from Mars Global Surveyor (MGS) such as altimetry data acquired by the Mars Orbiter Laser Altimeter (MOLA) and image data from the Mars Orbiter Camera (MOC). By incorporating these data into our new geologic mapping and associated studies of the martian south polar terrain, we have made significant advancements in the identification and interpretation of geologic units and features.

Mapping Approach. Previous geologic maps of the martian south polar region were compiled from Mariner 9 images by [1] and from medium-resolution Viking images by [2]. These maps have utilized mapping approaches that we revised for our south polar mapping.

As discussed in [3], mappable rock units can include (1) rock-stratigraphic units based on rock type (e.g., lava flows, impact breccia, and sedimentary deposits) and/or (2) allostratigraphic (unconformity-bounded) units that consist of event- or episode-related rock assemblages. Both types of units are used in terrestrial geologic mapping. Previous planetary mapping has strayed beyond these unit types and have included secondary tectonic or erosional structures or other features not related to primary materials and/or events (e.g., see discussion in [4]). We have applied allostratigraphic mapping approaches in our south polar geologic mapping. This has resulted in more conservative delineation of map units, most notably in the mapping of cratered highland materials. In addition, it is more informative as we institute new contact types [3] to document more fully the types of changes occurring across contact boundaries. We feel that this approach yields a meaningful expression of geologic history, while providing informative details regarding geologic complexities and data limitations.

Several contact boundary symbols from [5] were used to best display the relationships between adjacent material units, including *certain* (solid), *approximate* or *inferred* (dashed), *scratch* (no line), and *gradational* (thick, hachured line). Secondary structures such as ridge features, fractured terrains and mantles of secondary crater impact ejecta do not represent primary rock characteristics and have been mapped using various stipple patterns.

Results. Noachian materials within the study area consist of the cratered highland plateau sequence (Npl). These materials have been divided by [2] into units Npl_1 and Npl_2 based largely on the density of craters >10-km-diameter and <10-km-diameter respectively. Secondary modification features observed within areas of units Npl_1 and Npl_2 were used by [2] to further subdivide the highland plateau materials into the dissected unit (unit Npld), ridged unit (unit Nplr) and etched unit (unit Nple). Because these features are unrelated to the primary formation of the highland materials, we have reassigned outcrops previously mapped as units Npld, Nplr, and Nple to either unit Npl_1 or unit Npl_2. At the same time, we have been careful to map in appropriate detail the structures and morphologic features that had been previously used to separate the Noachian units. Since the main criteria in delineating units of Npl_1 and Npl_2 are crater density and modification state, in theory and practice where the two units are adjacent to each other, the nature of the contact is gradational. We also see local evidence of hiatuses between the units, such as in the emplacement of local deposits and the formation of tectonic and erosional structures. Therefore, where the highland units are in contact, our use of gradational contact lines is proving to be an effective tool in representing the event/episode relationship between the two units.

South polar Hesperian geology is broadly characterized by waning impacts, volcanism, tectonism, and the emplacement of the Dorsa Argentea Formation (DAF). The DAF was previously divided into two units by [2] whereas our 1:3,000,000-scale mapping has divided the DAF into 8 units consisting of six plains members (units Hda, Hdd, Hdc, Hdp, Hds, and Hdv) and the cavi (unit ANdc) and rugged members (unit Hdr). The lobate fronts yet lack of other typical volcanic-flow morphology of the plains units of DAF indicate that the units may be made up of debris flows [6]. We think that these flows, tens of meters to 200 m thick, may have originated by the discharge of huge volumes of slurry fluidized by ground water or

liquid CO_2, perhaps triggered by local impacts, igneous activity, or basal melting beneath polar deposits. The cavi and rugged members include irregular depressions, some with raised rims that penetrate the subsurface. The depressions may have formed by collapse due to expulsion of subsurface material in which local explosive activity built up the raised rims. Further, smaller eruptions of volatile-rich material may have resulted in coarse-grained, narrow, sinuous channel deposits within aggrading, fine-grained unconsolidated material perhaps produced by gaseous discharge of subsurface volatiles. Preferential erosion of the fines could have produced the Dorsa Argentea-type sinuous ridges associated mainly with the DAF.

Within the Amazonian south polar layered deposits (SPLD, unit Apl) of Planum Australe, erosional, depositional, impact, and possible tectonic features have been systematically mapped and their relation to SPLD formation and post-emplacement modification history has been investigated. Mapped features include linear and cuspate ridges, lineated terrain, trough scarps and valleys, buried craters, and primary and secondary impact-crater structures. We have also used MOC NA images and MOLA DEM's to assess the degree and extent of SPLD deformation evident within individual layers and sequences of layered deposits. We conclude that the PLD's are composed of porous unconsolidated layers that have not experienced significant basal melting or glacial flow, although localized boudin formation is evident among an upper sequence of layers within the stack [7]. We postulate that the PLD's eventually reached and maintained their present form following deposition without extensive flow deformation or redeposition. However, local resurfacing of the SPLD may have been effective at removing impact craters.

1:1,500,000-Scale Mapping of PLD's

As a follow-on study to our south polar regional mapping, we have begun a detailed geologic mapping study of the north and south polar layered deposits at 1:1.5M scale. The specific goals of this project are three-fold: (1) Construction of stratigraphic sections of the PLD and topographic mapping of prominent layers and layer sequences and investigation of intra- and interpolar stratigraphic and topographic variations in the PLD and residual ice caps, (2) detection and interpretation of structural deformation in the PLD, and (3) description and interpretation of the erosional history of the PLD.

Geologic mapping will be performed using a GIS-integrated, multi-dataset approach consisting of current and to-be-released mission-specific data products. The mapping base consists of MOLA-derived digital elevation models, shaded relief, slope and contour maps, all at resolutions at or exceeding 114 m/pixel below 87° latitudes. Above 87° latitudes, we will utilize Viking and (or) MOC stereo topography derived by M. Rosiek (USGS Photogrammetry Section) to improve the topographic definition in these areas. MOC WA stereo topography will result in a DEM with a spatial resolution no better than ~750 m horizontally and ~100 m vertically. Additional high-resolution data will be acquired by photoclinometry on frosted polar MOC NA images with assistance from L.A. Soderblom (USGS).

Viking (130 to 250 m/pixel), MOC NA (4 to 16 m/pixel) and THEMIS infrared (100 m/pixel) and visible (18 m/pixel) images will provide thermal, color, morphologic, and other surface properties information. Additional image-base products currently in development by B. Sucharski and E. Lee (USGS), such as the MOLA-registered Viking MDIM 2.1 and MOC WA MDIM 3.0 (~250 m/pixel), will be incorporated as they become available.

We are in the initial stages of the mapping project. As such, current tasks are focused on the acquisition and compiling of released data products. Specific tasks include ISIS-based processing of released THEMIS-VIS and spring and summer polar MOC-NA images. Following ISIS processing completion, the respective datasets will be mosaicked in order to provide high-resolution photogeologic mapping bases. The mosaicking process is highly adaptable, allowing the integration of future data releases with a minimum of mosaic re-processing. Initial THEMIS/MOC image mosaicking will be completed this summer, after which we will begin 1:1.5M-scale mapping of the SPLD. Initial results will be presented at the 3rd Mars Polar Science Conference.

References: [1] Condit, C.D., and Soderblom, L.A. (1978) *USGS Map I-1076***.** [2] Tanaka K.L. and Scott D.H. (1986) *USGS Map I-1802C* . [3] Tanaka K. L. et al., *this volume.* [4] Hansen V. L. (2000) *EPSL, 176,* 527-542. [5] Geologic Data Subcommittee (1999) *USGS OFR 99-430,* online version 1.0, http://geopubs.wr.usgs.gov/open-file/of99-430/. [6] Tanaka K. L. and Kolb E. J. (2001) *Icarus, 154,* 3-21. [7] Kolb E. J. and Tanaka K. L. (2001) *Icarus, 154,* 22-34.

GEOLOGIC MAP OF MTM -20272 AND -25272 QUADRANGLES, TYRRHENA TERRA REGION OF MARS. S.C. Mest[1,2] and D.A. Crown[1,3], [1]Department of Geology and Planetary Science, University of Pittsburgh, Pittsburgh, PA 15260; [2]Geodynamics Branch, NASA/Goddard Space Flight Center, Greenbelt, MD 20771 mest@kasei.gsfc.nasa.gov; [3]Planetary Science Institute, 620 N. 6th Ave, Tucson, AZ 85705.

Introduction: MTM quadrangles -20272 and -25272 (-17.5° to -27.5°, 270° to 275°) cover part of the highlands of Tyrrhena Terra north of Hellas basin. Geologic mapping allows detailed characterization of the cratered highlands, including impact crater morphologies, dissection by fluvial valleys, and formation of intercrater plains. The map area records a complex history of impact cratering and modification by fluvial and eolian activity [1-7]. Extensive networks of valleys dissect much of the area and have significant implications for past martian environmental conditions.

Geologic units were analyzed using Viking Orbiter and MOC images and MOLA topographic data. Viking image coverage ranges from 58 to 240 m/pixel; however, part of the map area is covered by 8-11 m/pixel images. High-resolution MOC coverage is sparse but was useful in characterizing geologic units at small scales and analyzing their spatial extents. MOLA data were used to identify relationships between valleys and impact craters, and to assess the distributions and stratigraphic positions of geologic materials.

Stratigraphy: Relative ages of geologic units were determined using stratigraphic relations and crater size-frequency distributions [7]. Craters were identified using MDIM 2 (231.4 m/pixel) and MTM (1:500K scale) photomosaics, and individual Viking Orbiter frames. This abstract focuses on the new units identified - dissected intercrater plains, valley floor, and crater floor materials, and the Millochau floor deposits - as well as the numerous fluvial features.

Dissected intercrater plains material: Dissected intercrater plains material (Ndip) contains well-incised networks of valleys and exhibits a surface shaped by impacts. In Viking images the plains show a smooth to irregular surface; irregularities result from a complex mixture of crater materials untraceable to specific source craters. Subtle mottling across the plains is due to uneven distribution of ejecta and eolian deposits. MOC images show high-standing areas of the plains contain many small (D<1 km) poorly preserved (eroded and (or) buried) craters, visible as shallow rimless depressions, and appear competent in nature whereas lower areas (floors of pits and craters) are filled with dark albedo sediments. The plains also exhibit layering where exposed along valley walls. Heavily dissected plains in the northern part of the map area are separated from smoother, less dissected plains to the south by a cluster of about twenty large (D>25 km) craters. MOLA data show the southern plains are ~600 m lower in elevation than to the north. MOC images show outcrops of intercrater plains are surrounded by dunes suggesting the southern part of the plains are being buried by eolian materials. Dissected intercrater plains is interpreted to consist of sequences of impact, volcanic, and sedimentary materials. Erosion by fluvial processes formed valley networks that dissect the plains. Eolian activity has since buried much of the southern plains. Crater size-frequency distributions show plains formation began in the Early Noachian Epoch, but continued into the Middle and Late Noachian.

Valley floor material: Valley floor material (HNvf) is found in most valleys in the map area. These deposits appear smooth in Viking images, but MOC images show the material consists of sediments mobilized to form dunes. The dunes are oriented perpendicular to the valley walls and most span the widths of the valleys. Most craters are buried by valley floor material, but several small craters superpose dunes, constraining the ages of floor material and the timing of intervalley flow. This suggests that the dunes are relatively stable and may indicate (a) the sediments are difficult to mobilize, (b) the wind velocities required to form dunes are no longer present, and (or) (c) the craters have acted to stabilize portions of the dunes and dune movement is still active in other areas. Valley floor material is believed to consist of sediments derived from the surrounding plains and deposited by water flowing through the valleys, mass wasting of valley walls, and eolian processes. Crater size-frequency distributions show ages ranging from Early to Late Noachian, but is designated as Late Noachian or younger from crosscutting relationships with the dissected intercrater plains.

Crater materials: Many craters display low-relief rims, smooth floors, and contain crater floor material (HNcf). Some deposits display lobate margins whereas others terminate gradually against the interior crater walls. Most craters have gullied interior walls suggesting that much of the floor deposits consist of eroded crater wall and rim material. Some craters breached by valleys indicate a portion of these deposits consist of eroded highland materials. Some component of crater floor material may also be lacustrine or eolian. No evidence for mass movements is found, as in other highland studies [8-13], but contributions from mass wasting are not ruled out. Crater size-frequency distributions suggest crater floor materials are Late Noachian to Early Hesperian in age.

Millochau (21.4°S, 275°W; D=114 km) shows terrains that suggest a complex geologic history and contains four distinct units: dune, etched, pitted, and rugged materials. MOC images allow these deposits to be identified and characterized separately from crater floor material. Mest and Crown [14] provides a more detailed description of the Millochau floor deposits than can be given here. The floor of central Millochau forms a plateau ~400 m above the surrounding floor, which is bounded on its northern and eastern edges by a scarp and a series of irregular depressions. Layers are exposed along the scarp boundary of the plateau and within knobs found in the depressions. The topographic expression of the plateau may represent a central peak buried by sedimentary, impact, and volcanic materials.

Rugged material (HNmr) forms irregular surfaces and extends from the central plateau to the base of the interior wall. Rugged material is interpreted to consist of sedimentary, volcanic, and impact-related (ejecta, impact melt) deposits that have undergone more degradation or are less resistant to erosion than pitted material. Pitted material (HNmp) covers the central plateau and shows a heavily pitted and cratered surface. Pitted material is believed to be composed partly of materials eroded from the interior wall of Millochau, but could also contain volcanic and impact-related (ejecta, impact melt) materials. Pits could be due to poorly preserved impact craters, collapse features, and (or) eolian-modified depressions. Etched material (HNme), found in the depressions that border the plateau, displays surface textures (smooth, lineated and irregular) and albedos distinct from pitted and rugged materials. Few fresh craters are observed within etched material, but some exposures contain craters that are being exhumed. Etched material is interpreted to be crater floor materials (sedimentary, volcanic, and impact materials) that have been exhumed. Collapse and (or) erosion (fluvial and eolian) are believed to be the main processes operating to expose these deposits. Dune material (Amd) occurs as patches that fill low-lying parts of other materials, is darker in albedo than underlying materials, and forms sets of long-wavelength (wavelengths ~40-170 m; avg = 70 m) and short-wavelength (wavelengths ~10-30 m; avg = 20 m) dunes, similar to those describe by [15]. Dune material is interpreted to consist of sediments eroded from other Millochau floor deposits, as well as crater wall and rim materials, and redistributed within low-lying areas by eolian processes.

The Millochau floor deposits have small areal extents and contain few large craters. Crater size-frequency distributions for these materials show ages ranging from Middle Noachian to Early Hesperian. Pitted material shows higher crater densities for all diameters. Rugged material shows lower densities (N(2) and (5)), consistent with its more degraded appearance. Age-determination for etched material was difficult; only four fresh craters (D>0.5 km) were identified, but based on its interpretation and the potential for geologically recent redistribution of unconsolidated debris, etched material is considered to be younger than pitted and rugged materials. Dune material contains no craters greater than 0.5 km in diameter and is designated Amazonian in age.

Fluvial Features: The map area is dissected by valleys that form open dendritic patterns on gradual slopes and (sub)parallel patterns on steeper slopes. MOC images show most valleys display rounded banks, layering along their walls, and dunes on their floors. MOLA profiles show valleys have v-shaped cross-sections; valley depths range from ~73 to 200 m and widths from ~0.9 to 10.5 km. The largest network dissects much of the map area southward to a grouping of large craters (24°S), and has tributaries that reach outside of the map area. The drainage basin enclosing this network, as well as several smaller networks, occupies an area ~300,000 km^2. The basin exhibits 4.5 km in relief with a max elevation near 3.5 km and a min near -1.0 km. The trunk valley of the larger network branches and rejoins upstream at least three times along its length. Smaller, less-incised (sub)parallel networks are found south of Millochau and typically head near the crater rim. The morphologic differences between these smaller networks and the larger network could be due to differences in (a) age, (b) lithology, (c) slope, and/or (d) the effect of broad-scale versus localized erosion.

Identification of clear relationships between valleys and craters is difficult due to coverage by low-resolution images. Several craters have dissected ejecta indicating valley formation post-dates crater formation. Viking images do not clearly resolve whether ejecta is found on the floors of these valleys, but MOLA profiles do not show significant changes in valley depth where ejecta is expected. It is possible that any ejecta in the valleys has been removed or redistributed. Craters that superpose valleys are observed, showing that some craters post-date valley formation. These craters do not appear to have caused any visible "damming" or diversion of water, which should be present if significant flow within these valleys was present at the time of impact. The above relationships suggest that most valley formation is relatively old with fluvial activity ceasing in the Late Noachian. Previous researchers [16,17] interpreted highland valleys, such as those mapped here, to have formed by mass wasting and sapping processes. However, the fact that valley widths and depths vary greatly along their lengths and many valleys head near crater rims suggests some component of runoff may be involved [3,4,16-19]. Furthermore, the ability to sustain an interconnected aquifer system in the highlands might be problematic over regional scales where subsurface materials may not be conducive for groundwater flow. Hydrologic modeling is being used to examine these problems in order to determine the fluvial evolution of the region [20].

Conclusions: Geologic mapping in the Tyrrhena Terra region reveals a surface that has undergone significant degradation and modification by impact, fluvial and erosional processes. Most of the materials mapped in this study are very old, ranging from Middle Noachian to Lower Hesperian in age. Surficial deposits, such as dune material, show evidence for activity in the Amazonian Period. The region shows complex relationships between craters and valley networks that dissect the intercrater plains. Lack of consistent high resolution coverage across the entire map area complicates interpretation of age relationships. The following summarizes the geologic history determined for this study area.

· Formation of Hellas and other large impact basins dominate geologic development early in the region's history, altering the topography to form sediment traps, and depositing large quantities of ejecta over much of the surface. Heavy bombardment during the Noachian also produced numerous large (D>10 km) craters, including Millochau.

· During the Early and Middle Noachian Epochs, intercrater plains formed by accumulation of layered sedimentary, volcanic, and impact-related materials. Fluvial processes eroded the plains and ejecta deposits forming well-incised networks of valleys and degrading various surfaces. As fluvial activity waned, craters continued to form, truncating and (or) burying some valley segments.
· During the Late Noachian and Early Hesperian Epochs craters were being degraded; gullies formed on interior walls and fill material accumulated on crater floors. Sequences of sedimentary, volcanic and (or) impact materials were emplaced on the floor of Millochau and subsequently degraded. Deposition within Millochau is related in part to erosion of the interior crater rim, but could also include contributions from eolian and lacustrine activity.
· Late Noachian and Early Hesperian Periods also involved deposition and remobilization of sediments within valleys and the southern dissected intercrater plains. Dune-forms suggest these sediments are mobile and composed of material deposited by valleys, impacts, or the wind.
· The most recent, and possibly ongoing, activity involves eolian emplacement of dune material in Millochau, erosion of the uppermost layers of the dissected intercrater plains, and redistribution of material throughout the area.

Determination of highland degradation in this and other areas of the circum-Hellas highlands is continuing. In comparison, geologic mapping in eastern Hellas [6,8,14,21,22] has shown that much of the fluvial and volatile-related features - such as valley networks, outflow channels, and debris aprons - are geologically "young" compared to Tyrrhena Terra. The significant differences between the ages, scales and morphologies of fluvial features in the two regions suggests (a) their geologies differ significantly, (b) the distribution of volatiles around Hellas basin varies greatly, and (or) (c) the processes of fluvial erosion were greatly dissimilar. MOLA data is being used in conjunction with mapping to document the styles and timing of the degradational processes. Specifically, watershed modeling is being conducted to further constrain fluvial activity in these highland terrains.

References: [1] Schaber G.G. (1977) *Geologic map of the Iapygia Quadrangle, Mars*, U.S.G.S. Misc. Inv. Ser. Map I-1020, scale 1:5M. [2] Greeley R. and J.E. Guest (1987) *Geologic map of the eastern equatorial region of Mars*, U.S.G.S. Misc. Inv. Ser. Map I-1802B, scale 1:15M. [3] Craddock R.A. and T.A. Maxwell (1993) *JGR*, **95**, 3453-3468. [4] Maxwell T.A. and R.A. Craddock (1995) *JGR*, **100**, 11765-11780. [5] Tanaka, K.L. and Leonard G.J. (1995) *JGR*, **100**, 5407-5432. [6] Mest S.C. and D.A. Crown (2002) *LPS XXXIII*, Abs. **#1730**. [7] Mest S.C. and D.A. Crown (2003) *Geologic map of MTM -20272 and -25272 quadrangles, Terra Tyrrhena region of Mars*, U.S.G.S., scale 1:500K, in review. [8] Mest S.C. and D.A. Crown (2001) *Icarus*, **153**, 89-110. [9] Grant J.A. and P.H. Schultz (1993) *JGR*, **98**, 11025-11042. [10] Grant J.A. and P.H. Schultz (1994) *LPS XXV*, 457-458. [11] Crown D.A. and K.H. Stewart (1995) *LPS XXVI*, 301-302. [12] Grant J.A. (1999) *Intl Jrnl of Impact Engin.*, **23**, 331-340. [13] Pierce T.L. and D.A. Crown (2003) *Icarus*, in press. [14] Mest S.C. and D.A. Crown, (2003) *LPS XXXIV*, Abs. **#1942**. [15] Edgett K.S. (2001) *LPS XXXII*, Abs. **#1181**. [16] Carr M.H. (1995) *JGR*, **100**, 7479-7507. [17] Carr M.H. (1996) Water on Mars, Oxford Univ. Press, New York. [18] Goldspiel J.M. et al. (1993) *Icarus*, **105**, 479-500. [19] Goldspiel J.M. and S.W. Squyres (2000) *Icarus*, **148**, 176-192. [20] Mest S.C. et al. (2002) *LPS XXXIII*, Abs. **#1892**. [21] Crown D.A. et al. (1992) *Icarus*, **100**, 1-25. [22] Leonard G.J. and K.L. Tanaka (2001) *Geologic map of the Hellas region of Mars*, U.S.G.S. Geol. Inv. Ser. I-2694, scale 1:5M.

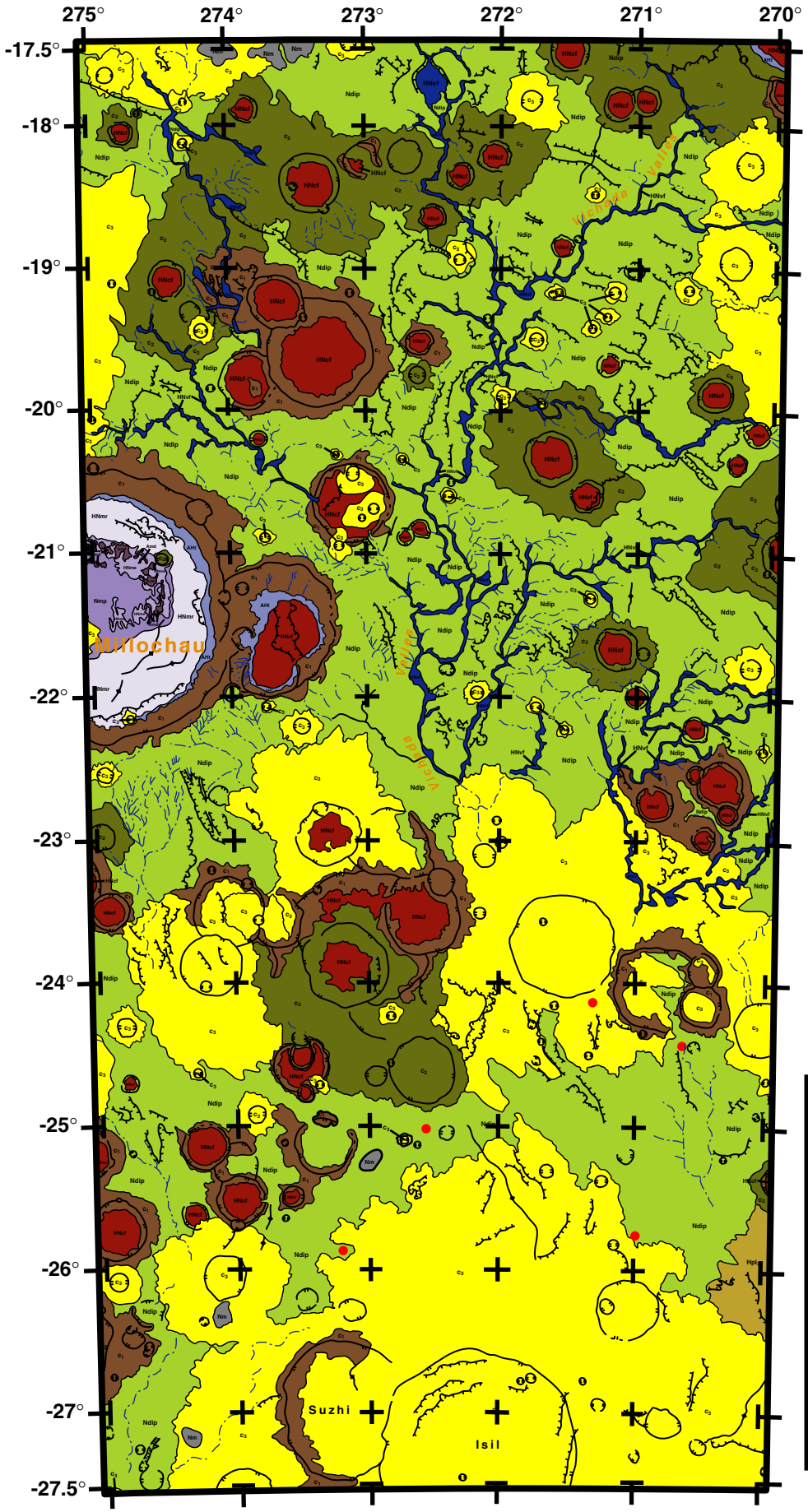

Geologic Map of MTM Quadrangles -20272 and -25272, Tyrrhena Terra Region of Mars

Scott C. Mest
and
David A. Crown

LEGEND

- Contact
- Ridge
- Scarp
- Channel
- Crater rim crest
- Degraded crater rim crest
- Indicates location of dune field observed within MOC images

Correlation Chart

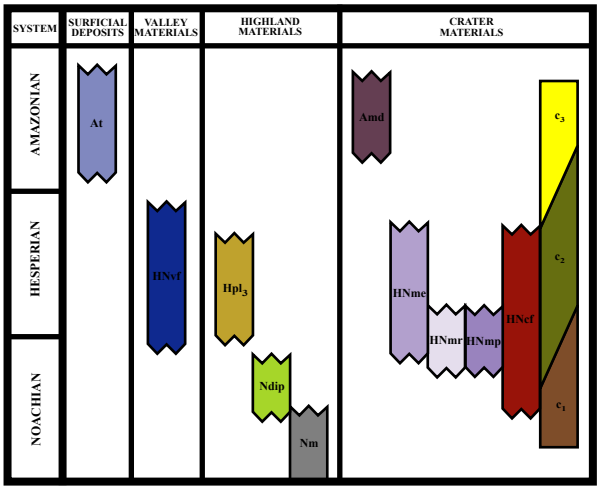

RESULTS OF MARS NORTHERN PLAINS GEOLOGIC MAPPING. Kenneth L. Tanaka, James A. Skinner, Jr., Trent M. Hare, Taylor Joyal, and Alisa Wenker; U.S. Geological Survey, 2255 N. Gemini Dr., Flagstaff, AZ 86001; ktanaka@usgs.gov.

Introduction. We are near completion of a geologic map of the northern plains of Mars at 1:15,000,000 scale, based mainly on Mars Global Surveyor (MGS) Mars Orbiter Laser Altimeter (MOLA) data, with significant contributions from Viking, MGS Mars Orbiter Camera (MOC) narrow- and wide-angle, and Mars Odyssey (MO) Thermal Emission Imaging System (THEMIS) images. Our objectives include reconstruction of the sedimentary, volcanic, tectonic, and erosional histories of materials and surfaces within and bordering the northern plains of Mars using the new MGS and MO data sets. In the process, we have also re-examined mapping techniques traditionally used for Mars and have adopted new approaches.

Methodology. We implement some geologic mapping methods in this map that differ to various degrees from previous approaches common to planetary geologic mapping but in most cases entail formally accepted techniques in terrestrial geologic mapping. We think that these approaches provide a clearer and more objective product than that of previous Mars geologic maps. Though some of these practices were previously employed to some extent, they are put to use in a more comprehensive and purposeful manner in this map of the northern plains of Mars.

First, as espoused by Hansen [1], we identify and map rock units based on their apparent geologic uniqueness as defined by their primary physical features, areal extent, relative age, and geologic associations. Primary features are those that formed during unit emplacement and may include lobate flow scarps, layering, albedo, and thermophysical character. Secondary features are those that are formed after the emplacement of the unit and may include fault scarps, yardangs, valley networks, and wind streaks and other aeolian debris. In many cases, delineating primary and secondary features requires careful observation and may be impractical or at least uncertain where overprinting of secondary features has masked, obliterated, or mixed with primary features. Furthermore, map units may consist of diverse, unknown or uncertain lithologies. This weakens the case for the rock-stratigraphic approach previously encouraged in Mars geologic mapping [2]. We find that a more tenable scheme for mapping complex units on Mars is to use *allostratigraphic* [3] or *unconformity-bounded* [4] units. This approach helps to discriminate geologic units chiefly by relative age, in which a significant hiatus can be inferred between overlying and adjacent units.

Second, we did not use morphology, albedo, terrain "type", or any other physical characteristics in map-unit names, because we find that such characteristics are highly variable within a single unit. Commonly, units are primarily delineated using relative age and geologic relations, which makes naming them based on physical characteristics unrealistic. Instead, we follow terrestrial methods in which units are named after appropriate geographic terms (e.g., "Isidis unit").

Third, we group units within six geologic provinces that showcase distinct regions of geologic activity. Also, we have a grouping for widespread units. Our unit symbols include a province designator with a small capital letter, where applicable.

Fourth, we institute a novel unit coloring approach, following a rainbow color scheme to represent age. Thus, Noachian and Early Hesperian units are magentas and purples, Late Hesperian materials are blues, Early Amazonian units are greens and yellows, Middle Amazonian units are oranges, and Late Amazonian units are reds.

Fifth, we attempt to more carefully define and map contact types using *certain, approximate, gradational, inferred,* and *inferred approximate* geologic contacts. These delineations are described in more detail in [5].

Our mapping was also enhanced by using Geographic Information Systems (GIS) software and adaptive mapping tools. These tools included stream digitizing using on-screen and separate drafting tablets over spatially co-registered MOLA and image data sets. Thematic maps, including median high-pass filter MOLA elevation data (i.e., the "detrended" maps of [6]) and other products contributed greatly to the identification and delineation of geomorphic features.

Results. We have identified 41 map units of which 34 fully or mostly postdate the Early Hespe-

rian (Figures 1 and 2). Cumulative crater densities for craters >5 and 16 km diameters have been compiled for each unit based on the crater database of N.G. Barlow (which is presently undergoing revision). We also have mapped wrinkle ridges (subdivided into symmetric, asymmetric, and subdued categories), scarps (including lobate, fault, depression, and channel types), channels, and lineaments. Stipple patterns have been designated to show polar residual ice, polygonal trough terrain, and thumbprint terrain.

Our mapping reveals some significant differences with previous mapping and stratigraphic studies, as follows:

Noachian. Applying our approach to unit definitions, we are conservative in delineating Noachian materials. The Libya unit comprises mainly Early Noachian massif-forming materials embayed by the Middle and Late Noachian Noachis unit that covers most of the ancient cratered highlands. Noachian material is inferred to make up the base of the Lunae unit layered sequence of lavas.

Hesperian. The Early Hesperian includes lavas of the Lunae and Amenthes units and mass-wasted and other plains-forming materials along the base of the highland/lowland boundary (HLB) [7]. The latter activity resulted in the knobby terrains along the HLB. Also, larger outcrops of crater ejecta and fill of Early Hesperian and younger age are mapped.

The Late Hesperian includes emplacement of volcanic flows on the northern part of Alba Patera, in Arcadia and southern Amazonis Planitiae, and on the Elysium rise. Mass-wasting, collapse, and other processes formed plains materials mostly lower in elevation than earlier plains deposits along the HLB [7], including the deposits flooring the fretted terrain of the Deuteronilus Mensae region. Within Xanthe Terra, early chaos development and outflow channeling occurred.

Amazonian. The Early Amazonian was the most intense period of activity in the map region. We redefine the base of the Amazonian based on the formation of the Vastitas Borealis materials, which include marginal (smooth with lobate margins and sinuous, medially ridged troughs; N(5)~64±5) and interior (thumbprint ridges, pitted cones, and polygonal troughs; N(5)~74±2) facies. These materials define a continuous deposit having a margin at nearly constant elevation (about -3800 m) and interpreted to be deposited in an ancient ocean [8-9]. The units embay materials deposited within the Chryse Planitia channel floors of Kasei, Maja, Simud/Tiu, and Ares Valles; potentially, the channel deposits are coeval with the Vastitas units as commonly thought [8-9], although this cannot be demonstrated stratigraphically [e.g., 7]. Some chaos development in Xanthe Terra probably ensued after channel dissection. Lavas were emplaced within Marte Vallis. Volcanism associated with Elysium Fossae troughs produced a broad field of lavas and dissected, lobate flows that may include lahars and ashflows covering eastern and central Utopia Planitia [10-11]. Although Syrtis Major Planum is predominantly Early Hesperian [12], the flows on the eastern flank in the map area have an Early Amazonian crater density. In the polar region, the Scandia unit includes domes and irregular mounds and depressions interpreted as mud volcanoes [7] or glacial features [13]. Also, dark, irregularly layered basal material of Planum Boreum, possibly a buried sand sea [14], was deposited.

The Middle Amazonian includes a deposit within Isidis Planitia remarkably similar to the trough, thumbprint ridge, and pitted cone morphologies of the Vastitas Borealis units, but much younger (N(5)~22±4). A possible channel connects the Isidis and Vastitas Borealis units and some of the pitted cones of the Isidis unit occur along cracks in Syrtis Major flows. Flows were emplaced separately in northern and southern Amazonis Planitia and much of the Medusae unit was emplaced at this time.

Finally, the Middle to Late Amazonian includes emplacement of a field of flows in southeastern Amazonis Planitia and the Olympus Mons aureoles, which partly cover the flows. In turn, younger deposits of the Medusae unit cover these units. In the Deuteronilus region, large debris aprons had been developing along the walls of large mesas, perhaps since much earlier times. A degraded mantle also overlies part of northwestern Utopia Planitia.

The very youngest materials in the map region include an extremely flat deposit in central Amazonis Planitia that may be the sediments of Marte Vallis dissection [15]. These are overlain by flows erupted from Cerberus Fossae that infill Marte Vallis and spread out part way into Amazonis

Planitia. In the polar region, Planum Boreum and surrounding plains were covered by thick sequences of layered deposits. These deposits were eroded back and partly covered by dunes.

References: [1] V.L. Hansen, EPSL 176, 527-542, 2000. [2] K.L. Tanaka et al., in Mars (H.H. Kieffer et al., eds.) UA Press, Tucson, p. 345-382, 1992. [3] North American Commission on Stratigraphic Nomenclature, AAPG Bull. 67, 84-875, 1983. [4] International Subcommission on Stratigraphic Classification of IUGS International Commission on Stratigraphy, International Stratigraphic Guide, GSA, Boulder, 214 p., 1994. [5] K. L. Tanaka and J.A Skinner, Mars 6 abs. #3129, 2003. [6] J.W. Head III et al., JGR 107, 10.1029/2000JE001445, 2002. [7] K.L. Tanaka et al., JGR 108, 10.1029/2002JE001908, 2003. [8] T.J. Parker et al., Icarus 82, 111-145, 1989. [9] V.R. Baker et al., Nature 352, 589-594, 1991. [10] E.H. Christiansen, Geology 17, 203-206, 1989. [11] K.L. Tanaka et al., USGS Map I-2147, 1992. [12] K.L. Tanaka, JGR 91, suppl., E139-E158, 1986 [13] K.E. Fishbaugh and J.W. Head III, JGR 105, 22,455-22,486, 2000. [14] S. Byrne and B.C. Murray, JGR 107, 10.1029/2001JE001615, 2002. [15] E.R. Fuller and J.W. Head III, JGR 107, 10.1029/2002E001842, 2002.

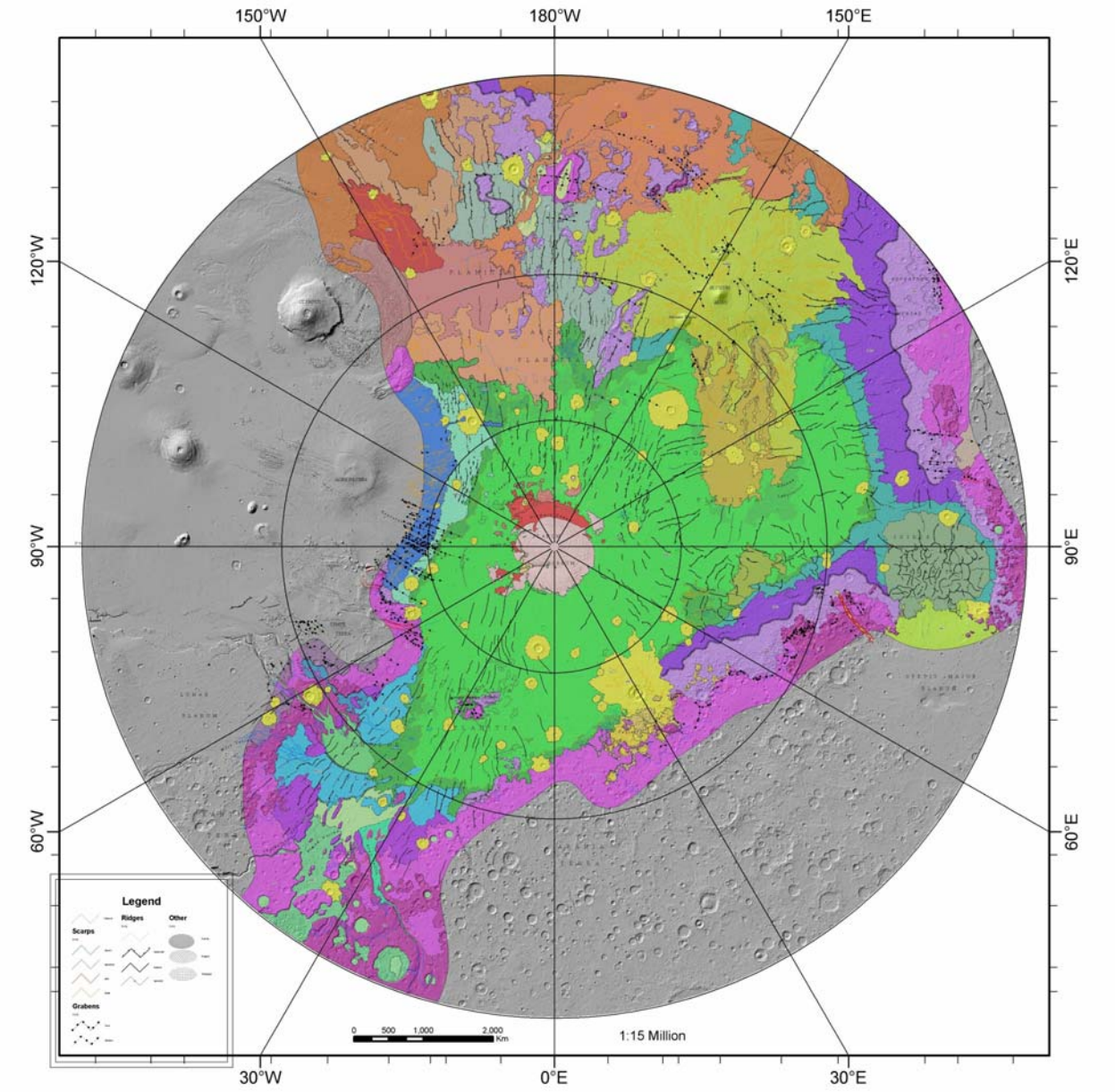

Figure 1. Geologic map of the northern plains of Mars.

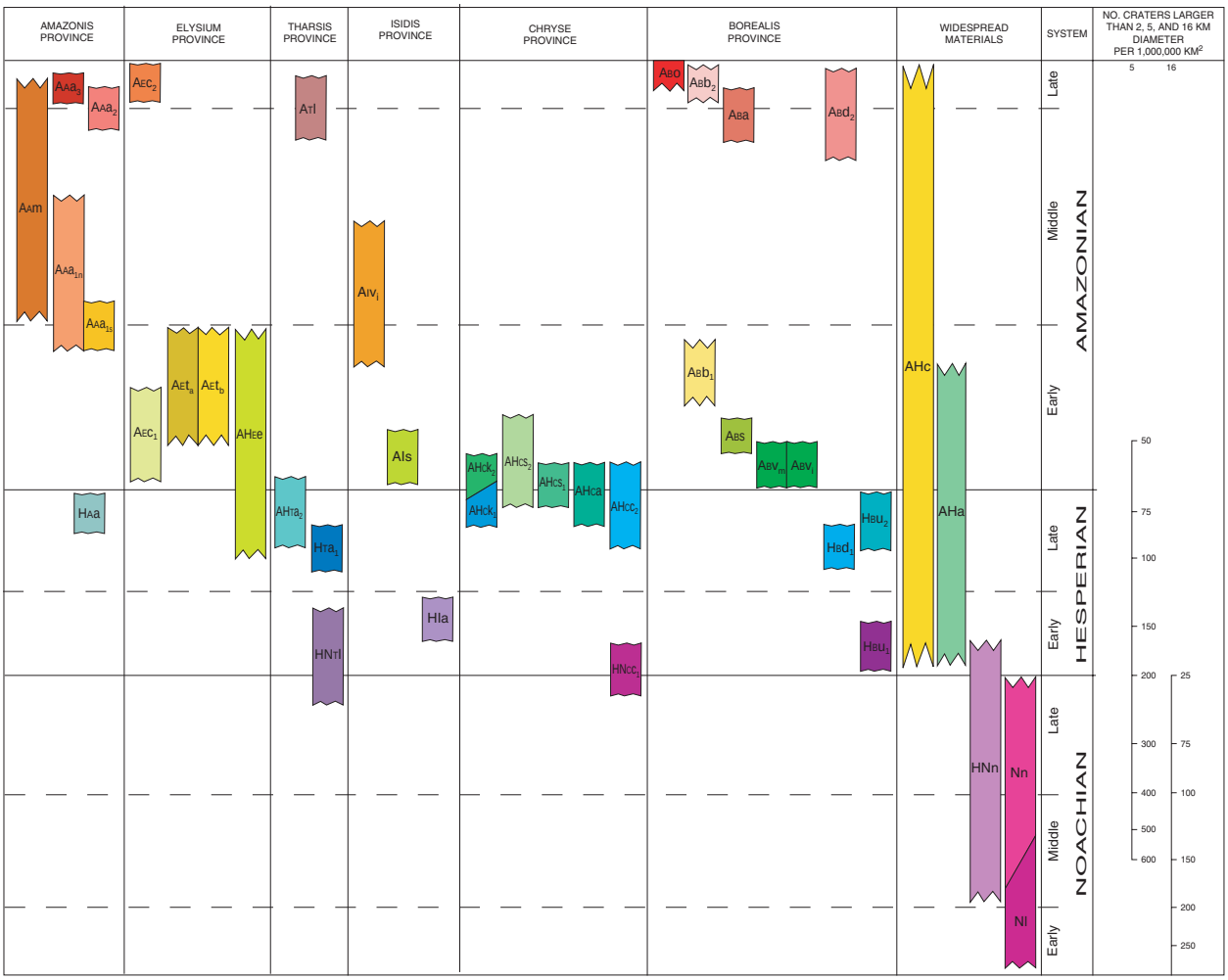

Figure 2. Correlation of map units in the northern plains of Mars.

GEOLOGIC EVOLUTION IN MARGARITIFER SINUS, MARS, AS REVEALED BY 1:500,000 GEOMORPHIC MAPPING

K.K. Williams[1] and J.A. Grant[1], [1]Center for Earth and Planetary Studies, National Air and Space Museum, Smithsonian Institution, Washington, DC 20013-7012, grantj@nasm.si.edu.

Introduction. Geologic mapping of portions of the Margaritifer Sinus region (0º-45º W, 0º-30º S) [1-3] at 1:500,000 continues (Figure 1). This work builds on neighboring mapping [4, 5], and includes definition of drainage basin morphology and hypsometry. Results indicate that the region has experienced an extended period of fluvial modification likely related to precipitation-recharged supply and limited runoff that was focused towards the Chryse trough [6, 7]. On the western flank of the trough, the Uzboi-Ladon-Margaritifer (ULM) system flows northward, draining 11 X 10^6 km^2 or ~9% of Mars [6]. The ULM outflow system incised and infilled the terrain as it crossed relief associated with ancient multi-ringed impact basins [7, 8]. The signature of the ULM drainage system on topography is pronounced in MOLA data of the region (Figure 1). By contrast, the valley systems of Samara and Paraná-Loire Valles on the eastern flank of the trough are two of the best integrated valley systems on Mars [1]. They drain more than 540,000 km^2, or ~0.5% of Mars. All drainages within Margaritifer Sinus were active from the Late Noachian to the Mid-Hesperian, and resulted in storage and subsequent release of water from Margaritifer basin at the head of Ares Vallis [2] (Figure 1).

Nearly completed mapping of MTM -20012 and -25012 quadrangles (Figure 2) [3] covers much of Paraná Valles, the depositional Paraná basin, and the head of the NW-flowing Loire Valles. Results here are for mapping in MTM quadrangles -10022 and -15022. These two quadrangles include the confluence plain formed by the Samara and Loire Valles and the valles southwest of Margaritifer basin, an area that has been greatly modified by erosion and deposition caused by multiple episodes of water transport [3, 6, 7].

Geologic History of Margaritifer Sinus. The geologic history of this region was discussed by [1-3] and is summarized here. Previous mapping at 1:2M and 1:500K [2, 4, 5] determined that the Ladon and Holden impact basins [7, 8] are the oldest features in Margaritifer Sinus. Three subsequent resurfacing events in the Noachian deposited competent materials that may be

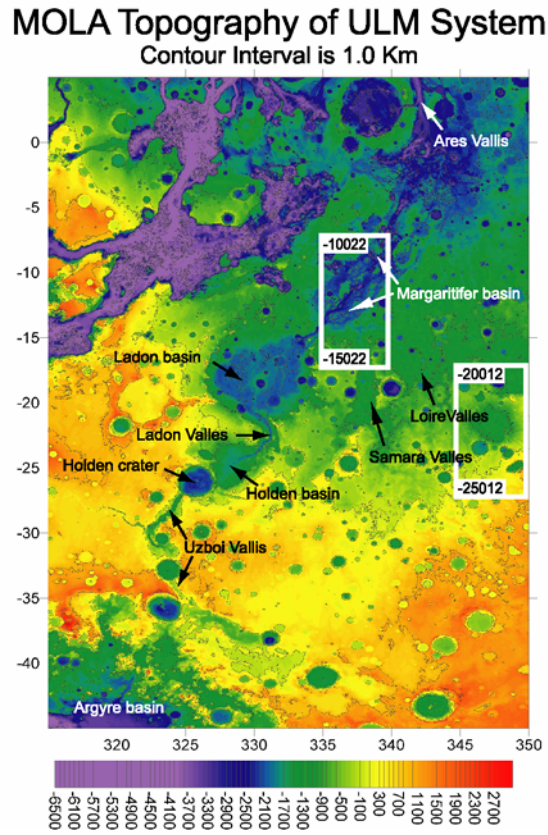

Figure 1. MOLA topography of Margaritifer Sinus. White boxes show areas being mapped. The area covered by MTM quadrangles -10022 and -15022 (upper left box) contains Margaritifer basin. (from Fig. 1 in [9])

volcanic or of alternate origin [3]. During the Late Noachian and the Early Hesperian, segments of the ULM system and other valleys in the area were incised and low-lying areas were infilled. The channel and valley formation in Margaritifer Sinus was concurrent with increased geomorphic activity elsewhere on Mars [1-3, 10]. Later, in the Early to Mid-Hesperian (N5 ages of 200 to 70), a localized resurfacing event emplaced material that embays all valleys and channels (Figure 2).

Margaritifer basin is included in MTM quadrangles -10022 and -15022, which form the centerpiece of the ongoing mapping. Within the basin, smooth plains embay most adjacent surfaces and higher areas of older terrain.

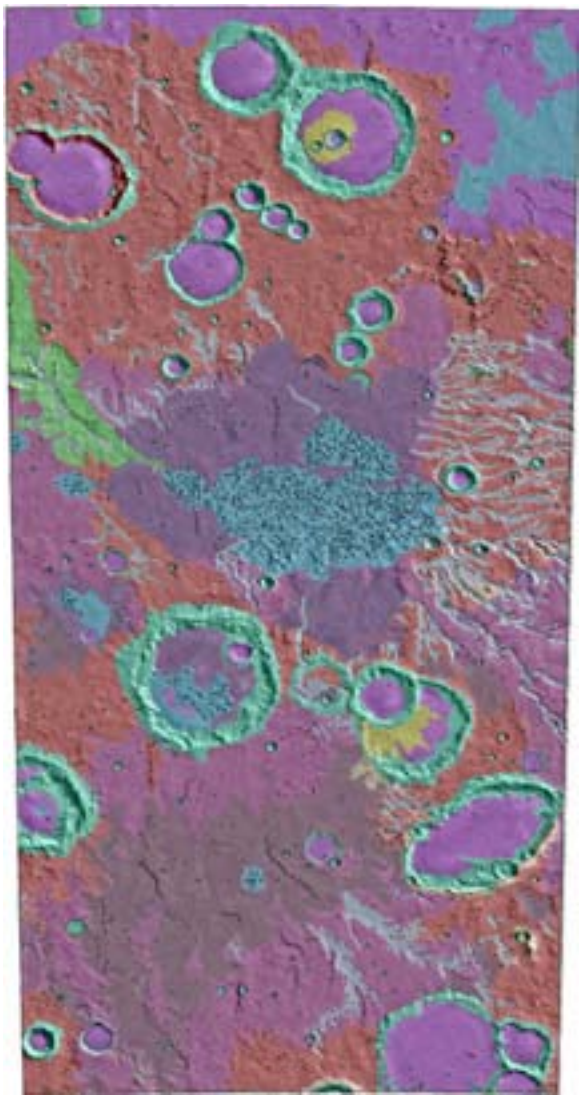

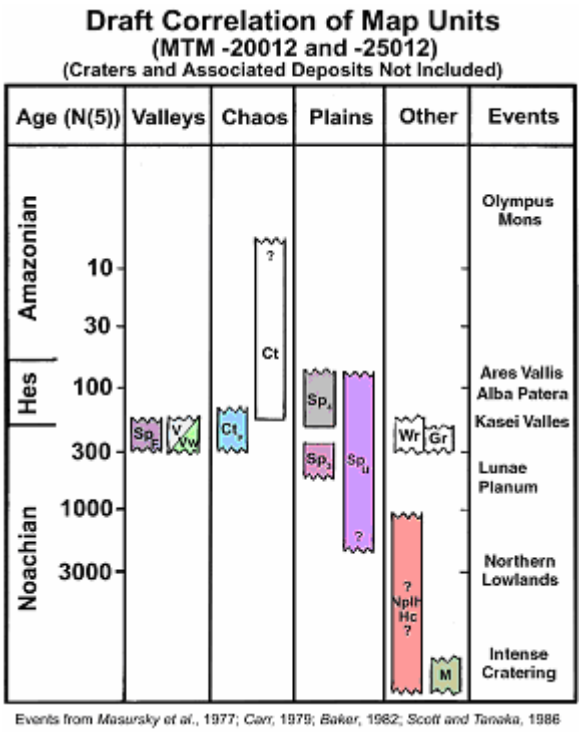

Figure 2. Preliminary map (left) of MTM-20012 and -25012 quadrangles [3]. North is to the top. Correlation of map units (above) is modified from figures in [1] and [2]. Map and correlation of map units do not yet incorporate standard symbols or colors.

These older terrains were emplaced earlier, have since been eroded by subsequent fluvial activity, and are now embayed by younger deposits. The northeastern portion of the basin is disrupted by collapse features associated with Margaritifer and Iani Chaos. Margaritifer basin may have been the location of considerable ponding, subsurface infiltration, and storage of water [2]. Release of this stored water likely resulted in formation of Margaritifer and Iani Chaos and incisement of Ares Vallis to the north. The Margaritifer Sinus region records a long history of repeated water collection, transport, storage, and discharge starting with incisement of the Ladon and Holden impact basins and ending in formation of Ares Vallis.

Mapping of MTM-10022 and -15022. Most surface features within these two quadrangles are the result of erosion or deposition due to water. Figure 3 is a Viking MDIM2 mosaic showing this area. Poor resolution (~250 m/pixel) coverage of the southern third of Figure 3 masks contacts between depositional and erosional surface units. Coverage in these two quadrangles by Mars Orbiter Camera (MOC) Narrow Angle and Wide Angle and THEMIS images is fairly dense within Margaritifer basin and the area north of there, but coverage is sparse south of Margaritifer basin.

Interestingly, although image resolution in the southern third of Figure 3 complicates mapping, MOLA topography reveals important information about the courses of Samara and Loire Valles. Figure 4 is a perspective view of MOLA data looking north over the area in Figure 3. Margaritifer basin is prominent as the wide, green area in the center. The low chaos regions are shown in dark blue, and a regional decrease in elevation from south to north is apparent. The orange area in Figure 4 marks the course of Samara Valles, whereas Loire Valles emerges from the east and joins Samara Valles prior to emptying into Margaritifer basin. A late stage

water transport and resurfacing event took place through Margaritifer basin and is defined by the youngest (lowest) channel of the basin. This channel is interrupted by collapse associated with local chaos (7.5 S, 22.5 W) near the center of Figure 3. Continued mapping in this area seeks to refine the sequence of transport, ponding, and discharge in the area of Margaritifer basin as related to other regional geologic events.

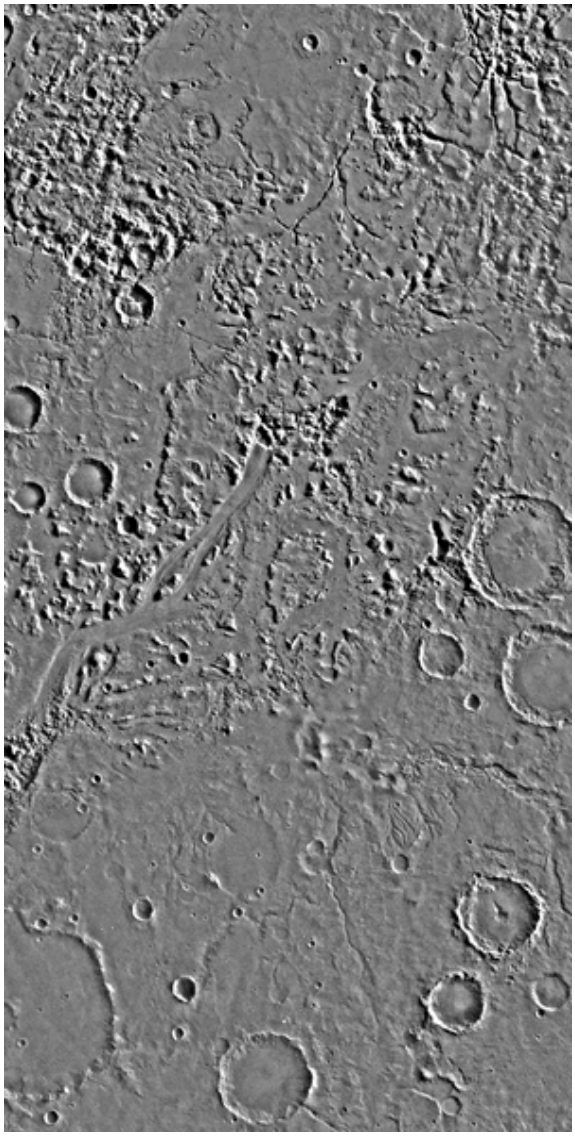

Figure 3. Viking image mosaic of MTM -10022 and -15022 quadrangles. Margaritifer basin runs SW-NE though the center of the image.

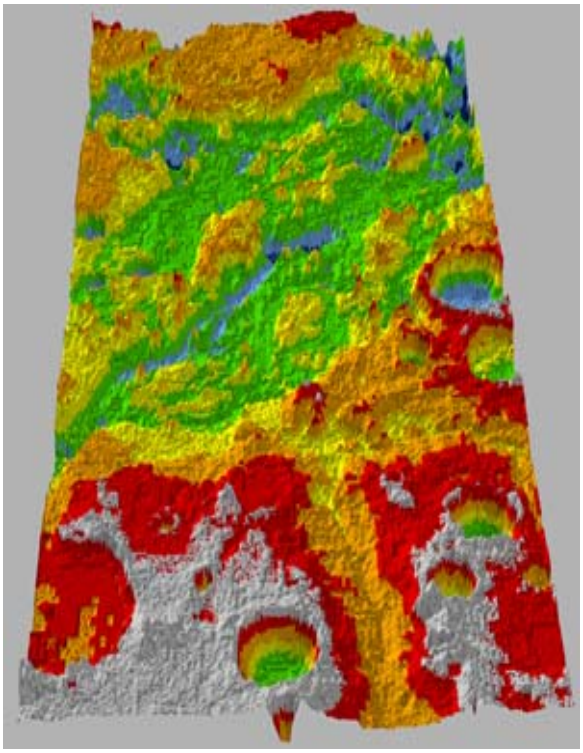

Figure 4. North-looking perspective of MOLA topography in the area covered in Figure 3. Note Samara Valles running from the south and intersecting Loire Valles before both meet Margaritifer basin. Blue colors are low elevation and reds and grays are high.

References. [1] Grant, J.A. (2000) Geology, 28, 223-226. [2] Grant, J.A. and T.J. Parker (2002) JGR, 107(E9), 5066. [3] Grant, J.A. and D.A. Clark (2002) Planetary Mappers Meeting (abstract). [4] Parker, T.J. (1985) Master's Thesis, California State Univ., LA, 165. [5] Parker, T.J. (1994) Ph.D. Thesis, USC, LA. [6] Banerdt, W.B. (2000) Eos, 81, P52C-04. [7] Saunders, S.R. (1979) USGS I-1144, USGS. [8] Schultz, P.H. et al. (1982) JGR, 87, 9803-9820. [9] Grant, J.A. and T.J. Parker (2002) LPSC XXXIII. [10] Scott, D.H. and K.L. Tanaka (1986) USGS Misc. Inv. Series Map I-1802-A, USGS.

GEOLOGIC MAPPING OF MARS (EASTERN PORTION OF THE MEDUSAE FOSSAE FORMATION) AND VENUS (V15 QUADRANGLE - BELLONA FOSSAE). James R. Zimbelman, CEPS/NASM MRC 315, Smithsonian Institution, Washington, D.C. 20013-7012; jrz@nasm.si.edu.

Introduction: This report summarizes results obtained for mapping projects supported by NASA PG&G grant NAG5-11743. The grant identifies topical problems for both Mars and Venus, with science objectives that make use of geological mapping results. This report gives results presented at the 2003 Mappers meeting held at Brown Universitry in June, 2003.

Mars Mapping: Geologic mapping of the Medusae Fossae Formation (MFF) on Mars is being carried out in support of a science objective to identify and interpret the stratigraphic relationships within and around both eastern and western exposures of MFF near the equator of Mars, for use in evaluating specific hypotheses of origin for these unusual materials. Two Mars Transverse Mercator (MTM) quadrangles were mapped previously at 1:500,000 scale and combined for eventual publication at 1:1M scale on a single map sheet. This mapping effort identified three subdivisions within both the upper (Amu) and middle (Amm) members of MFF, with clear stratigraphic contact relationships at several places within the map area. Results from the detailed mapping were extended to a regional view through geologic mapping at 1:2M scale, which will be published at 1:4M scale (Fig. 1). The three subdivisions of both the upper and middle members can be traced across much of the eastern portion of MFF. The regional mapping was aided greatly by topographic data obtained from the Mars Orbiter Laser Altimeter (MOLA) through collaborators H. Frey and S. Sakimoto. The MOLA data led directly to the identification of an exhumed channel below unit Amm_1 [1], that appears to be part of a collection of outflow features northwest of the Tharsis region [2]. Efforts are still underway to compile "truth tables" for the numerous published hypotheses of origin for MFF [see 3], based on both the observed properties of the Martian materials and literature about terrestrial examples of the proposed mechanisms of origin. Assessments to date indicate that both the ignimbrite [4-6] and the aeolian materials [5, 7-9] hypotheses are the most viable alternatives with regard to the new data sets from Mars Global Surveyor (MGS). THEMIS infrared imaging data are showing layering within the MFF units as revealed by changes in the thermal properties of the exposed materials (Fig. 2). Following submission of the combined MTM 05142 and 00142 maps and the eastern regional map, work will begin on a western regional map covering MC-15SE and MC-23NE (15° N to 15° S, 180° to 202.5° W). Daytime THEMIS images will likely provide important new insights for the regional mapping; Kelly Bender (ASU) is collaborating with the PI in this effort.

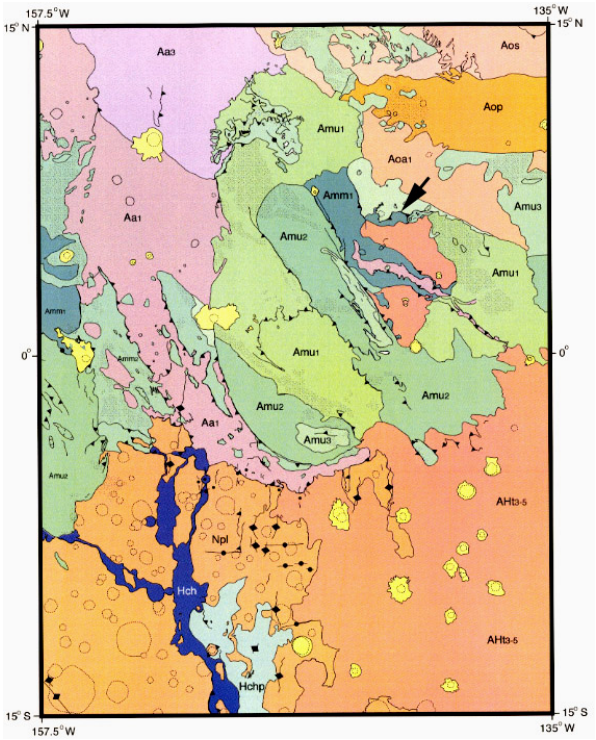

Figure 1. Regional geologic map of the eastern portion of MFF, corresponding to MC-8SE (top) and MC-16NE (bottom). Mapping was carried out at 1:2M scale, to be published at 1:4M scale. Arrow shows approximate location of Figure 2.

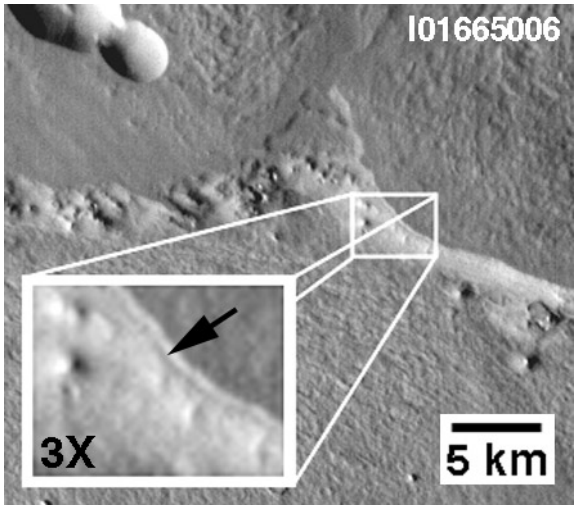

Figure 2. Portion of THEMIS image I01665006, daytime thermal infrared. A cliff of Amm_3 unit shows a darker (cooler) layer (inset, arrow), implying the materials are more compacted than the rest of the unit. Daytime THEMIS images hold great potential for revealing many important new details in MFF.

Venus Mapping: Venus mapping efforts are in support of the science objective of identifying and interpreting stratigraphic relationships in the northern lowland plains of Venus, to provide constraints on global resurfacing models. Geologic mapping of the Kawelu Planitia (V16) quadrangle on Venus is now complete, compiled at a scale of 1:5M based on mapping at FMAP scale that preserves the full resolution of the Magellan SAR data. A revised version of the V16 map will be submitted soon; no unit boundaries changed on the map, but the correlation chart underwent considerable change following discussion at recent Mappers meetings. Detailed stratigraphic information was extracted from the V16 map for lobate plains flow units around the Sekmet Mons volcano, which provides new insights into the possible resurfacing of the northern lowland plains; this work is described in a manuscript that is now in press in JGR-Planets [10]. Experience gained in revising the V16 map was crucial to carrying out mapping of the Bellona Fossae (V15) quadrangle.

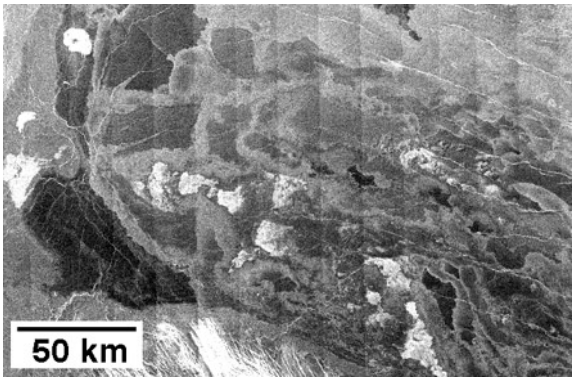

Figure 3. Fea Fossae lava flows, part of a recent study of fifteen lava flows on five planets [11, 12]. Portion of Magellan SAR mosaic, centered on 29°N, 216°E.

Fewer stratigraphic relationships are evident among the lobate plains in V15 than were observed in V16, but local volcanic centers do display a sequence of volcanic flows (Fig. 3; 11, 12). The stratigraphic information is represented in the correlation chart for the V15 map (Fig. 4), which also illustrates the style of correlation chart derived for the revised V16 map. Regional plains, lacking distinctive attributes in the Magellan SAR data or other remote sensing data sets, are abundant in both the V15 and V16 quads. However, at present there is no way to verify (or to test) that the regional plains are the same materials within each quad, let alone across the adjacent quads. The correlation chart is a compromise in an attempt to portray stratigraphic information that is consistent within a given quad, but also to show readers the considerable uncertainty associated with each unit. An outcome of the 2002 Mappers meeting was a decision

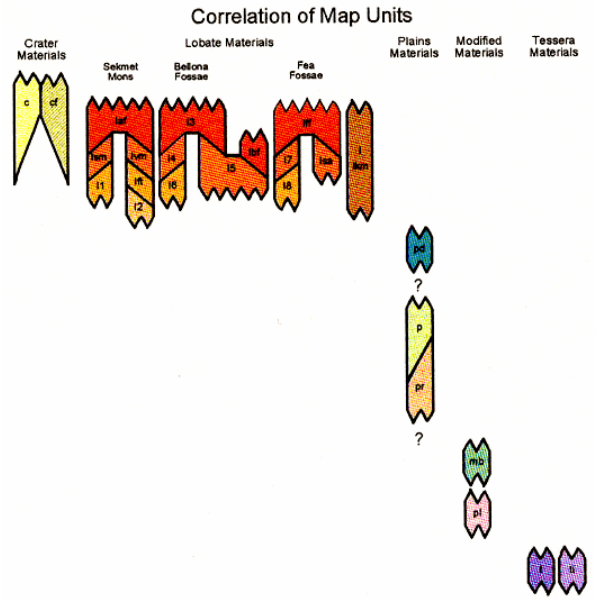

Figure 4. Relative stratigraphy of geologic units in the V15 map. Hachured lines indicate uncertainty in vertical extent of unit, but relative vertical position is consistent with mapped relationships. Sloping lines indicate time-transgressive contact between units.

to attempt to clarify what each mapper intends to show by their correlation charts. The GEMS working group will coordinate the compilation of the correlation chart information, in order to provide better understanding (if not uniformity) between charts of different maps.

References: [1] J.R. Zimbelman et al., Geol. Soc. Am. Abs. Prog., 32(7), A303, 2000. [2] J.M. Dohm et al., JGR-Planets, 106(E6), 12301-12314, 2001. [3] J.R. Zimbelman et al., LPS XXX, Abs. #1652, LPI (CD-ROM), 1999. [4] Scott, D.H., and K.L. Tanaka, JGR, 87, 1179-1190, 1982. [5] Scott, D.H., and K.L. Tanaka, U.S.G.S. Misc. Invest. Series Map I-1802-A, 1986. [6] M.G. Chapman et al., U.S.G.S. Misc. Invest. Series Map I-1962, 1989. [7] Ward, A.W., JGR, 84, 8147-8166, 1979. [8] Carr, M.H., Water on Mars, pp. 133-6, Oxford Univ. Press, New York, 1996. [9] Wells, G.L., and J.R. Zimbelman, Arid Zone Geomophology, 2nd ed. (D.S.G. Thomas, Ed.), pp. 659-690, Wiley & Sons, New York, 1997. [10] Zimbelman, J.R., Flow field stratigraphy surrounding Sekmet Mons volcano, Kawelu Planitia, Venus, in press in JGR-Planets. [11] J.R. Zimbelman et al., Eos, Trans. AGU, 83(47), Abstract P71B-0457, F831, 2002. [12] M.N. Peitersen et al., Eos, Trans. AGU, 83(47), Abstract P71B-0458, F831, 2002.

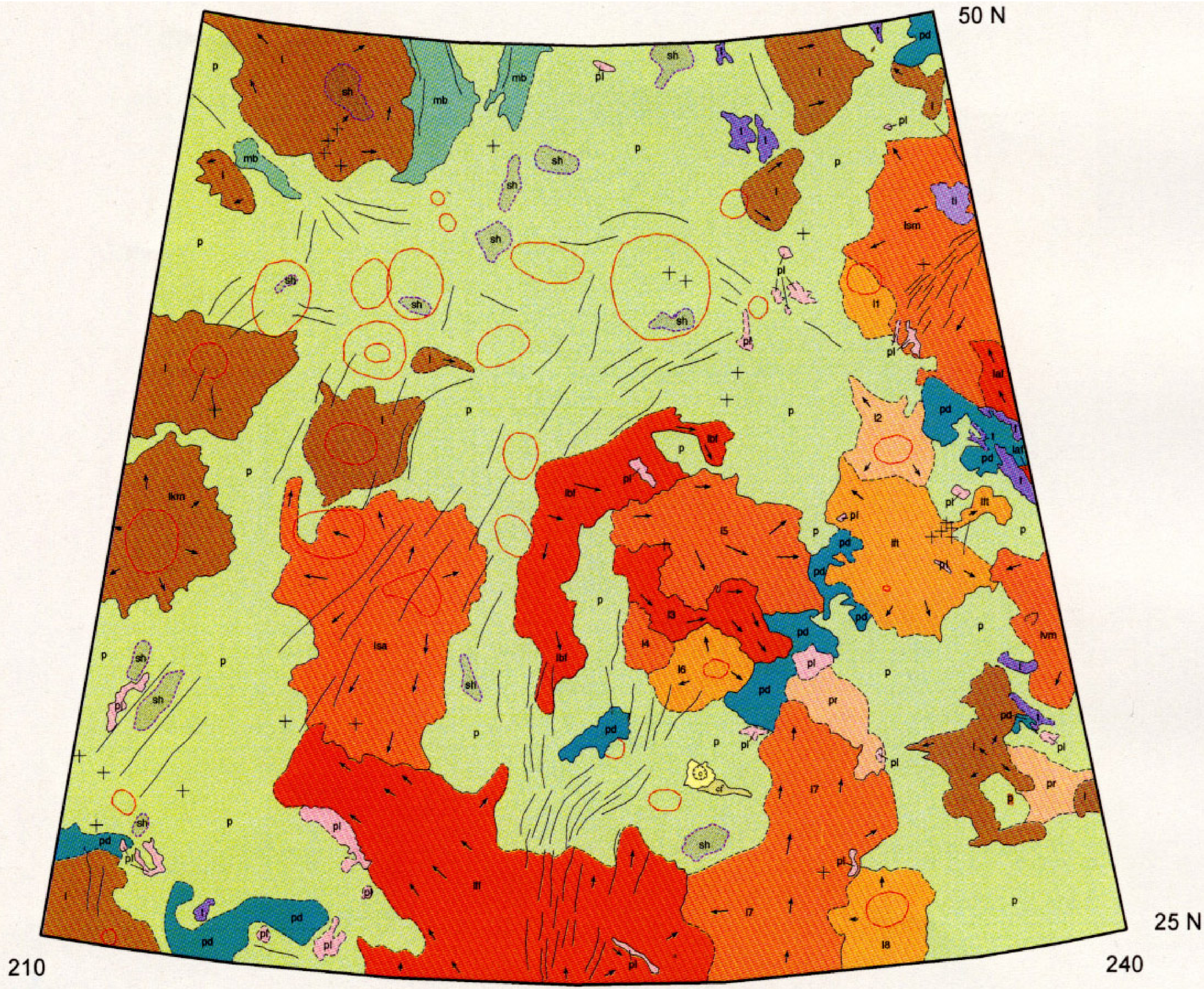
50 N
25 N
210
240

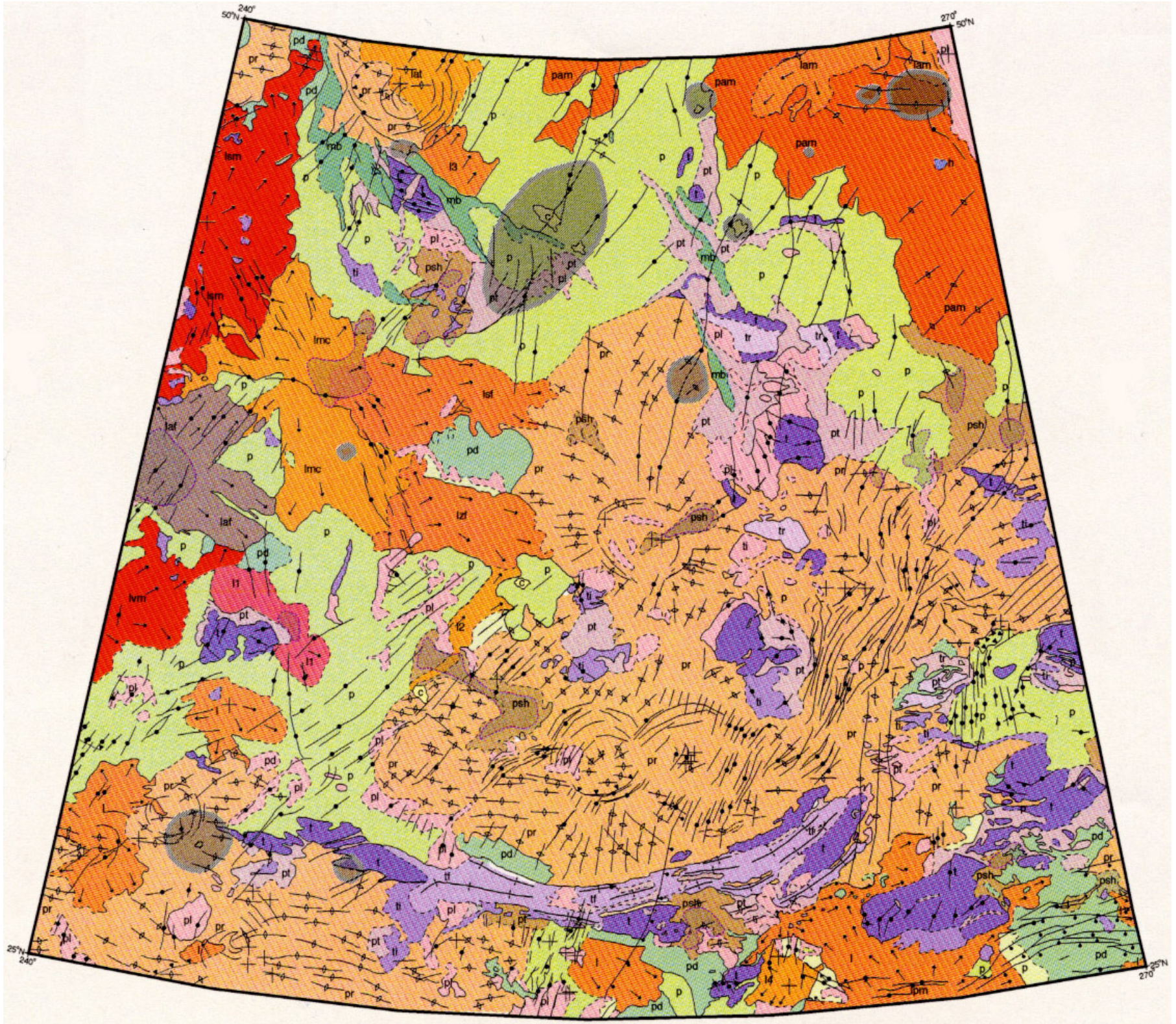
240°
50°N
270°
50°N
25°N
240°
270°
25°N
pd
pr
lat
pam
lam
pl
lsm
mb
l3
pt
p
h
psh
ti
lmc
lsf
tr
lzf
lvm
l1
l2
l4
lpm

CHARACTERIZATION OF VENUS MIDLANDS (V57 FREDEGONDE, AND V3 MESKHENT TESSERA QUADRANGLES) AND DEVELOPING CRITERIA TO TEST GEOLOGICAL HISTORY MODELS: J. W. Head[1] and M.A. Ivanov[1,2]; [1]Dept. of Geological Sciences, Brown University, Providence, RI 02912 USA, [2]Vernadsky Institute, RAS, Moscow, Russia.

Introduction: The first-order global topography of Venus revealed by Magellan [1] is composed of three major components: 1) lowlands (<0 km, ~11% of Venus) forming circular and elongated basins, 2) highlands (>2 km, ~9% of Venus) composed primarily of steep-sided plateaus, and 3) midlands (0-2 km, ~80% of Venus, rolling plains [2]) that lie between basin and highland margins. The midlands are the location of a wide variety of features and structures including coronae, novae, rift zones, ridge and fracture belts, and extensive volcanic plains. This distribution of topography raises some fundamental questions. How and when did the major components of Venus topography form? How do the specific features of the midlands relate in time and space to the lowlands and highlands? What are the implications for the geologic history of Venus?

There are two proposed end-member models for the correlation of regionally observed sequences of units. In the first, the sequences in different regions appear to be repetitive [3,4]. The individual units are thus considered to be broadly time correlative rather than time transgressive. This has been termed a "directional" (implying a specific set of global trends in the evolution of Venus), or a "synchronous" model (implying that the individual sequences of events are broadly synchronous globally). Alternatively, the observed sequence of units is interpreted to be due to specific volcano-tectonic regimes, similar to Wilson cycles on Earth, which occur at different times in different parts of the planet [5]. In this case, the local sequence of units represents only local or regional time-dependent sequential styles of endogenic activity. This has been termed a "non-directional" (implying that the individual sequences represent local conditions occurring at different times in different places), or a "diachronous" model (implying that the sequences of events are not synchronous globally).

The midlands characterize the majority of the surface of Venus and documentation of sequences of events among units and structures is thus very important to constrain the applicability of the models to the geologic history. As with the mapping of most planetary bodies [6-8], several different approaches have been employed to define and characterize geological units, to map structures, and to establish stratigraphic relationships, geological sequences and columns, and correlation charts [9-14]. One of our goals is to contribute to the discussion of these different approaches by continuing detailed mapping of the Venus midlands, employing different approaches and addressing how our results relate to the issues involved.

Midlands: Documentation of Key Features and Relations. The V57 Fredegonde quadrangle in the southern hemisphere and the V3 Meskhent Tessera quadrangle in the northern hemisphere (Figs. 1-3) contain the array of features necessary to characterize many aspects of the midlands and their transition to other topographic provinces.

The Fredegonde quadrangle (V-57) covers the transition from Lada Terra in the west to relatively small (several hundreds of km across) lowland basins in the east. The edge of Lada Terra is characterized by several large coronae interconnected by swarms of grooves that form large corona-groove chains extending for several thousands of kilometers. The chains resemble in many aspects the corona-rift zones at the margins of large equidimensional basins such as Lavinia (V55) and Atalanta (V4) Planitiae [15,16] and typically are accompanied by extensive young lava flows and prominent belts of linear deformation.

The mapping in this quadrangle offers the opportunity to characterize the transitional zones between midlands and lowlands and establish the sequence of events within the corona-groove zones and to assess the relative timing among them and other features, such as volcanic plains, ridge belts, and edifices. For instance, the preliminary first-order observation made during reconnaissance stage of mapping within the V-57 area is that vast regional plains embay ridge belts (Fig. 1a) whereas corona-groove zones appear to postdate the plains (Fig. 1b).

The Meskhent Tessera quadrangle (V3) connects large lowlands (Atalanta Planitia to the east) and highlands (Ishtar Terra: Fortuna Tessera to NW and Dekla Tessera to SW). Prominent belts of grooves and ridges characterize the elongated lowland between Fortuna and Dekla Tesserae. Dekla Tesserae connect two large tessera regions, Tellus and Laima Tesserae. Meskhent Tessera dominates the NE portion of the quadrangle (Tethus Regio) and several small elongated and equidimensional lowlands occupy the central portion of the area. The eastern portion of Ishtar Terra and Tethus Regio are separated by local lowland occupied by Tusholi Corona. In the east-central part of the area, Fakahotu Corona appears to be at the western end of a chain of coronae interconnected by belts of fractures and graben. The chain makes a large arc that runs along the western edge of Atalanta Planitia. There is evidence for tectonic activity at Fakahotu that predates regional plains (Fig. 2a) and for young volcanic flows that are superposed on regional plains (Fig. 2b).

The V3 quadrangle displays a rich array of features typical of the transition to both lowland basins and the highlands. The major goals of mapping in the Meskhent Tessera quadrangle are as follows. 1) Document types of units and structures. 2) Establish the sequence of events among them. 3) Assess the relative timing of formation of the main topographic features. 4) Assess the importance of the corona-fracture chain at the western edge of the

Atalanta basin. 5) Characterize the transitional zones between midlands to lowlands and midlands to highlands.

References: 1) Ford, P.G. and G.H. Pettengill, *JGR*, 97, 13103, 1992; 2) Masursky, H.et al., *JGR*, 85, 8232, 1980; 3) Basilevsky, A.T. and J.W. *JGR*, 105, 24583, 2000; 4) Ivanov, M.A. and J.W. Head, *JGR*, 106, 17515 2001a; 5) Guest, J.E., and E.R., *Icarus*, 139, 56, 1999; 6) Wilhelms, D.E., The geologic history of the Moon, *US Geol. Surv. Spec. Pap., 1348*, - p.302, 1987; 7) Wilhelms, D.E., Geologic mapping, *in: Planetary Mapping*, R. Greeley and R.M. Batson eds. 208, 1990; 8) Tanaka, K.L., USGS Open File Report 94-438, 50 p., 1994; 9) Senske, D.A. et al., *LPSC (Abstr.), XXV*, 1243, 1994; 10) Tanaka, K.L. et al., *in:* Venus II, Phillips et al., eds, 667, 1997; 11) Basilevsky, A.T. and J.W. Head, *EMP* 66, 285, 1995a; 12) Basilevsky, A.T. and J.W. Head, *PSS* 43, 1523, 1995b 13) Basilevsky, A.T. and J.W. Head, *JGR*, 103, 8531, 1998; 14) Hansen, V.L., *EPSL* 176, 527, 2000; 15) Ivanov, M. A. and J. W. Head, *USGS Geol. Inv. Ser., Map I-2684*, 2001; 16) Ivanov, M. A. and J. W. Head, *USGS Geol. Inv. Ser., Map I-2792*, 2003

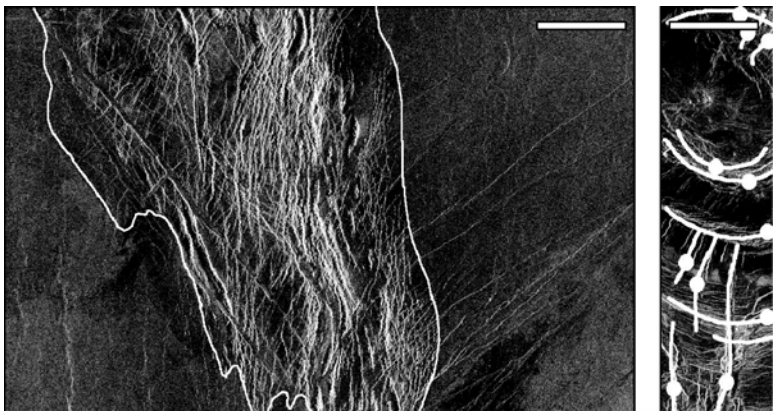

Figure 1. Fredegonde quadrangle (V-57). a) Regional plains embay the ridge belt of Oshumare Dorsa. b) Lava flows and graben at Dunne-Musun Corona postdate the background of regional plains. Scale bars are 50 km.

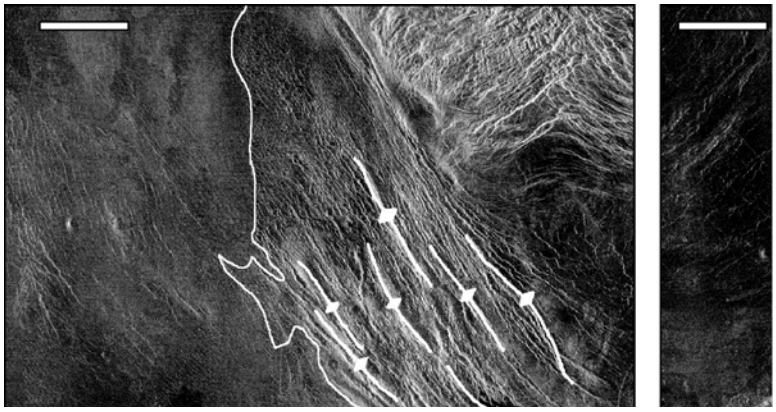

Figure 2. Meskhent Tessera (V-3) quadrangle. Regional plains embay tectonic structures at SW corner of Fakahotu Corona (a) and some lava flows at the NW flank of the corona (b) are superposed on regional plains. Scale bars are 50 km.

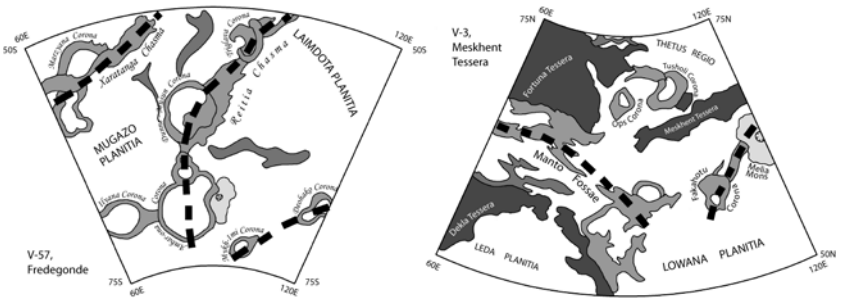

Figure 3. Geologic sketch maps of V57 (Fredegonde) and V3 (Meskhent Tessera) quadrangles. Thick dashed lines show the principal structural trends.

LAKSHMI PLANUM QUADRANGLE (V-7) VENUS. M. A. Ivanov[1,2] and J. W. Head[2]. [1]Vernadsky Institute, RAS, Moscow, Russia, mishaivn@mtu-net.ru, [2]Dept. of Geological Sciences, Brown University, Providence, RI, USA, james_head_iii@brown.edu.

Introduction. Lakshmi Planum dominates the western portion of Ishtar Terra and represents one of the most spectacular features on Venus [1]. Lakshmi Planum is a high-standing (about 3-4 km above MPR) plateau surrounded by the highest Venusian mountain ranges. The surface of the plateau is covered by morphologically smooth plains. Two distinctive volcanic centers, Colette and Sacajawea Paterae occur in the middle of the plains. The unusual characteristics of Lakshmi Planum have led to a variety of interpretations of its mode of origin ranging from hot spot to collision hypotheses [2,3 and reference therein]. The V-7 quadrangle portrays the planum itself and its surroundings (Fig. 1). The mapping in this area allows us to document specific features of Lakshmi Planum and establish the sequence of events in the formation and evolution of this major feature on Venus. As the first stage of our mapping project we undertook reconnaissance mapping within the V-7 quadrangle in order to outline the principal features in this area and develop a preliminary model of the sequence of events there.

Topographic and stratigraphic characteristics of major features within the V-7 Quadrangle. Lakshmi Planum, which is about 2000 km across, occupies the northern half of the V-7 quadrangle. A broad zone of complexly deformed terrain surrounds the roughly circular structure of Lakshmi Planum at intermediate elevation (Fig. 1). *Southern Border:* In the South, two major scarps, Vesta Rupes in the north and Ut Rupes to the south, define this zone. The major features of this transition zone are small fragments of tessera terrain (e. g. Clotho Tessera) and linear belts of grooves. The lava plains of the lowland of Sedna Planitia, the surface of which is topographically flat, broadly embay these terrains. The southeastern corner of the quadrangle is occupied by numerous lava flows of Neago Fluctūs. The flows emanate from Muta Mons at intermediate elevation and flow down toward the vast lowland of Sedna Planitia. The flows embay the terrains of the transition zone and the surface of Sedna Planitia as well. *Western Border:* In the West, the large Omosi-Mama Corona, which is the source of the apparently young Djata Fluctus, is the main feature of the transition zone. *Northwest, North and Northeast Borders:* Large tessera massifs, Atropos Tessera and Itzpapalotl Tessera (out of the V-7 area), make a giant arc that embraces Lakshmi Planum from the northwest, north, and northeast.

Mountain Belts. The most important features of Lakshmi Planum are mountain belts that make an almost complete zone outlining the relatively flat interior of the plateau (Fig. 1). The mountain range of Danu Montes borders the southern edge of the plateau. Danu Montes form a wide arc (about 1500 km long) the top of which rises about 1.5-2 km above the surface of Lakshmi Planum. The highest point of the Montes is around 335°E and the height of the range is lower toward the eastern and western edges. The southwestern sector of Lakshmi Planum between about 60-65°N shows little evidence for mountain belts but the western and northwestern edges of the Planum are bordered by the mountain range of Akna Montes. Akna Montes form a compact zone (about 1000 km long and 250 km wide) with the highest area between 65-70°N that stands about 3 km above the surface of Lakshmi Planum. The northern and partly northeastern edges of the Planum are bordered by Freyja Montes that stand about 3-3.5 km higher than the adjacent surface of Lakshmi. The mountain range of Freyja Montes consists of latitudinal and longitudinal branches. The first is short, wide (about 500 km long and 200-300 km wide), higher, and straight. The second is smaller in all respects and is slightly convex to Lakshmi Planum. These mountain ranges, as well as Maxwell Montes to the east (outside of V-7), consist of tightly packed elongated parallel ridges 5 to 10 km wide and resemble to some extent the common ridge belts elsewhere on Venus [4]. At the contacts with the interior plains of Lakshmi Planum, there is abundant evidence for embayment of the mountain by the plains. At the longitudinal branch of Freyja Montes, however, the interior plains appear to be slightly ridged, conformal to the strike of the mountain belt.

Interior Plains. The interior surface of Lakshmi Planum is generally flat, slightly tilted toward the south and lacks significant tectonic structures such as those that are very abundant at the edges and outside of the planum. The interior of Lakshmi displays three types of materials. The most widespread are plains with moderate and uniform radar albedo and deformed by a network of wrinkle ridges. Morphologically, these plains represent a complete analog to regional plains of Venus [5,6] that occur, in particular, on the surface of Sedna Planitia. Stratigraphically lower than the intra-Lakshmi regional plains are materials heavily deformed by tectonic structures. Although these materials are not in direct contact with the mountain ranges, within both Akna and Freyja Montes there are inclusions of similar materials embedded in the ridges of the mountain belts. Stratigraphically higher than the regional plains within Lakshmi are volcanic plains consisting of numerous radar brighter and darker flows that bear almost no tectonic deformation. The flows are clearly related to two major volcanic centers, Colette and Sacajawea Paterae, and are analogous to the youngest lava plains on Venus that surround distinct centers such as large volcanoes [7-10].

Sequence of events. Our first-order observations and preliminary mapping within the V-7 quadrangle are summarized as the following general sequence of events during the formation and evolution of Lakshmi Planum: 1) The oldest features within the area of our mapping appear to be the heavily tectonized materials that are embayed by the intra-Lakshmi regional plains. 2) The mountain belts and the transition zone of complexly deformed terrains around Lakshmi may be somewhat younger but very detailed mapping is necessary to establish an order of events between these features. 3) The mountains and the transition zone are embayed by vast regional plains both from inside (within Lakshmi Planum) and outside (in Sedna Planitia). Neither in Lakshmi Planum nor outside is there direct evidence for the sources of these plains. 4) The latest activity within the area under study was volcanism at several distinct centers that produced the lava flows of Neago Fluctūs and Djata Fluctus to the southeast and west of Lakshmi and around Colette and Sacajawea Paterae within the Planum.

References. 1) Barsukov, V.L., et al., *JGR*, 91, D399-D411, 1986, 2) Kaula, W.M., et al., *JGR*, 97, 16085-16120, 1992, 3) Kaula, W.M., et al., Ishtar Terra *in: Venus II Geology, Geophysics, Atmosphere, and Solar wind environment, S.W.Bougher, D.M. Hunten, and R.J. Phillips eds., Univ. Arizona Press Tucson,* 789-900, 1997, 4) Banerdt W.B., et al., Plains tectonics on Venus *in: Venus II Geology, Geophysics, Atmosphere, and Solar wind environment, S.W.Bougher, D.M. Hunten, and R.J. Phillips eds., Univ. Arizona Press Tucson*, 901-930, 1997, 5) Head, J.W. and A.T. Basilevsky, *Geology*, 26, 35-38, 1998, 6) Basilevsky, A.T. and J.W. Head, *JGR*, 103, 8531-8544, 1998, 7) Price, M., , et al., *JGR*, 101, 4657-4671, 1996, 8) Namiki, N. and S.C. Solomon, *Science*, 265, 929-933, 1994, 9) Ivanov, M. A. and J. W. Head, *JGR*, 106, 17515-17566, 2001, 10) Ivanov, M. A. and J. W. Head, Geologic map of the Lavinia Planitia (V55) quadrangle *USGS Geol. Inv. Ser., Map I-2684* 2001.

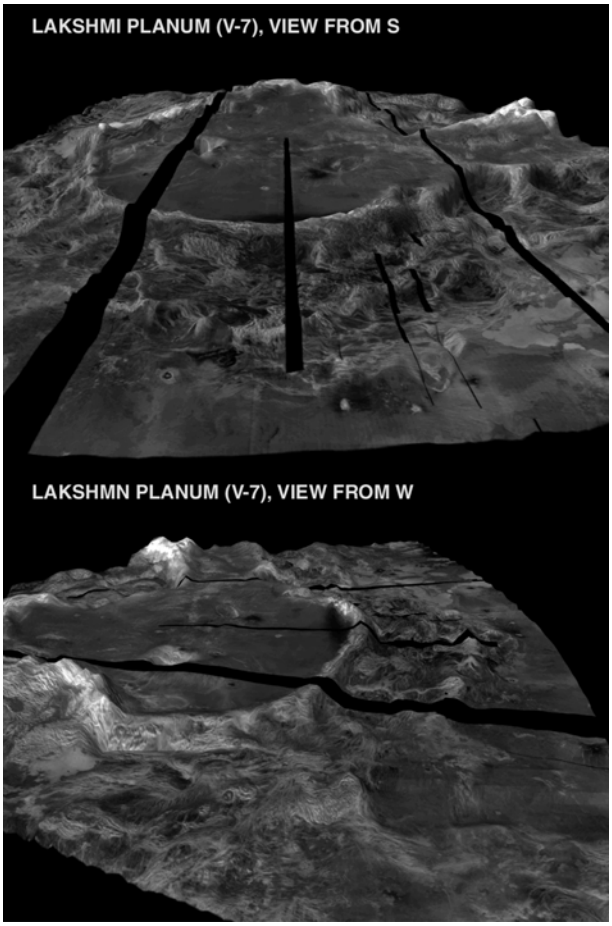

Figure 1. Two perspective views of Lakshmi Planum and its surroundings within the V-7 area. Vertical exaggeration is about 1:50.

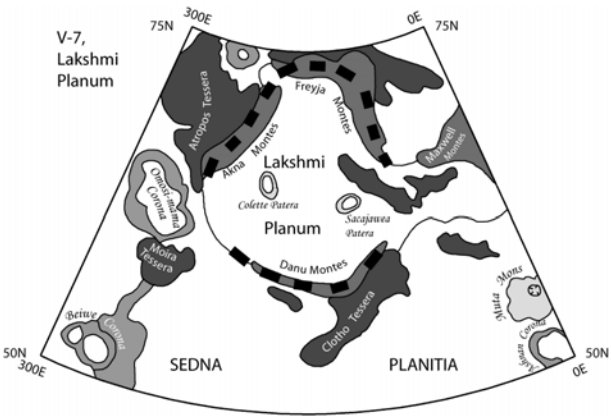

Figure 2. Sketch map of the Lakshmi Planum (V7) quadrangle. Thick dashed lines indicate the principal structural trends.

RESULTS FROM ONGOING MAPPING OF THE NEMESIS TESSERAE (V14) QUADRANGLE, VENUS.

Eric B. Grosfils, Geology Department, Pomona College, Claremont, CA 91711 (egrosfils@pomona.edu).

Introduction: The Nemesis Tesserae quadrangle (25-50°N, 180-210°E) is located within Ganiki Planitia, north of Atla Regio, south of Vinmara Planitia, and southeast of Atalanta Plantia. The region contains a diverse array of volcanic-, tectonic- and impact-derived features, and the objectives for the ongoing mapping effort are fivefold: 1) explore the formation and evolution of previously identified radiating dike swarms within the region, 2) use the diverse array of volcanic deposits to test further the neutral buoyancy hypothesis proposed to explain the origin of reservoir-derived features, 3&4) unravel the volcanic and tectonic evolution in this area, and 5) explore the implications of 1-4 for resurfacing mechanisms.

Approach: Ongoing mapping and analysis of the geology within the Nemesis Tesserae quadrangle builds upon integrated interpretation of multiple datasets. The primary mapping base is a single, georeferenced, 250 m/pixel[1], lambert conformal conic-projected Magellan radar image, co-registered in ArcGIS 8.3 with topography and remote sensing (e.g., emissivity, etc.) datasets. Complementing this mapping configuration, similar resolution synthetic stereo data (at 10x vertical exaggeration) viewed on an adjacent screen provide powerful topographic insight into material unit boundary locations and stratigraphy. Finally, georeferenced FMAP resolution (75 m/pixel) radar data, sinusoidally projected to a central meridian of 195°E and then digitally mosaicked within ArcGIS, are also employed; all units defined during mapping on the lower resolution lambert base can be reprojected "on the fly" during a simple cut-and-paste operation in ArcGIS so that they co-register with the sinusoidally projected FMAP images, yielding a quick and efficient way to use high resolution data to refine problematic unit boundaries and stratigraphic relationships.

A Comment on Involving Undergraduates. Extensive involvement of undergraduates during the past several years has been an important component of the "methods" employed for the project to date, and I report briefly on my experiences here in the hope that they will be of benefit to others who seek to involve undergraduates productively in their mapping efforts. To date I have leveraged student funding provided by my mapping grant more than fourfold (via PGGURP, funds from Pomona College, and via selected use of independent study credit), allowing me thus far to work with 4 students in the summer of 2001 (all of whom co-authored LPSC abstracts [1-3]), 1 in the fall of 2001, 7 in the spring of 2002 (3 of whom continued collaboration in the fall of 2002 to produce an LPSC abstract [4]), and 1 in the spring of 2003. The students, ~35% men and 65% women, have ranged in background from several with only one geology class (freshmen) to one who had just completed his senior year of college. My experiences to date suggest that the most productive way to involve undergraduate students is to engage a large group at a single time; there are pros and cons to doing this during the summer or within an academic semester [5]. Either configuration, however, allows the group to solve many problems (software issues, etc.) with minimal assistance. It also promotes a healthy and synergistic opportunity for the students to compare observations and test hypotheses—an important component of their education as science students—and allows me to focus my collaborative time with them upon exploring and helping to guide their scientific efforts and upon integrating the mapping and science results they produce, maximizing forward progress for the quadrangle mapping effort as a whole. Other configurations I have tried have not been as productive for the students and have generally hindered my ability during that period to make forward progress on the project as a whole, requiring as much or more of my time and yielding less science return. I would be happy to discuss these matters further with interested parties.

Selected Observations and Results: Mapping to date has providing insight into several interesting science questions, only a few of which are described here.

Giant Radiating Dike Swarms. The V14 quadrangle contains three features interpreted as radial dike swarms. Extensive study of similar features preserved in the geologic record on Earth has revealed a great deal about how such swarms originate, but because of poor preservation little is known about the detailed configuration of the magma source regions (beyond the general statement that they are normally mantle plume sites) or the scale/nature of any associated surface volcanism [6]. Observations in V14 indicate that both the magma source regions and surface expressions of similar dike swarms on Venus are highly diverse. For example, one (previously unidentified) swarm, with lineaments extending fairly uniformly to lengths of ~200-400 km and radiating through ~180° of arc, emanates from a broad topographic dome 250 km in radius, the crest and flanks of which are characterized principally by a cluster of small shield volcanoes and associated lava flows. These characteristics suggest a

[1] This translates, when viewed at full resolution, to an effective mapping scale of about 1:1M.

small, deep-seated (sub-crustal?) plume, with dike alignments governed in large part by the stresses associated with formation of the dome [cf 6 and references therein]. The second swarm, which radiates through 360° of arc and is similar in size, has a single, unnamed volcano at the focus, and the flanking flows from this edifice both cover and are cut by dike-related fracturing suggesting an interplay between intrusive and extrusive volcanism characteristic of a shallow crustal magma reservoir [cf 7]. Finally, the third dike swarm contains at least two distinct radial lineament sets, the focal regions of which are separated by ~200 km [8]. The oldest, centered upon a subdued annular structure, fans across ~270 degrees of arc out to distances of at least 150 km, but one prominent subswarm extending northeast toward Bellona Fossae exceeds 1000 km in length. The younger radial system, centered upon an unnamed volcano, is characterized by dikes fanning through ~360 degrees of arc across at least 125 km (a small handful of dikes extend twice this distance). In this case, the flows from the edifice cover but are not cut by the dikes, suggesting that the intrusive phase of volcanism ceased prior to when the most recent surface deposits were emplaced. Considered together, it appears that lateral migration of the magma source region has occurred with time and interestingly, unlike what has been documented for novae on Venus [9,10], the older center has longer continuous fractures and greater fracture-to-fracture spacing than the younger one, suggesting the possibility that there is further information to be gleaned about the subsurface plumbing from the character of the surface record. Study of the radiating dike systems and comparison with the terrestrial record and other swarms on Venus is continuing.

Neutral Buoyancy. Mapping to data has revealed well over thirty major reservoir-derived features in the quadrangle, but the total number of features in the quadrangle is too small for a meaningful Chi-squared test of the neutral buoyancy hypothesis [7]. Our results do indicate, however, that criteria used to define volcano and dike swarm elevations in previous studies [e.g., 11,12] may not be effective if the amount of post-emplacement deformation observed in the pseudostereo data for V14 is at all typical.

Structural Deformation. Prominent extensional and compressional lineaments occur throughout the quadrangle, but in general several patterns are observed. Extensional lineaments occur in three primary forms: 1) sets which are geometrically linked to specific volcanic features, such as the dike swarms described above and several coronae and smaller annular features, 2) sets concentrated into linear, topographically elevated belts, and 3) those which significantly deform (and in many cases define) the tessera in the region. While very small-scale distributed fracturing pervades the plains, no distinctive regional tectonic patterns are otherwise observed. Compressional lineaments also occur in several primary configurations: 1) as regional, often arcuate systems of wrinkle ridges in low-lying plains areas, 2) as sets concentrated into linear, topographically elevated belts, and 3) as narrow sets immediately adjacent to the edges of areas with steeply elevated topographic boundaries. The stratigraphic and tectonic implications of the observed deformation continue to be a focus of intense study.

Pyroclastic Deposits? An intriguing region of homogeneous, rough, radar-bright "feathery" deposits—similar to units interpreted by others as pyroclastic materials [13]—occurs within V14. As with previously mapped examples no vents are observed and the materials blanket and bury tectonic lineaments in the area; however, the deposits mapped in V14 are not spatially affiliated with a corona rim. They do lie, however, along the southeast edge of the 500 km dome and complex magmatic center with which the first dike swarm described earlier is affiliated, suggesting that volatile-rich eruptions on Venus may derive from small, deep-seated plumes.

Impact Cratering. The V14 quadrangle contains 11 impact craters and 4 "splotch" craters. Two of the craters—Yablochkina and Akiko—are affiliated with areally extensive radar dark haloes that blanket the surrounding plains and make unit differentiation in the affected areas quite challenging; only one large crater (Nadira) has no halo deposit whatsoever. One of the most interesting craters, however, is also one of the smallest: Unitkak has a diffuse-appearing, radar-dark streak several kilometers wide that extends away from the crater in a straight line across more than 500 km.

References: [1] Polit, A. T., et al. Abst#1673 (CD-ROM). *LPSC XXXIII*, 2002. [2] Pelletier, S. P., and Grosfils, E. B. Abst#1863 (CD-ROM). *LPSC XXXIII*, 2002. [3] Doggett, T. C., and Grosfils, E. B. Abst#1004 (CD-ROM). *LPSC XXXIII*, 2002. [4] Waldron, A. C., et al. Abst#1060 (CD-ROM). *LPSC XXXIV*, 2003. [5] Grosfils, E. B. *Geol Soc Amer Mtg. 34*, 304, 2002. [6] Ernst, R. E., et al. *Ann Rev Earth Planet Sci, 29*, 489-534, 2001. [7] Head, J. W., and Wilson, L. *J Geophys Res, 97*, 3877-3903 1992. [8] Grosfils, E. B., and Ernst, R. E. Abst#1808 (CD-ROM). *LPSC XXXIV,* 2003. [9] Krassilnikov, A. S., and Head, J. W. Abst#1463 (CD-ROM). *LPSC XXXIII*, 2002. [10] Basilevsky, A. T., and Raitala, J. *Planet Space Sci 50*, 21-39, 2002. [11] Grosfils, E. B., and Head, J. W. *Planet Space Sci 43*, 1555-1560, 1995. [12] Keddie, S. T., and Head, J. W. *Planet Space Sci 42,* 455-462, 1994. [13] Campbell, B.A., and Clark, D.A. USGS Open-File Report, 02-412, 29-31, 2002.

GEOLOGIC MAP OF THE GREENAWAY QUADRANGLE (V-24), VENUS

Nicholas P. Lang and Vicki L. Hansen, Department of Geological Sciences, University of Minnesota-Duluth, Duluth, MN 55812 (lang0604@tc.umn.edu)

Introduction: The Greenaway quadrangle (*Figure 1*) occupies an ~8,400,000 km^2 equatorial swath of lowlands and highlands on Venus. This region (0-25° N., 120-150° E.) includes parts of Llorona and Niobe Planitiae and is bounded by crustal plateau Thetis Regio to the south, Rusalka Planitia to the east, and Gegute Tessera to the west. The northern three-fourths of the quadrangle are part of the vast lowlands, or planitia, which cover ~80% of the planet.

Although early VMAPS convey the plains as simple, monotonous regions, detailed mapping of a representative portion of the plains reveals that Venus' plains can consist of structurally and volcanically complex regions marked by extensive development of small-shield and coronae-sourced flows that interact with tectonic structures and long-wavelength topography.

Our mapping is part of a larger, ongoing project aimed at understanding the geologic evolution of the venusian planitia.

Methodology: Geologic mapping, according to standard guidelines [1, 2], is conducted digitally using Mercator projection of a 225-m/pixel Magellan SAR base. Synthetic stereo, Magellan altimetry data, and full-resolution (75-m/pixel) normal and inverted Magellan SAR framelets are used in mapping.

Basal Materials: Large patches of ribbon-bearing tessera terrain, or ribbon terrain, outcrop along the western and southern boundaries of V-24, but kipuka of ribbon terrain are common across the quadrangle. V-24 ribbon terrain hosts a variety of secondary structures including NW and NE-trending ribbons, NW-trending folds, intratessera basins, and graben.

Patches of pervasively deformed terrain (mapped as basal materials, undifferentiated) containing NW-trending tightly-spaced lineaments outcrop across the quadrangle and are typically spatially associated with ribbon terrain. Lineament type is generally difficult to distinguish, although both folds and fractures occur locally. All patches have a low topographic expression and they are locally embayed and/or are partially covered by flows sourced from coronae and/or small shields. The continuity of trend in the NW-trending lineaments in isolated outcroppings suggests that these localized patches comprise a large NW-trending deformation belt buried by younger flows. Some patches appear to dissect ribbon terrain suggesting that parts of the deformation belt are locally younger than ribbon terrain.

A suite of NE-striking fractures outcrop in an ~1000x300 km topographic warp in SE V-24. The warp is embayed by flows from coronae and small shields, but preserves an area that appears to have undergone a complex history of volcanism with subsequent NE fracturing followed by more volcanism and reactivation of fracturing. We map this region as a composite unit bl (Llorona Planitia basal materials).

Coronae: Eight coronae dot the quadrangle. Four coronae (Kamadhenu, Kubebe, and two unnamed coronae) occur as a small chain along a NE-trending topographic arch that divides V-24 into two NE-trending basins. Kubebe and the two unnamed coronae exhibit lobate volcanic flows that extend past their respective annuli. Kamadhenu does not exhibit evidence of such activity. Instead, we interpret Kamadhenu volcanic flows to source from several small shields all contained inside the annulus. It is possible that Kamadhenu magmatism was similar to that of the other coronae but that evidence of such flows has been covered by younger material, or flow evidence has been erased through weathering. Individual shield flows are difficult to delineate because they coalesce to form an amorphous flow field mapped as the Kamadhenu shield field.

Rosmerta Corona boasts the most extensive flows in V-24 with individual flows possibly extending greater than 1000 km and into three adjoining VMAPs (V-23, V-35, and V-36). Immediately north of Rosmerta is a northerly-trending fracture belt that dissects ribbon terrain and apparently provided numerous conduits for flows to spill north onto the planitia. Radial fractures that extend from Rosmerta are most likely the surface expression of a dike swarm.

Abundia and Nintu Coronae in NW V-24 exhibit apparently localized volcanic flows. Both coronae are extremely subdued and have amphitheater-like morphologies lacking the traditional raised rim of other coronae.

Blai Corona sits on the southern edge of V-24 and extends into northern V-36. Blai exhibits a radial fracture pattern and associated flows embay the surrounding ribbon terrain.

Flows also extend from Boann Corona to the north and from Ituana Corona to the east.

Small-Shields: Small shields are the most dominant feature across V-24. Conservative estimates of shield densities range from 3,550-10,550 shields/10^6 km^2, but actual densities may be much greater strongly suggesting that shields may play an extremely dominant role in volcanic resurfacing of the planitiae in this area. Based on their distribution, shields are divisible into two broad categories: shield clusters and shield plains. Shield clusters are local concentrations of shields typically inside or immediately surrounding a corona. Shield plains are broad distributions of shields across expansive regions [3].

Impact Structures: 19 impact structures are identified in V-24. Two craters have rough floors and are surrounded by dark haloes, three craters have a smooth floor, but highly degraded haloes, and 14 craters have smooth floors and no surrounding halo. All craters have a raised rim and visible ejecta blanket; some ejecta materials continue for over a hundred kilometers from the rim and some are likely fluidized deposits. Ejecta from crater Wilder, superposed on Gegute Tessera, is embayed and partially covered by small-shield flows.

Structure: Wrinkle ridges, graben, and regional lineaments dominate structural deformation of plains materials.

The wrinkle ridges describe a broad E-ENE pattern across the map with their highest density in the NE of V-24. Some wrinkle ridges may exist locally as inversion structures where earlier formed fractures were filled by lava and later contracted [4].

V-24 graben appear to be generally spatially associated with corona-related activity and have a dominant northerly trend.

Regional lineaments most likely represent the traces of faults, fractures, dikes, and/or joints. Trends vary from NNW to NNE and cannot be associated with any particular event.

Discussion: Mapped units represent material deposited during a specific event of geologic history. The exceptions to this are units bl and the widespread pvu (volcanic plains, undifferentiated) which are composite units and are not stratigraphically coherent over their entire area. Thus, these two units cannot be used in correlating map units across the quadrangle. To correlate units across V-24, stratigraphically coherent units must either interact or be stratigraphically placed in reference to a widespread marker bed [e.g. 5]. V-24 displays limited interaction between mapped units making correlation nearly impossible and strongly inhibiting the derivation of a detailed geologic history. However, based on map-scale cross-cutting relationships, a very general sequence of events for V-24 may be deduced: 1) Deposition of surface materials followed by subsequent formation of ribbon terrain, 2) formation of the NW-trending deformation belt, and 3) formation of the NE-trending topographic arch with concurrent coronae volcanism. Although some patches of the deformation belt locally dissect ribbon terrain, this does not prove the deformation belt is entirely younger than ribbon terrain. Initiation of Rosmerta, Abundia, Kubebe, and Boann volcanism cannot be constrained, but associated flows parallel the basin trend indicating at least some volcanism post-dated formation of the arch. Shield clusters may represent late-stage corona volcanism and, hence, their timing is locally constrained. Shield plains make up a large part of unit pvu and their timing is difficult to constrain, but may have occurred throughout the history of V-24.

References: [1] Tanaka, K.L., et al., (1994) *The Venus Geologic Mapper's Handbook* 2nd ed., USGS Open-file Report 94-438, 68p. [2] Hansen, V.L., (2000) *EPSL*, 176, p. 527-542. [3] Aubele, J.C., (1995) *GSA-Aw/P*, 27 (6), p. 209. [4] Hansen, V.L., et al., (2002) *LPSC XXXIII* #1121. [5] Compton, R.R., (1985) *Geology in the Field*, John Wiley and Sons, New York, p. 85.

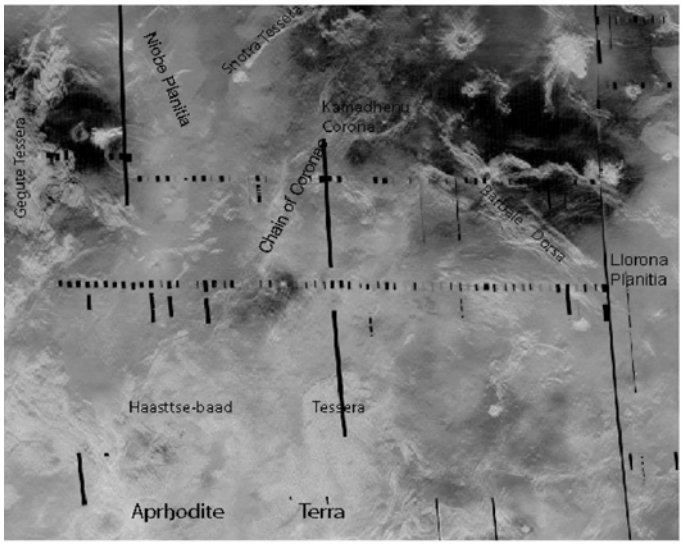

Figure 1: Normal SAR image of the Greenaway Quadrangle showing the names and locations of major features.

The Geology of the V39 Taussig Quadrangle. A. W Brian[1,2] and E. R. Stofan[1,2], [1]Proxemy Research, 20528 Farcroft Lane, Laytonsville, MD 20528, [2]Dept of Earth Sciences, UCL, Gower Street, London, WC1E 6BT, awb@star.ucl.ac.uk

Introduction. The Taussig Quadrangle (V39) of Venus extends from 0°-25°S latitude and 210°-240°E longitude. The region is 2632.2 km north-south by 3158.6 km east-west and has an area of 8.10×10^6 km^2. It is bounded by Atla Regio to the north-west, Ulfrun Regio to the north, Wawalag Planitia to the south and Hinemoa Planitia to the north-east. It contains 13 impact craters, 3 large volcanoes, 8 paterae, 24 coronae, a 3900 km long section of the Parga Chasmata rift system and parts of Hinemoa and Wawalag Planitiae. Elevations within the area vary from 4.3 km above to 3.6 km below the mean planetary radius (MPR, 6051.84 km, [1]). Emissivity values within the quadrangle vary from 0.52 to 0.95 with the average 0.85 (similar to the mean emissivity of 0.845 for the Venusian surface [1]). There appears to be a dichotomy in values between the materials to the northeast of the rift (e.g. units *pl*, *puT*, *pf fC2* and *fM1*) and those to the south (e.g. units *prT*, *pli*). This is most likely attributed to separate plains and volcanic flow materials that contain minerals with different dielectric constants.

We have mapped the quad using standard photogeologic mapping techniques [e.g. 2, 3] using full resolution F-Maps, Magellan image data on CD-ROM and synthetic stereo images. The synthetic stereo images were particularly useful in determining stratigraphic relations between units and the role of the region's topography in the construction of the different landforms. They were of particular use in understanding the complex deformation associated with the chasma regions. Unit contacts in some places were found to be distinct and well defined by crosscutting relationships, but in others were only noticeable through digital manipulation of the F-Map data. Additional Magellan data sets such as emissivity, reflectivity, altimetry and roughness were also used.

Plains Units. Ten distinct plains units are identified within the quadrangle based on morphologic and stratigraphic relationships: Densely Fractured Plains (unit pdf), Hilly Plains (unit ph), Taussig Uniform Plains (unit puT), Shield Plains (unit psh), Lineated Plains (unit pli), Fractured Plains (unit pf), Lobate Plains (unit pl), Undulating Plains (unit pu), Taussig Regional Plains (unit prT) and Smooth Plains (unit ps). The scale of each of these plains units varies from <100 km^2 to over 100,000 km^2.

The Taussig Regional Plains materials (unit prT) are the most extensive plains unit in the area covering approximately 30% of the quadrangle. They are characterised by relatively low backscatter coefficients, with small-scale variations in backscatter visible throughout. Some individual flows can be recognised within the unit at F-MAP scale, which suggests that *prT* materials could be a collection of many volcanic flows with similar radar backscatter. Densely Fractured Plains materials (unit *pdf*) (e.g. 23.5°S, 222.5°E) are located throughout the quadrangle. They have strong radar backscatter coefficients that represent highly deformed materials with very rough surfaces. All the outcrops consist of inliers rising above the surrounding materials, which embay them. Most blocks are 50-75 km across although some may be slightly larger. Some pdf materials show multidirectional deformation but no dominant trends are observed within the quadrangle. The unit is embayed by eighteen different other units, but there is no evidence to suggest all pdf materials are the same age or of the same origin over the whole of the quadrangle. The materials are interpreted to be earlier highly deformed plains materials and/or possibly the upstanding rims of old coronae.

Volcanic Centres. V39 contains three named large volcanoes (>100 km diameter flow apron) (Mbokomu and Gwen Montes, and Fedchenko Patera), along with 24 intermediate (10-50 km diameter) volcanic centres. The quad also contains eight paterae that vary in caldera size from 40 km to 160 km. The most prominent of these are Ledoux, Jotuni and Villepreux-Power Paterae. All the volcanic centres and many of the paterae have extensive volcanic flow aprons that superpose their surrounding units. Most flows have variable radar backscatters and vary in morphology from sheet to highly dendritic. Mbokomu Mons is 240 km wide and sits on the Jokwa Linea branch of the Parga Chasmata rift system. Its shape is not typical of other classic venusian volcanoes (e.g. Sif and Sapas Montes) and is more plateau-like leading some authors [4, 5] to classify it as a corona. We are investigating its geology further but have mapped it here as a large volcano.

Coronae. Twenty-five coronae are located within the quadrangle ranging in diameter from 100 to 600 km. Fourteen of the coronae in the region have identifiable and mappable units that are interpreted to be volcanic in origin. They are found in two main geological settings: those formed within the plains and those formed on or within the rift. There are twelve 'plains' coronae and thirteen 'rift' coronae. Several coronae show complex histories. For example, Onenhste Corona (19S,221E) deforms plains unit *pli*, and therefore postdates it. These plains are deformed by radial and concentric fractures associated with the

corona. Several units (unit *prT, ef, uco2*) truncate much of the radial deformation where they embay unit *pli*. Other radial fractures emanating from the centre of Onenhste however cut these units indicating that there have been at least two stages of deformation (possibly associated with secondary uplift of the corona) over the evolution of the feature. The secondary fracturing also cuts the flow unit *fOn* suggesting that this deformational event occurred after its emplacement in the centre of the corona.

Structure. V39 is dominated by the complex troughs, ridges and fractures of the Parga Chasmata rift system. The main region of deformation runs diagonally north-west to south-east through the area, although several other zones of fractures branch away from the main system.

The rift system displays a complex geological history, intertwined with the formation and development of the coronae and volcanoes along its length. The timing of individual tectonic events is unclear, but it is evident that both volcanism and rifting have overlapped in time. The majority of the rifting in the area postdates the formation of the local plains, with subsequent volcano and corona development along the system (e.g., at Mbokomu Mons and Maram Corona) displaying cross-cutting relationships with several generations of tectonic activity. The youngest tectonic events appear to be long (hundreds of kilometres) parallel sets of south-east trending graben that run along the main zone. The majority of these graben cross-cut earlier associated rift flows and fractures.

Geologic History and Stratigraphy. The geologic history of the Taussig Quadrangle is a complex one that has been dominated by both volcanism and tectonism. A vast array of volcanic and tectonic landforms has been produced suggesting that these processes have been both repetitive and ongoing. Volcanism has occurred dominantly in the form of volcanic centres, lava flow deposits associated with coronae, extensive lava sheets, and clusters of small edifices. Tectonism has dominated in the form of large scale extensional rifting, belts of fractures and graben, clusters of radial and concentric fractures and faults and small scale wrinkle ridges. By assessing the stratigraphy of all these units and structures, a history of the region has been determined.

The earliest visible materials (unit *pdf*) are presumed to have been ancient volcanic units, subsequently disrupted by severe tectonic deformation. This was followed by the emplacement of further volcanic plains (units *ph, pli, pf*) combined with small edifice formation in the form of the shield plains (unit *psh*) in the north. Structural deformation of these older plains represents the action of different stress fields at different times. The widespread regional plains (units *prT*, and *pl*) formed after these events, embaying older units and leaving upstanding outcrops of deformed material.

Concurrent with all but the very earliest, and subsequently highly deformed, plains materials, has been corona, volcano and rift development. Coronae have formed in a number of plains units and throughout the history of the area and many show repeated episodes of volcanism and tectonism that overlap with the units that surround them. Several coronae are considered to be sites of long-term geologic activity with multiple episodes of volcanism and annulus formation. Rifting has dominated at least in the latter stages of the evolution of the area, but the initiation of this large-scale extension could have started even before the emplacement of the widespread regional plains. Volcanism has also occurred throughout the history, but is most prominently represented by some of the youngest materials, in the form of large volcanic edifices and extensive lava flow fields. Impact cratering has occurred throughout the history of the region, but provides very little constraint on surface unit ages.

These observations suggest to us that different styles of volcanism and tectonism have repeatedly occurred through the visible history of this part of Venus. Volcanism associated with coronae, large volcanoes and calderas is seen throughout much of the stratigraphic column overlapping with the formation of the widespread regional plains. There is no evidence to suggest that these processes occurred in discrete episodes as suggested by Basilevsky and Head [6] and therefore this study indicates that the geology of the Taussig Quadrangle favours a non-directional history of evolution [8].

References: [1] Pettengill, G. H. et al., *J. Geophys. Res*., 97:13,091-13,102, 1992. [2] Wilhelms, D. E., *Planetary Mapping*, Edited By R. Greeley and R. M. Batson, *Cambridge University Press*, 1990. [3] Tanaka, K. L., *U. S. Geol. Surv*., Open File Report 94-438, P 50, 1994. [4] Crumpler, L. S. et al., In *Venus II*, Edited By S. W. Bougher, D. M. Hunten, and R. J. Phillips, *Univ. of Ariz. Press, Tucson*, 1997. [5] Stofan, E. R. et al., *J. Geophys. Res*., 97:13,347-13,378, 1992. [7] Basilevsky, A. T., and J. W. Head, *Planet. Space Sci*., 48:75-111, 2000. [8] Guest, J. E., and E. R. Stofan, *Icarus*, 139:55-66, 1999.

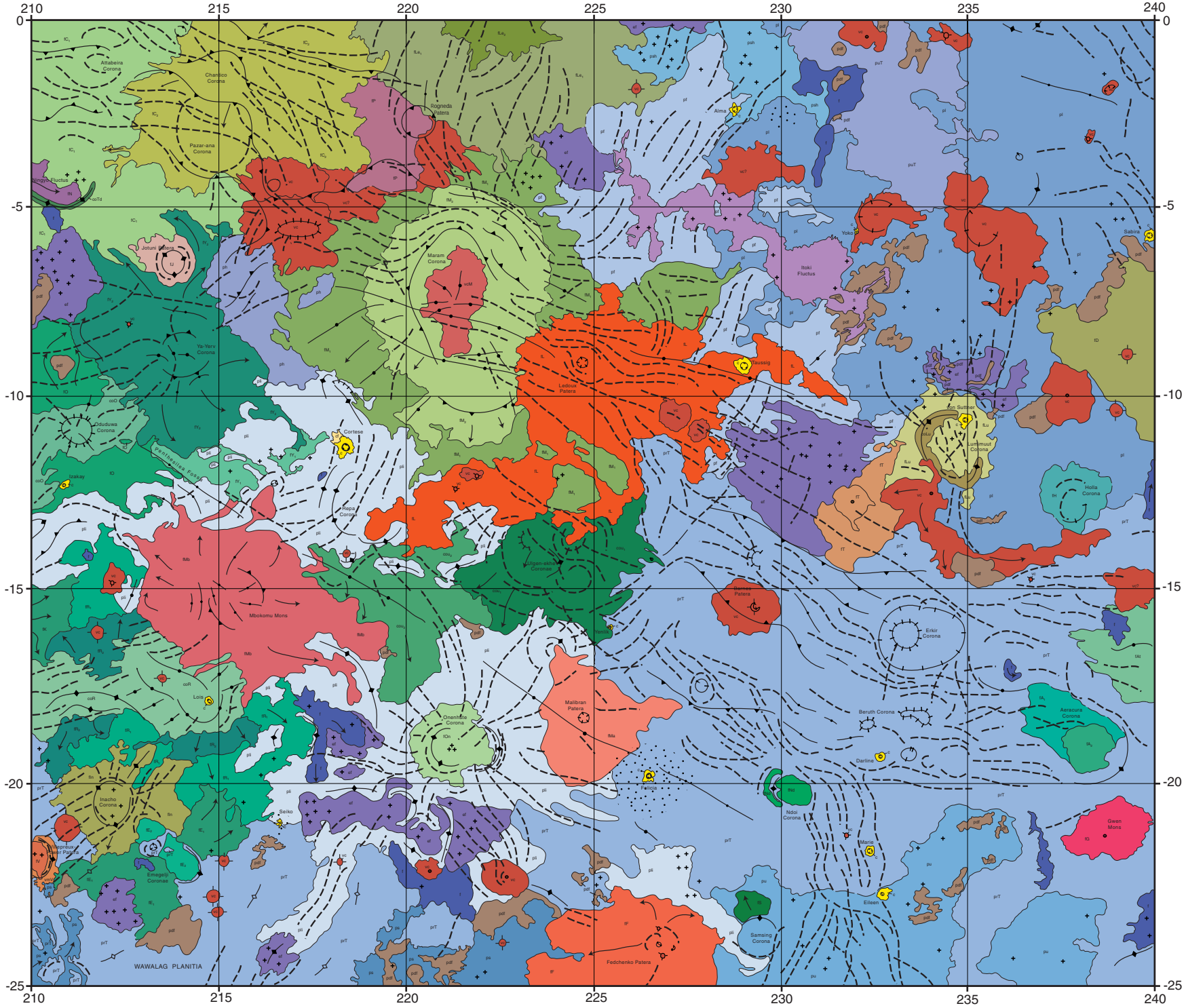
210
215
220
225
230
235
240
0
-5
-10
-15
-20
-25
WAWALAG PLANITIA
Attabeira Corona
Chanico Corona
Pazar-ana Corona
Rogneda Patera
Alma
Jotuni Patera
Maram Corona
Itoki Fluctus
Yoka
Sabira
Ya-Yerv Corona
Taussig
Ledoux Patera
Von Suttner
Lummuut Corona
Oduduwa Corona
Cortese
Parthenelea Fossa
Izakay
Holla Corona
Hopoi Corona
Mbokomu Mons
Bernea Patera
Erkir Corona
Lois
Onenmiw Corona
Malibran Patera
Beruth Corona
Aeracura Corona
Darline
Falicia
Inacho Corona
Seiko
Ndoi Corona
Gwen Mons
Emegelji Coronae
Eileen
Samsing Corona
Fedchenko Patera

PRELIMINARY GEOLOGIC MAPPING OF HELEN PLANITIA QUADRANGLE (V52), VENUS. Ivan Lopez[1] and V.L. Hansen[2]. 1. Departamento de Matematicas y Fisica Aplicadas y Ciencias de la Naturaleza. ESCET. Universidad Rey Juan Carlos. C/Tulipan s/n, 28933 Mostoles, Madrid. Spain. Add your email address Ivan. 2. Department of Geological Sciences. University of Minnesota-Duluth, 1114 Kirby Drive, Duluth, MN 55812. (E-mail:i.lopez@escet.urjc.es)

Introduction.

The Helen Planitia Quadrangle (V52) is located in the southern hemisphere of Venus between 25º-50ºS and 240º-270ºE, covering an approximate surface of 8,000,000 km^2 between the mesolands of Eastern Parga Chasmata and the lowlands of Helen Planitia. It is bound to the east by the corona-dominated volcanic rise of Themis Regio and to the west by Wawalag Planitia. The mean altitude of V52 ranges from 0 to 2 km over the mean planetary radius (6051.84 km), although some areas of Helen Planitia in southern V52 lie lower. The area includes a large number and high morphological variety of coronae, large volcanoes, deformation belts, and other volcanic and structural features distributed among regional plains materials, allowing the study of their relative age relationships, interactions and evolutionary sequence.

The previous mentioned characteristics make V52 a great area for addressing the following questions: a) what are the different styles of tectonic and volcanic activity present in a mesoland-lowland transition zone? b) What is the geologic history of these areas of transition and what role do large tectovolcanic structures such as coronae and volcanoes play in resurfacing? c) What is the relationship of these large structures with other styles of volcanism (e.g. small shields) and tectonism within the quadrangle?

Data sets and mapping techniques used in this work.

Geologic Mapping is at the base of descriptive analysis in geology. A map provides in one glance the distribution of primary and secondary structures, contact locations and styles, limits of material units, and possibly relative ages of materials and structures. The map forms a tool for unraveling the geologic history of an area. This ongoing mapping follows the philosophy outlined by [1-2] and used in the mapping of other venusian quadrangles (e.g., V37, V25 and V35).

Mapping is conducted in both Mercator and Lambert projection of left and right-looking normal and inverted Magellan SAR images (225-250 m/pixel) and left-looking synthetic stereo radar images (450m/pixel). The main goal of early stages of mapping is to determine the location, distribution, and nature of primary and secondary structures present at this map scale and to make a first attempt to determine major material units for further mapping. Detailed mapping of selected areas using full resolution Magellan SAR data (75 m/pixel) is ongoing.

Structures.

Secondary structures occur across the study area. In mapping secondary structures we discriminate, where possible, between local deformation trends-structures formed in relationship with large tectovolcanic features (e.g. radial and concentric fractures formed during corona formation) and large deformation trends of regional significance (e.g. chasmata and dorsa).

Principal regional fracture trends.

1) NW-SE fracture trend. Close-regularly-spaced fractures that dominate over graben. This fracture suite is restricted to northwestern V52 and is interpreted to be locally reoriented to E-W direction by the effect of the local stress field formed in relation to large tectovolcanic features, coronae and large volcanoes (e.g. Chuginadak Mons). The fracture suite predated formation of a N-striking fracture suite that dominates southern V52.

2) N-striking fracture suite. This fracture suite, present across V52, is the main direction in the southern half of the quadrangle. It is composed mainly of fractures, but parallel graben are also present. This fracture suite forms areas of concentrated deformation such as in Ajina Fossae, where the interfracture spacing decreases.

3) WNW-ESE trending fabrics (Parga Chasmata). With this direction we observe single lineaments and also paired straight lineaments, interpreted as graben. These lineaments connect coronae associated with Parga Chasmata and in many cases merge with coronae annular fractures. Some scarps are also recognizable. This direction dominates northern V52, and represents the region mark by the high apparent strain.

Local fracture suites.

The large number of tectovolcanic features found in the study area produced local fracture suites and locally modify the orientation of regional structures. This large number is also accompanied by a large diversity in tectonic and volcanic style including: coronae, montes, novae, paterae and radial fractures systems, interpreted by some authors as the surface manifestation of deep radial dyke swarms [3].

Compressive deformation: folds and wrinkle ridges.

Different trends of wrinkle ridges occur within V52. Wrinkle ridges with N-trending wrinkle ridges dominate the western and central part of the quadrangle, whereas NW-trending wrinkle ridges dominate the southwestern part of V52. This trend is also present in the northern part but occurs in a localized fashion. NW-trending wrinkle ridges parallel Tsovinar Dorsa, the largest contractional deformation belt present in the area formed by large ridges marked by folds. Other families of wrinkle ridges occur around large tectovolcanic features (e.g. Oanuava Corona) but are locally distributed and seem not to have regional significance.

Materials.

Basement

a) Tesserae. As observed in other quadrangles, tessera terrain is the oldest local unit where time

relations with other materials can be determined. There are different types of tessera terrain outcropping in V52, although the characteristics of the outcrops (i.e. isolated tessera outcrops surrounded by younger volcanic materials) make time relations between the different types of terrain impossible to establish. In V52 we have found ribbon-bearing tessera (the ribbons trend consistently ENE) and graben-dominated tessera outcrops occur across the entire quadrangle.

b) Pervasively deformed terrain. Small outcrops of highly fractured terrain occur within V52. This type of terrain presents a closely spaced NW lineament trend although a N direction is present in some outcrops. The lineaments are so closely spaced and pervasive that it is impossible to determine the previous characteristics of the deformed material. In southern V52 the fracture terrain appears together with other basement materials in large inliers that follow a NW trend (e.g. Sopdet Tesserae) but it also forms as isolated small kipukas surrounded by younger volcanic materials. Age relations between the various tessera terrains and this unit are indeterminate; like tessera, this unit forms the oldest local unit.

Post-basement volcanic materials.

A number large volcanotectonic features, associated with Parga Chasmata, comprise the origin of numerous volcanic flows that give shape to northern V52.

A large igneous flow unit composed of multiple individual flows mainly covers northern V52. The origin of this unit can be generally traced to an unnamed corona formed in Parga Chasmata although some flows seem to originate from fractures of the Parga Chasmata fracture belt. This large flow can be classified as a transitional flow field according to the classification for this type of deposits established by [4]. The flow material postdates some coronae and some volcanic edifices to the south, filling the interior lows of the coronae. The flow represents several flow units, and displays well-defined internal structure, lobate flow structure and irregular boundaries. It preserves some primary structures that give important information regarding its flow direction (i.e. ropy structure) and eruption style (i.e. channels) and that also helps to establish the time relationship of this unit with other flows. The limits of this unit are not clear on its E and SW limits and have been traced as approximate or transitional with the surrounding materials. This large flow clearly predates the flows originated in Lalohonua Corona in the Galindo Quadrangle (V40) and in an unnamed volcanic structure located next to this corona.

The second large unit present in northern V52 comprises materials associated with Oanuava Corona, a multiple corona located south of Parga Chasmata. The materials of this corona present a higher radar backscatter that the surrounding materials and a reticulate pattern texture that helped define the unit limits. The limits of the unit are very clear to the west where the presence of some primary structures and flow directions allow us to establish the timing with the large igneous flow unit described above which clearly predated this second unit. The limits to the east are not as clearly defined, nor are the relations with the large flow and other units.

Central V52 hosts many tectovolcanic features (coronae, large volcanoes and radial dyke swarms), as well as volcanic features such as shield fields and small paterae. Some units associated with shields and small volcanic edifices clearly postdate large units formed in relationship with coronae and chasmata.

Large differences in surface radar properties in the volcanic materials that cover central V52 and the large number of volcanic edifices could indicate that many materials and flows are present in central V52. Nevertheless, the mapping of these units is still on progress and the origin of much of these materials is still to be traced.

The central and southern parts of V52 host an incredibly large number of small shields that partially cover, mask, or veil large areas; shields both postdate and predate various secondary structures and materials (tesserae, previous volcanic materials, etc). These shields occur in relation with large tectovolcanic structures (coronae and radial dyke swarms) but they also occur with no apparent relation to large features. The role that this shield material, first recognized by Aubele [5] could play in the resurfacing of the large plains of Venus has been described by [6]. This type of volcanism could be of a great important as a major source of resurfacing in southern V52.

Sopdet Tesserae and Tsovinar Dorsa separate Helen Planitia from the central part of the quadrangle. Both the tesserae outcrop and the deformation belt follow a NW-trend that marks the limit between these two areas that represent differences in number and style of the volcanic features. This part of V52 is devoid of large tectovolcanic features such as coronae or volcanoes, although the area hosts large areas with a high concentration of small shields. Other primary volcanic features such as large channels (e.g. Sinann Vallis) are also present.

Impact structures. V52 preserves 11 craters, some with bright halos (e.g. Adaiah) and outflow materials (e.g. Wollestonecraft and Rose). They are distributed across the quadrangle although the most craters occur in central V52. V52 also hosts two dark splotches in the southern part of the quadrangle.

References. [1] Tanaka, K.L., et al., (1994) *The Venus Geologic Mapper's Handbook* 2nd ed., USGS Open-file Report 94-438, 68p. [2] V.L. Hansen, (2000) Earth Planet. Sci. Lett. **176**, 527-542. [3] Ernst et al, (1995) Earth Science Reviews **39**, 1-58. [4] Lancaster et al., (1995) Icarus **118**, 69-86. [5] Aubele, J.C. (1995) Geological Society of America-Annual meeting, Abstract with Programs, 27 (6), p.209 [6] V.L. Hansen and L.F. Bleamaster, (2002) LPSC XXXIII, 1061.

CORONAE AND RIFTING IN V53 AND V28: INSIGHTS FROM GEOLOGIC MAPPING. E. R. Stofan[1,2] and J.E. Guest[2], [1]Proxemy Research (20528 Farcroft Lane, Laytonsville, MD 20882, ellen@proxemy.com), [2]Department of Geological Sciences, University College London, UK.

Introduction: We have been mapping the geology of Hecate Chasma (V28) and Themis Regio (V53) quadrangles at 1:5,000,000 scale as part of the NASA Planetary Geologic Mapping Program. Both of these quadrangles cover parts of the chasma systems that encircle Venus. In each quadrangle, there is a close association of rifts or fracture belts and coronae, as well as unusual amounts of volcanism (e.g., 1). Our motivation for mapping these regions is to better understand the relationship between corona formation and rifting, to investigate the relationship between rifting and volcanism, including at coronae, and to determine the stratigraphic relationship of plains-forming units.

Quadrangle Overviews. V28. The Hecate Chasma Quadrangle (V28) extends from 0°-25° N. latitude, 240°-270° longitude. Hecate Chasma is an extensive rift system (e.g., 2) that lies in a lowland region (Hinemoa Planitia) in the northern hemisphere of Venus. Hecate Chasma consists of several rift systems, low-lying plains units, coronae and numerous small volcanic edifices including shields, domes and cones. The quadrangle contains several intermediate to large volcanoes, including Polik-mana Mons and Lama Tholus. There are fourteen coronae in the quadrangle, the largest of which is the 525 km diameter Taranga Corona. There are eight impact craters in the V28 quadrangle. The overall topography of V28 consists of low-lying plains located slightly below Mean Planetary Radius (MPR, 6051.84, [3]).

In V28, we have mapped ten plains materials units. Fifteen units associated with named volcanic edifices have been mapped, along with flow materials emanating from unknown sources or from chasmata fractures. Eleven units associated with coronae have been mapped, with several coronae having no associated materials units. In addition, tessera and impact crater materials have been mapped.

V53. The Themis Regio Quadrangle (V53) extends from 25°S - 50°S latitude, 270° - 300° longitude, and encompasses the Themis Regio highland, surrounding plains, and the southernmost extension of Parga Chasmata. The overall topography of V53 consists of low-lying plains lying slightly below Mean Planetary Radius (MPR, 6051.84, [3]) surrounding the Themis highland. The lowest points in the quadrangle are along the Parga Chasmata rift and in the troughs around several coronae at about 2 km below MPR. The area covered by this quadrangle is part of a larger region known as the Beta-Atla-Themis (BAT) region, which contains an unusually high concentration of volcanic features [1]. There are 12 impact craters in the quadrangle.

Six plains units have been mapped in V53, as have 9 units associated with specific named volcanic edifices. Multiple flow materials units associated with unnamed or unknown sources have also been mapped. Twenty corona materials units are mapped, along with tessera and impact crater materials.

Plains Mapping. In the two chasma regions, more plains materials units have been mapped than in our previously mapped quadrangle, V-46 (Aino Planitia) (in press, 2003). In V53 and V-28, no regional-scale plains units have been identified; plains units scale tends to be on the order of 100's

of kms rather than 1000's of kms. The plains units in these quadrangles are frequently not in contact, making identification of a definitive stratigraphy difficult. In V28, all of the plains materials units to the south of the rift have an unusually high concentration of volcanic edifices.

Corona Characteristics. In both Parga/Themis and Hecate Chasmata, coronae are located along the rift, to the north and to the south of the rifts. Coronae in both quadrangles exhibit all forms of coronae topographic shapes [4], including depressions, rimmed depressions, plateaus and domes.

In V-28, multiple segments of the rift are present. Along one section of the rift, we have mapped only volcanoes, along another only coronae, and both types of features on the main segment of the rift. Some coronae along the rift do not have much associated volcanism; coronae with the most associated volcanism in these quadrangles are located at least 500 km off the rifts. Most of the coronae formed synchronously with the rifting, although some clearly predate the rifts and others postdate extensional deformation.

A strong association between volcanism and coronae along rifts has been noted elsewhere on the planet [5]. In these quadrangles, most of the more volcanic coronae are located in Themis Regio, previously identified as a possible hotspot (e.g., 6).

Conclusions. We interpret the majority of coronae along Parga and Hecate Chasmata to support a passive origin (e.g., 7). Some of the coronae along the rift have large amounts of associated volcanism, while others do not. In addition, several coronae off rift have more associated volcanism than the features along the rift. Therefore, while extension clearly plays a role in the amount of volcanism associated with coronae (e.g., 5), it is not the only contributing factor. Coronae at Themis Regio possibly have larger than normal amounts of volcanism due to the possible mantle plume beneath the rise.

The high number of plains units, coronae and volcanoes in these two quadrangles result in a very horizontal stratigraphic column, as few units are in direct contact. The scale of resurfacing in these quadrangles is on the scale of 100's of kilometers, consistent with the fact that they lie in the most volcanic region of Venus.

References. [1] Crumpler, L.S.,et al. 1997. In *Venus II*, eds. Brougher, S.W., Hunten, D.M. & Phillips, R.J. University of Arizona Press, Tucson, 697-756. [2] Hamilton, V. E., and E. R. Stofan, Icarus, 121, 171-194, 1996. [3] Ford, P.G., and Pettengill, G.H., 1992, Journal of Geophysical Research, v. 97, no. E8, p. 13,103-13,114. [4] Smrekar, S.E. and E.R. Stofan (1997) *Science*, 277, 1289-1294. [5] Magee, K.P. and J.W. Head 1995. *J. Geophys. Res*. **100**, 1527-1552. [6] Stofan, E. R., S. E. Smrekar, D. L. Bindschadler, and D. A. Senske. 1995. *J. Geophys. Res*. 100: 23,317-23,327. [7] Hansen, V.L. and R.J. Phillips 1993. *Science* **260**, 526-530.

GEOLOGIC HISTORY OF LADA TERRA, VENUS: MAPPING OF V-61, MYLITTA FLUCTUS, AND PRELIMINARY MAPPING OF V-56, LADA TERRA, QUADRANGLES. M. A. Ivanov[1,2] and J. W. Head[2]. [1]Vernadsky Institute, RAS, Moscow, Russia, mishaivn@mtu-net.ru; [2]Brown University, Providence, RI, USA, james_head_iii@brown.edu.

Introduction. Lada Terra is a large (from 300°E to 120°E and from 60°S to 80°S) elevated region on Venus. It is characterized by a wide variety of features, among which coronae play the most important role. The western portion of Lada Terra is dominated by the very large (~800 km), Quetzalpetlatl Corona [1,2], and smaller coronae typically arranged in linear zones characterize the rest of this topographic province. To the northwest and northeast, the lowlands of Lavinia and Aino Planitiae border Lada Terra. The two quadrangles, V-61 and V-56 cover the western and central portions of Lada Terra and the whole structure of Quetzalpetlatl Corona, show the transition from Lada Terra to the surrounding lowlands, and display the major structural trends at the edges and in the interior of Lada Terra. During our mapping in the V-61 area [3,4] and reconnaissance mapping within V-56 quadrangle we have analyzed the nature and age of the topographically highest large corona (Quetzalpetlatl) and documented the most prominent structural trends, their nature, and timing.

Area of V-61 quadrangle. (Fig. 1 a). *Quetzalpetlatl Corona*: The most spectacular feature of this quadrangle [3,4] is Quetzalpetlatl Corona, represented here by its western half. The annulus is the structurally most prominent part of the corona, and consists of densely spaced ridges up to 10 km wide. The ridges make up an arc-like belt outlining the northern and northwestern sectors of the corona. A topographic moat partly filled with lavas is adjacent to the belt on its outward side and there is no counterpart to the ridge belt/moat complex in the southern portion of Quetzalpetlatl. The corona is also a large volcanic center. Relatively young lava flows cover the interior of Quetzalpetlatl and the vast area around it. The sources of the flows appear to be close to the center of Quetzalpetlatl (Boala Corona and a longitudinally oriented swarm of graben that runs from Boala toward the northern edge of Quetzalpetlatl).

Structural Trends. Several distinct structural trends characterize the area within the V-61 quadrangle. In the lowlands of Lavinia and Helen Planitiae, several continuous topographic ridges (Morrigan Linea, Penardun Linea, etc.) separate the vast lowlands into a series of secondary basins [6-7]. Morphologically, these zones consist mostly of ridge belts and relatively old units broadly embayed by regional plains. Kalaipahoa Linea that represents a swarm of graben and hosts two coronae (Kamui-Huci in the West and Jord in the East) introduces another structural trend. Kalaipahoa Linea makes a broad arc that topographically corresponds to the edge of Lada Terra. The graben of Kalaipahoa Linea cut regional plains and appear to be partly contemporaneous with the younger lava flows emanating from Quetzalpetlatl. Jord Corona, and Tarbell Patera adjacent to it, are the sources of the gigantic Mylitta Fluctus [8] that flows down the regional slope into the lowland of Lavinia Planitia.

Area of V-56 quadrangle. (Fig. 1 b). The western portion of this area is characterized by the eastern half of Quetzalpetlatl Corona that bears the same basic characteristics as in the V-61 quadrangle. The ridge belt/moat complex outlines the northern portion of the corona and has no counterpart in its southern part. The vast apron of young lava flows covers the regional slopes away from the corona. The apparent sources of the flows are Erzulie Mons and a cluster of small shields in the southeastern sector of Quetzalpetlatl.

The main difference of the V-56 area from the V-61 quadrangle is that it contains two large massifs of tessera terrain (Cocomama and Lhamo Tesserae). These tesserae appear to be the oldest terrain in the scene and establish the oldest structural trends in the quadrangle. Cocomama Tessera dominates the central portion of Lada Terra and the Lhamo Tessera is a part of a regional highland ridge that borders the eastern edge of Lavinia Planitia [9]. In the northeastern corner of the quadrangle, within the lowland of Aino Planitia, a double fork-like topographic ridge consists of Asiaq and Kuldurok Dorsa. This ridge is made up of ridge belts and is broadly embayed by regional plains. By its topographic, morphologic, and stratigraphic characteristics the Asiaq and Kuldurok Dorsa belt strongly resembles the old structural zones occurring in the V-61 quadrangle within the lowlands surrounding Lada Terra.

Two very prominent young structural zones characterize the V-56 area. The first occurs in the northwestern corner of the area and is a continuation of the Kalaipahoa Linea. The most important feature of this zone within the V-56 quadrangle is Eithinoha Corona (~400 km). The swarms of graben that characterize the Kalaipahoa Linea structural zone run along the edge of Lada Terra and cut through Lhamo Tessera suggesting the superposition of the older and younger zones in one area. The second large zone is in the central portion of the quadrangle. It is oriented longitudinally and consists of a chain of relatively small coronae interconnected by swarms of graben. This zone is split into three branches at about 65°S, 40N. The most prominent, western, branch, which is characterized by the large (~350 km) Otygen Corona, merges with the Kalaipahoa Linea in the northwestern corner of the quadrangle. The central branch apparently dies out at the northern edge of Lada Terra and the eastern branch runs into the eastern portion of it (out of the V-56 area).

Summary of the History of Lada Terra and Quetzalpetlatl. Our analysis of the two neighboring quadrangles reveals preliminary evidence for the progressive change of volcanic and tectonic styles as a function of time at the regional scale within Lada Terra. 1) Cocomama Tessera, which is heavily embayed by all types of volcanic plains and occurs in the center of Lada Terra, may represent an outcrop of the ancient basement of this region. 2) The relatively older structural zones that are embayed by regional plains and represented mostly by the ridge belts (e. g. Morrigan Linea, Kuldurok Dorsa, etc.) are restricted within the lowlands and rarely occur within the highland of Lada Terra. 3) Quetzalpetlatl Corona may represent a long-lived structure if its northern rim is a fragment of a ridge belt. The rim, however, may be due to internal corona evolution, which is suggested by the spatial association of it with the moat. This kind of association commonly occurs at a number of large coronae [10-12]. 4) The youngest structural trends represented by the corona-rift zones occur within the elevated Lada Terra region [13]. In contrast to the older zones, the corona-rift chains do not extend into the lowlands, are absolutely dominated by extensional structures, and the sources of young vast lava flows typically occur along these zones.

References. Stofan, E.R., et al., *JGR*, 97, 13347-13378, 1992, 2) Stofan, E.R., et al., Coronae on Venus: Morphology and origin *in: Venus II Geology, Geophysics, Atmosphere, and Solar wind environment, S.W.Bougher, D.M. Hunten, and R.J. Phillips eds., Univ. Arizona Press Tucson*, 931-965, 1997, 3) Squyres, S.W. , et al., *JGR*, 97, 13579-13599, 1992; Ivanov, M. A., and J. W. Head, Geologic Map of Mylitta Fluctus Quadrangle (V-61), Venus, submitted to *U.S. Geol. Inv. Ser*., 2003, 4) Ivanov, M. A., and J. W. Head, Geologic Map of Mylitta Fluctus Quadrangle (V-61), Venus, this volume, 2003, 5) Banerdt W.B., et al., Plains tectonics on Venus *in: Venus II Geology, Geophysics, Atmosphere, and Solar wind environment, S.W.Bougher, D.M. Hunten, and R.J. Phillips eds., Univ. Arizona Press Tucson*, 901-930, 1997, 6) Ivanov, M. A. and J. W. Head, Geologic map of the Lavinia Planitia (V55) quadrangle *USGS Geol. Inv. Ser., Map I-2684*, 2001, 7) Roberts, K.M., et al., *JGR*, 97, 15991-16016, 1992, 8) McGill, G. and N. Bridges, Geologic map of the Kaiwan Fluctus Quadrangle (V-44), Venus, *USGS, Geologic Investigation Series, Map I-2747, Scale 1:5,000,000*, 2002, 9) Janes, D.M. and S.W. Squyres, *JGR*, 100, 21173-21187, 1995, 9) Schubert, G. and T.D. Sandwell, *Icarus*, 117, 173-196, 1995, 11) Ivanov, M. A. and J. W. Head, Geologic map of the Atalanta Planitia (V44) quadrangle *USGS Geol. Inv. Ser., in edit* 2002, 12) Magee, K.P. and J.W. Head, *JGR*, 100, 1527-1552, 1995.

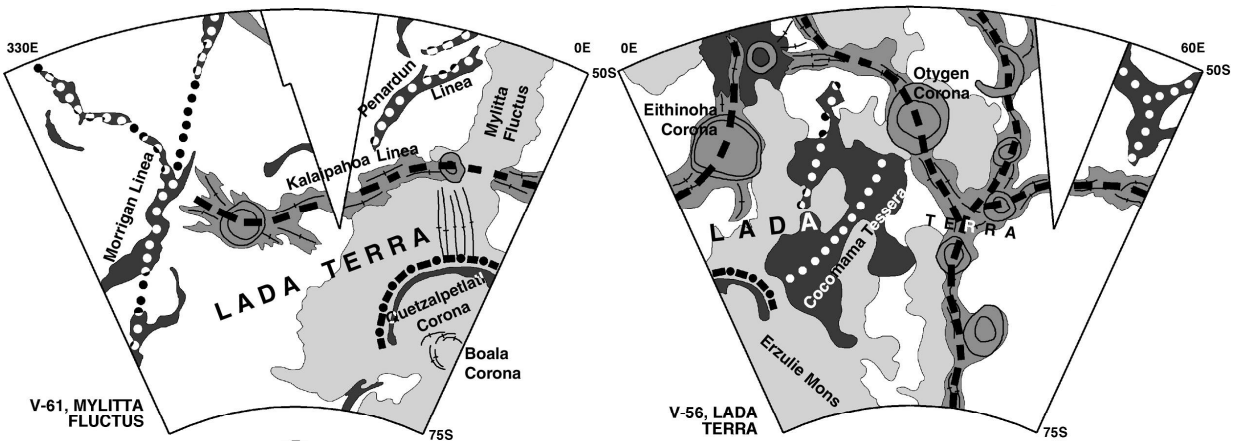

Figure 1. Sketch maps of V-61 and V-56 Quadrangles. Dark gray indicates older structural zones, young corona-rift zones are shown in gray, and light gray shows young lava flows. Strikes of structural trends are shown in dotted (old) and dashed (young) lines.

GEOLOGIC MAP OF THE MYLITTA FLUCTUS QUADRANGLE (V-61), VENUS: M.A. Ivanov[1,2] and J. W. Head[2], 1 - Vernadsky Institute, RAS, Moscow, Russia; 2 - Dept. of Geological Sciences, Brown University, Providence, RI 02912 USA.

Introduction: The Mylitta Fluctus Quadrangle (V-61, 50-75°S, 300-360°E, Fig.1) covers the southern part of Lavinia Planitia (a basin-like lowland [1], 1.5-2 km deep) and the western part of the Lada Terra upland (~3 km high). Lavinia Planitia has complex patterns of deformational belts [2,3] and Lada Terra hosts several large coronae, including Quetzalpetlatl [4], connected by belts of fractures and graben [5,6]. Large lava flows complexes (fluctūs) emanate from some coronae in Lada [7]. The characteristics of Lavinia Planitia suggest the large-scale mantle downwelling there [1,8] and the specific features of Lada Terra are consistent with mantle upwelling [9].

The major questions addressed by geological mapping in the Mylitta Fluctus area are as follows. 1) What is the sequence of events in the formation and evolution of large-scale lowlands and uplands on Venus? 2) What are the characteristics and timing of formation of the transition zone from Lada Terra to the surrounding lowlands? 3) How do the units in the map area compare with each other and what information do they provide concerning models for Venus global stratigraphy and tectonic history? In our analysis we have used traditional methods of geologic unit definition and characterization for the Earth [10] and planets [11] appropriately modified for radar data [12].

Stratigraphy: Although we have mapped tectonic structure independent of material units, in a few cases tectonic features are such a pervasive part of the morphology that it becomes part of the definition of a unit. In other cases, the approach depends on scale and density of structures. Here we summarize the stratigraphic units mapped in the quadrangle. *Densely lineated plains (pdl)*. This unit is characterized by relatively flat surfaces and swarms of dense (<1 km apart) subparallel lineaments. *Ridged and grooved plains (prg)*. This unit has relatively high radar albedo and is commonly deformed by relatively broad (~5-10 km wide) ridges tens of kilometers long. *Shield plains (psh)*. Abundant small shield-shaped features (from a few km to 10-20 km in diameter, many with summit pits) characterize this unit. *Wrinkle ridged plains (pwr_1 and pwr_2)*. These units are morphologically smooth plains material of intermediate-dark to intermediate-bright radar albedo complicated by networks of wrinkle ridges. The lower unit (pwr_1) is relatively homogeneous and the upper unit (pwr_2) has slightly higher albedo and lobate boundaries in places. *Shield cluster (sc)*. The surface of this unit is morphologically similar to that of shield plains but, in contrast, is tectonically intact and displays distinct lava flows superimposed on the plains nearby. *Smooth plains (ps)*. This unit is tectonically intact and has uniform and typically low albedo. *Lobate plains (pl_1 and pl_2)* have numerous flow-like internal elements and unit boundaries are typically lobate. The lower unit *(pl_1)* is characterized by a subdued pattern of the flows and the upper unit *(pl_2)* has very prominent pattern of the flows. *Impact crater materials (c)* include impact craters and related deposits.

Geologic history: The distribution of the mapped units in space and time allows outlining the geologic history within the Mylitta Fluctus quadrangle. In contrast to many other areas on Venus where tessera forms the oldest material unit [13-15], the V-61 quadrangle represents a vast tessera-free area. This suggests that either tessera never formed there or it was completely covered by subsequent lava plains units. The densely lineated volcanic plains (unit pdl), thus, represent the oldest exposed unit in the map area. The deformation patterns in pdl are very dense, unidirectional, and were formed due to extension. Fragments of pdl occur within the upland and lowland parts of the map area suggesting a more extensive presence of the unit in the subsurface. Following the emplacement and deformation of pdl, a less intensely deformed plains unit was emplaced (unit prg). The most important features of prg are ridges that are very pervasive in places. Occurrences of the unit form a large (SW-NE) zone of broad arches within the lowlands. The arches run roughly parallel to the edge of Lada Terra. In the NE corner of the map, however, small fragments of prg are within the Lada upland. The material of prg and its deformation separate the lowlands around Lada Terra into secondary small-scale basins.

After emplacement and deformation of prg, a plains unit characterizing by abundant small volcanoes (shield plains, psh) was emplaced. The morphology of this unit indicates widespread local and shallow magma sources during its emplacement. The lack of broad ridges within psh means that regional compressional stresses had waned in intensity before emplacement of the unit. Subsequent to the formation of shield plains the style of volcanism changed [16]. Instead of abundant small volcanoes, vast plains (units pwr_1 and pwr_2) were emplaced from sources that are now rarely visible. The wide extent of these units and the presence on their surface of narrow sinuous channels within the quadrangle and elsewhere [17-18] suggest a high-effusion-rate mode of emplacement from a few sources. The units pwr_1, pwr_2, and psh were deformed by wrinkle ridges during and subsequent to their emplacement. Some wrinkle ridges are oriented consistently with the tectonic fabric typical of prg. Thus, the deformation recorded in these units appears to be consistent in trends but reflects a decrease in the intensity of deformation with time.

The V-61 quadrangle displays a rich geological record of relatively late (post wrinkle ridged plains) volcanic and tectonic activity. Abundant occurrences of smooth plains (unit ps) in many places tend to occur near distinct volcanic centers, which indicates that smooth plains at these localities are morphologically smooth and homogeneous facies of late volcanism in the map area. Lobate plains (units pl_1 and pl_2) that were emplaced after

formation of wrinkle ridges are almost completely restricted within the upland of Lada Terra and related to two major sources in the northern and central parts of the upland. The latest volcanic activity has led to formation of enormous lava complexes (fluctūs) near these centers. There are no large or medium-sized volcanoes associated with these regions, however [19]. This suggests that the eruptions that produced the fluctūs were probably not persistent enough to form prominent volcanic constructs. Volcanism at the time of formation of ps and pl played a significant role in resurfacing and continued to operate as an important factor in formation of the extensive flood-like plains units. Of the nine impact craters seen in the map area one (Alcott) is embayed by pl flows. Within the map area there are no craters possibly cut by tectonic structures.

There are clear trends in the evolution of tectonic regimes within the Mylitta Fluctus Quadrangle. Contractional deformation decreased in intensity from higher level associated with the formation of ridge belts (unit prg) to lower levels associated with deformation of regional plains (units pwr_1 and pwr_2) by pervasive structures of wrinkle ridges. Contractional structures are absent within younger units suggesting seizing of compressional stresses by the time of units emplacement.

Extensional deformation that overprints densely lineated plains (pdl) and forms groove belts (gb) and rift zones (rt) appears to have an opposite trend. Fractures in pdl are narrow, pervasive, and do not form belt-like concentrations. The subsequent extensional structures are organized into belts the individual structures of which on average become progressively broader as a function of time. It is important to note that some occurrences of older groove belts continue the general trend of younger rift zone. This suggests that the rift probably inherited the structural trend of groove belts and may be a result of reactivation of a precursor deformation belt. Thus, the general orientation of tension stresses appears to be stable through a significant part of geologic history within the quadrangle, from before the emplacement of regional plains to the time of formation of lobate plains.

References:

1) Bindschadler, D.L. et al., *JGR*, 97, 13,495, 1992; 2) Squyres, S.W., et al., *JGR*, 97, 13579, 1992; 3) Solomon, S.C., et al., *JGR*, 97, 13,199, 1992; 4) Stofan, E.R., et al., *JGR*, 97, 13347, 1992; 5) Baer, G. et al., *JGR*, 99, 8355, 1994; 6) Magee, K. P. and Head, J. W., *JGR*, 100, 1527, 1995; 7) Roberts, K.M., et al., *JGR*, 97, 15991, 1992; 8) Simons, M. et al., *GJI*, 131, 24, 1997; 9) Kiefer, W.S. and Hager, B.H., 1991, *JGR*, v. 96, 20947, 1991; 10) American Commission on Stratigraphic Nomenclature, AAPGB, 45, 645, 1961; 11) Wilhelms, D.E., 1990, Geologic mapping, *in:* Planetary mapping, R. Greeley and R.M. Batson eds. 208, 1990; 12) Tanaka, K.L., USGS Open File Report 94-438, 50 p., 1994; 13) Ivanov, M.A., and Basilevsky, A.T., 1993, *GRL*, 20, 2579, 1993; 14) Ivanov, M.A., and Head, J.W., *JGR*, 101, 14861, 1996; 15) Hansen, V.L. et al., *in:* Venus II, Phillips et al., eds, 797, 1997; 16) Head, J. W. et al., *LPSC 27*, 525, 1996; 17) Baker, V.R. et al., *in:* Venus II, Phillips et al., eds, 757, 1997; 18) Basilevsky, A.T., and Head, J.W., *GRL*, 23, 1497, 1996; 19) Crumpler, L.S. and Aubele, J.C., *in:* Encyclopedia of Volcanoes, 727, 2000

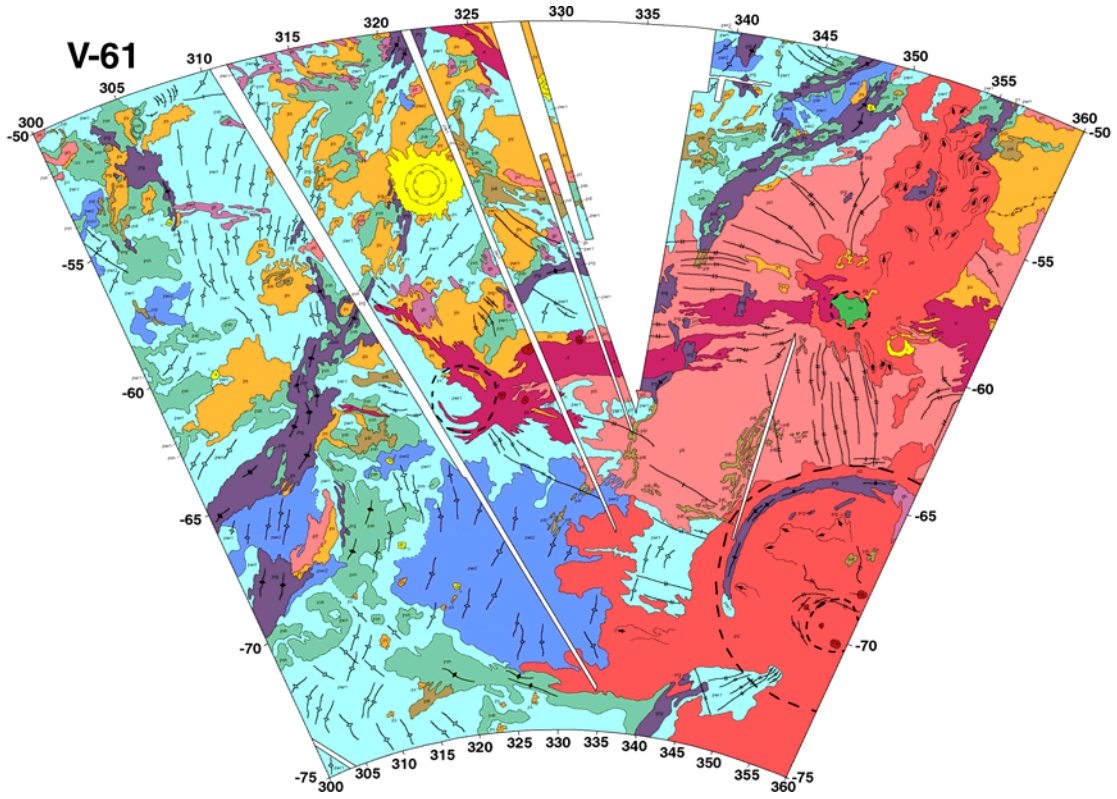

GLOBAL GEOLOGICAL MAPPING OF EUROPA: STRATEGY AND UPDATE.

P.H. Figueredo[1], K. Tanaka[2], D. Senske[3], T. Hare[2], R. Greeley[1], and T. Becker[2]; [1]Dept. Geological Sciences, Arizona State U., Tempe, AZ 85287-1404 (figueredo@asu.edu); [2]U. S. Geological Survey, 2255 N. Gemini Dr., Flagstaff, AZ 86001; [3]Jet Propulsion Laboratory, 4800 Oak Grove Dr., Pasadena, CA

Introduction

Knowledge of the global distribution of Europan geologic units in time and space is a necessary step for the synthesis of the results of the Galileo mission and in preparation for future exploration (namely, by the Jupiter Icy Moon Orbiter (JIMO)) of the satellite. We have initiated the production of the first global geological map of Europa, using the recently published global photomosaic of Europa (USGS Map I-2757) as a base map. This photomosaic covers most of the satellite and combines Voyager and Galileo images at variable spatial resolution. The map will be produced entirely in GIS format for analysis and combination with other datasets.

Strategy

We expect to produce a global geological map at 1:10M scale and several high-resolution insets (1:5M scale), on a separate sheet, that will illustrate the morphologic and stratigraphic complexity of Europa's surface. Different mappers will be responsible for mapping different classes of features, to allow the application of uniform criteria for the distinction of units and sub-units, cross-checking, and detailed assessment of the relations with other units. Given the uneven resolution of the base photomosaic, stratigraphic relationships from all high-resolution Galileo observations will be extrapolated onto the global context.

One of the principal objectives of this project is to establish a global stratigraphic framework for Europa. In the absence of a well-developed cratering record, this goal will be achieved using the global network of lineaments. Stratigraphic information will be displayed and synthesized in correlation charts showing age variations relative to latitude and longitude. The results with be contrasted, revised, and expanded with the aid of GIS routines tailored to compile a stratigraphy based on the relative ages of prominent lineaments that form broad arcs across Europa's surface (B. Pappalardo, *personal communication*, 2003).

The minimum dimension for mapping a feature as a unit is 20 km (2mm on the map); smaller features of interest can be mapped as structures or dots showing their location. Albedo mantles should be mapped with a stippled pattern superimposed on the underlying unit. A preliminary unit-symbol format is proposed, where unit $XYz_{\#}$ consists of X, stratigraphic age; Y, region; z, feature type; and $_{\#}$, sequence number and/or feature subtype).

Update

With assistance from J. Blue (USGS Nomenclature Specialist), we have proposed formal names for 14 *lineae* (lineaments) and one *regio* (region) that are key for stratigraphic studies. The careful examination of the global lineament network has shown that the existing image coverage, even with broad regions of km/pixel resolution, will allow some degree of stratigraphic control throughout most of the satellite. In addition, we have revised the base photomosaic for completeness and geodetic control quality. A new version, including all available data, is likely to be generated shortly.

Because of our focus on stratigraphy, we opted for the distinction and mapping of *allostratigraphic* (aka, unconformity-bounded) and *lithostratigraphic* units in

our global map (cf., Skinner and Tanaka, 2003). Using this method, we expect to use the major tectonic and chaos formation events (marked with a star in Figure 1) to bracket any other geologic feature or event. We have applied this approach on the independent mapping of a test region in the equatorial trailing hemisphere (Figure 2). All mappers identified similar units and stratigraphic relations, and only minor differences in the level of detail, nomenclature, and symbology resulted. We have begun the mapping phase of our project with the region between 140° and 250° longitudes.

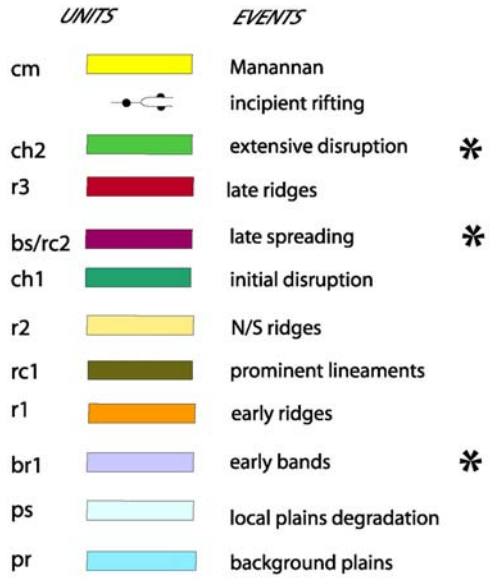

Figure 1. Sequence of map units for Europa test region shown in Figure 2.

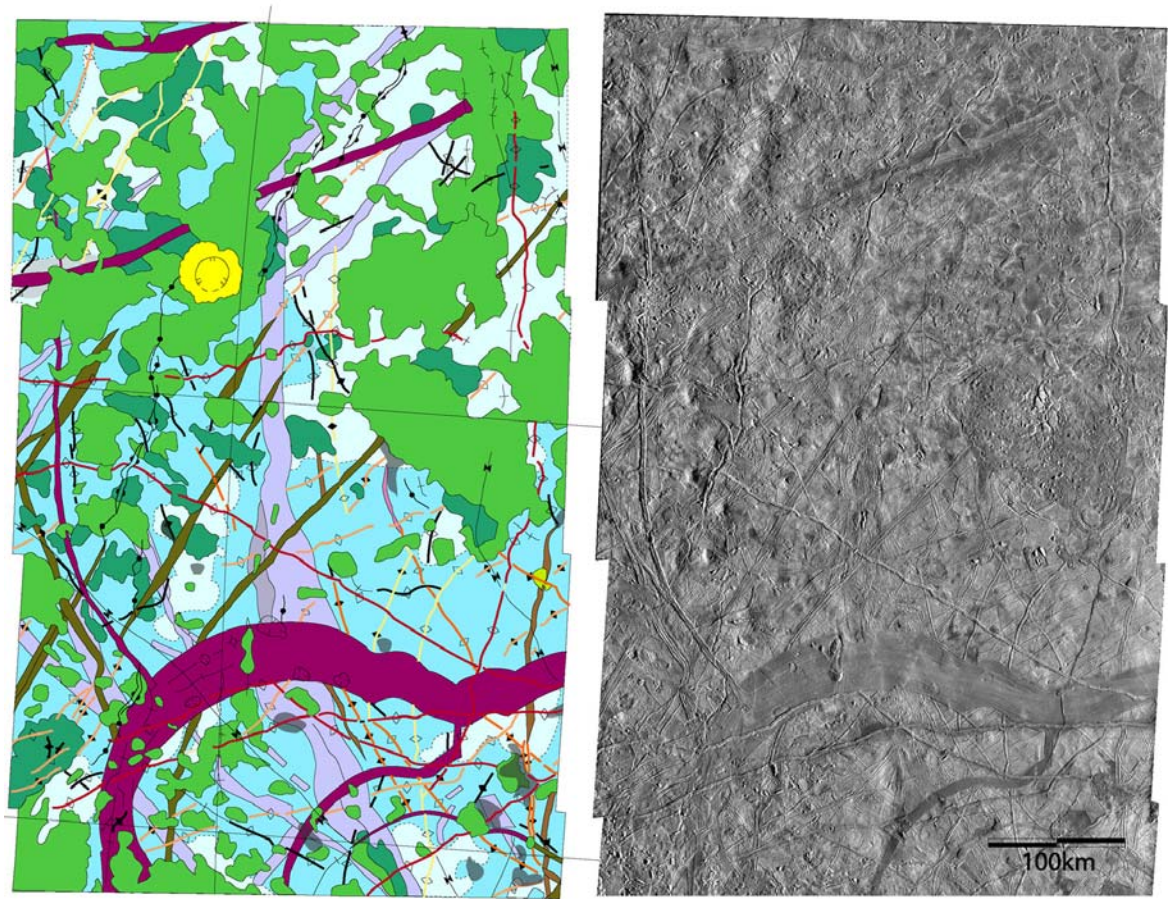

Figure 2. Geologic map (left) and photomosaic of Galileo images (right) of a region on Europa where each mapper independently produced a geologic map to develop mapping approaches and test consistency of results.

GLOBAL MAPPING OF BRIGHT TERRAIN ON GANYMEDE: A POST-GALILEO VIEW OF UNITS AND STRUCTURES. Geoffrey C. Collins[1], James W. Head[2], G. Wesley Patterson[2], Robert T. Pappalardo[3], and Louise M. Prockter[4]. [1]Wheaton College, Norton, MA 02766 (gcollins@wheatonma.edu); [2]Department of Geological Sciences, Brown University, Providence, RI 02912; [3]LASP, University of Colorado, Boulder, CO 80309; [4]Applied Physics Laboratory, Laurel, MD 20723.

Geologic mapping of Ganymede based on Voyager data has divided Ganymede terrain units into three basic classes: light material, dark material, and crater materials [1-3]. Almost two thirds of the surface of Ganymede is covered by light material, also known as bright terrain.

Bright terrain on Ganymede is pervasively cut by "grooves," which are topographic troughs, often occurring in closely packed sets. Voyager-based studies of grooves generally interpreted them as extensional tectonic features [4-5], and Galileo-based studies have confirmed this interpretation, though with more apparent extensional strain than Voyager-based studies had considered [6-7]. The ridges and troughs that make up the grooves are characterized by hundreds of meters of topographic relief [5,8], and a characteristic spacing of about 5 to 10 km [9].

In principle, geological map units are material units and should be independent of structure [10], and most workers adopt this approach. In planetary mapping, however, exceptions have often been made due to the local and regional dominance of structural features, the synoptic and remote sensing aspect of the data, and the scale of the mapping (e.g., [11]). On Earth, rock-stratigraphic units are defined as "...a subdivision of the rocks in the Earth's crust distinguished and delimited on the basis of ....observable physical features... [commonly lithologic]... and independent from time concepts... and... inferred geologic history..." [10]. In planetary mapping stratigraphic units must be defined largely by remote sensing and so it is difficult to approach the process of geologic mapping of planetary crusts with a strict 'lithologic' definition of units. As outlined by Wilhelms [11], planetary mappers use the broader definition of rock-stratigraphic units as those "distinguished and delimited on the basis of observable physical features", which might include surface morphology, albedo, etc. (see also [12]).

The distinction and individual mapping of structures, or their inclusion in the definition of a unit, is clearly a function of the scale of mapping. What might be mapped separately as individual structures at a scale of 1:100,000 would very likely be included as part of a unit definition or characterization at a scale of 1:15M. Bright terrain on Ganymede offers mappers such a conundrum. At high resolution, the faults which make up the grooved terrain are clearly visible and can be mapped individually. At the regional or global scale, such a map of structures would be incomprehensible due to the density of features, and it would thus be best to map areas with similar structural characteristics as separate units.

All Voyager-based maps separated smooth light material from light material with grooves, and further separated grooves into three classes: subdued, sharp, and throughgoing or conspicuous grooves. Throughgoing grooves were mapped along their length as features, while subdued and sharp grooves were mapped as units with a feature showing representative groove trends. Some mappers also added graben or graben-like structures to describe large grooves [2], or used a separate description for reticulate or overlapping grooves [3].

In high resolution Galileo images, we were not able to distinguish consistent morphological differences between units mapped as sharp grooves and features mapped as throughgoing grooves. The basic difference is the linear extent of these structures, and whether they are truncated by younger structures. The faults which make up these features are dominated by the tilt-block morphology [7]. There is also a continuous gradation at high resolution between units mapped as light smooth material and units mapped as subdued grooves. These areas are dominated by topography that is locally flat, with dark lineaments and occasionally graben-like structures cutting through them [7].

We believe the best way to map the bright terrain is to divide it into three units, which are distinguishable at the global scale, and which have distinct morphological differences at high resolution.

The first unit is subdued material: Material with subdued topography and a low density of grooves. This unit covers most of what has been previously mapped as smooth bright material, and some of the subdued grooved bright material. An example of subdued material is shown in figure 1.

The second unit is grooved material: Material consisting solely of groove lanes. This unit covers the sharp grooved bright material, the throughgoing grooves, and some of the subdued grooved bright material.

The third unit is undivided material. This unit is necessary because a significant portion of Ganymede has not been imaged at a resolution sufficient to distinguish subdued material from grooved material.

Dividing the bright terrain units by groove morphology does not lead to a clear age relationship among these units. Subdued and grooved material appear both early and late in the stratigraphic sequence interpreted in high-resolution target areas [13-14]. By using cross-cutting relationships among the faults in the bright ter-

rain, we can derive the age relationships among the bright terrain units. This has already been done for some sections of Ganymede, using three age units in Uruk Sulcus [13] and Nun Sulci, four age units in western Sippar Sulcus [14], and five age units in eastern Sippar Sulcus and the leading hemisphere [15]. The youngest grooves on Ganymede form a network of connected structures that can be traced across the globe [16], but correlation of the older units and determination of the optimal number of age units to use for global stratigraphic correlation in the final map are yet to be determined.

References: [1] B. Lucchitta et al., USGS Map I-2289, 1992; S. Croft et al., USGS Map I-2328, 1994; R. Wagner et al., USGS Map I-2497, 1995; J. Underwood et al., USGS Map I-2534, 1997; D. Wilhelms, USGS Map I-2442, 1997; [2] S. Murchie and J. Head, USGS Map I-1966, 1989; R. DeHon et al., USGS Map I-2388, 1994; [3] J. Guest et al., USGS Map I-1934, 1988; G. McGill et al., USGS Map I-2459, 1997; [4] E. Shoemaker et al., Satellites of Jupiter, 435-520, 1982; [5] E. M. Parmentier et al., Nature 295, 290-293, 1982; S. Squyres, Icarus 52 545-559, 1982; [6] G. Collins, GRL 25, 233-236, 1998; R. Pappalardo and G. Collins, J. Struct. Geol., submitted; [7] R. Pappalardo et al., Icarus 135, 276-302, 1998; [8] B. Giese et al., Icarus 135, 303-316, 1998; [9] R. Grimm and S. Squyres, JGR 90, 2013-2021, 1985; J. Patel et al., JGR 104, 24,057-24,074, 1999; [10] ACSN, AAPGB, 45, 645, 1961; [11] D. Wilhelms, USGS IP 55, 1972; D. Wilhelms, Cambridge, 208, 1990; [12] J. Head et al., Icarus, 33, 145, 1978; [13] G. Collins et al., Icarus, 135, 345, 1998; [14] G. Collins et al., LPSC XXIX, 1319, 1998; [15] J. McBee and G. Collins, LPSC XXXIII, 1449, 2002; [16] G. Collins, LPSC XXXIII, 1783, 2002.

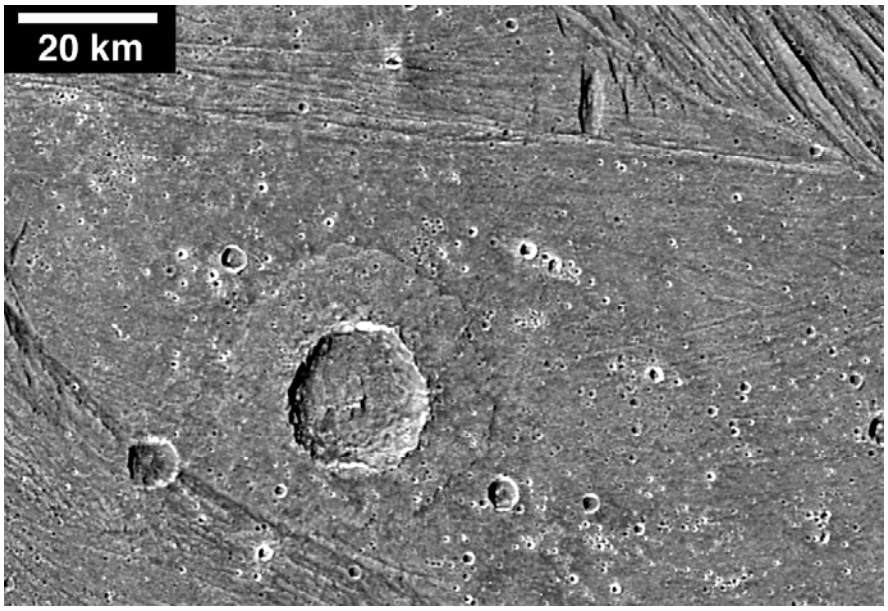

Figure 1. Subdued material in the bright terrain at high resolution, from the G28 smooth terrain observation in Harpagia Sulcus. In the upper right corner is grooved material.

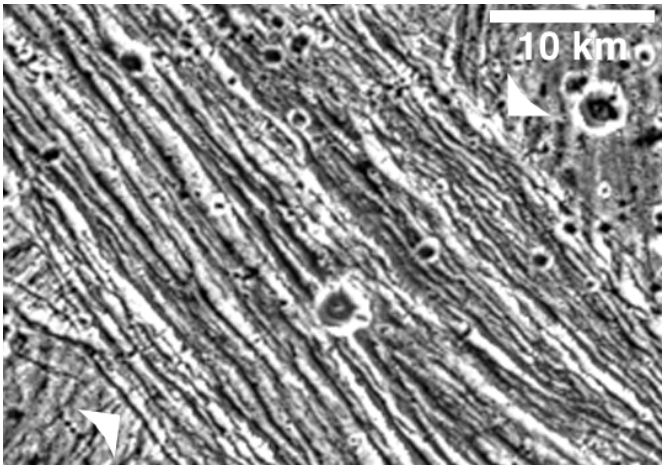

Figure 2. Grooved material in the bright terrain at high resolution, from the G1 Uruk Sulcus observation. The grooved material lies between the two arrows, and the material in the upper right and lower left corners is subdued material.

GLOBAL MAPPING OF GANYMEDE AT 1:15M SCALE: DEFINING DARK TERRAIN. G. Wesley Patterson[1], James W. Head[1], Geoffrey C. Collins[2], Robert T. Pappalardo[3], and Louise M. Prockter[4]. [1]Department of Geological Sciences, Brown University, Providence, RI 02912 USA (james_head@brown.edu); [2] Wheaton College, Norton MA 02766, [3]LASP, University of Colorado, Boulder, CO 80309; [4]Applied Physics Laboratory, Laurel, MD 20723.

Introduction: Dark terrain on Ganymede occurs as isolated areas (regiones) of polygonal, rounded, or irregular outline and is distributed randomly across its surface. The size of these polygons varies from >3000 km across (Galileo Regio) to slices of terrain <10s of km long. In total, ~500 polygons of dark terrain have been identified comprising 35% of the surface of Ganymede [1].

Dark terrain is generally accepted to be >4 Gyr old [2, 3] based on measured crater densities. It is commonly transected by linear to sublinear furrows ~10km wide and up to 100s of km long [4]. Galileo high resolution images suggest that dark terrain is composed of a relatively thin, dark lag deposit overlying brighter icy material, and has been modified by sublimation, mass wasting, ejecta blanketing, and/or tectonism [5, 6].

Geologic maps produced at the 1:5M scale have divided dark terrain polygons into numerous geologic units based typically on perceived differences in overlying structure and/or apparent surface albedo. We are preparing a global geologic map of the satellite at the 1:15M scale and there are a number of issues that must be considered. These include: 1) Developing unit definitions that encompass all characteristics identified in previous quadrangle maps, 2) Validating distinguishing characteristics between previously mapped units using high resolution Galileo images, and 3) Determining whether or not the distinguishing characteristics of previously mapped units would be visible at a scale of 1:15M.

Discussion: From 1984 through 2001 geologic maps of fifteen quadrangles of Ganymede were produced, each by different authors. Several of the dark terrain units defined were common among the various maps including: 1) furrowed material– forms arcuate troughs flanked by rims that are estimated to be ~100 km high [7], 2) lineated material– has faint parallel to subparallel lineations and 1 to 5 km wide linear depressions that are less straight, less regularly spaced, and less even in width than grooves in light materials [8], and 3) undivided material – dark materials whose characteristics are difficult to identify because of poor resolution of images [9]. We plan to adopt these general units at the 1:15M scale.

Some units are unique to a particular quadrangle however, and assessing which of these merits inclusion at the scale of the global map is necessary. Figure 1 shows a Voyager 2 image of the Uruk Sulcus region which overlaps the Jg-8 Uruk Sulcus quadrangle as well as the Jg-12 Osiris quadrangle. Near the border of the two quadrangles (dashed line), *Guest et al.* [7] identified a reticulate unit consisting of material cut by two or more sets of grooves 20 to 70 km long and 4 to 8 km wide intersecting at angles ranging from 30° to 90°. They also identified a dark grooved unit consisting of material of low but variable albedo cut by closely spaced grooves (about 12 km apart) 25 to 100 km long and about 5 km wide which is similar in texture to light grooved material but forming less regular patterns. A dark vermicular unit is also identified whose albedo tends to be lower than that of other dark cratered materials with a surface that is generally rough and cut by sinuous troughs a few tens of kilometers long and as wide as 5 km.

Wilhelms [10] also defines three dark terrain units in this area. There is a reticulate unit defined as being cut by short grooves meeting at high angles with an apparent albedo intermediate between typical dark and light materials. There is a dark reticulate unit which is simply defined as similar to the reticulate unit but with a lower apparent albedo and there is a dark furrowed unit described as widely spaced furrows a few kilometers wide that have raised, scalloped, ragged rims.

The similarities between the reticulate and grooved units of the two quadrangles indicate that they could be combined into a single "reticulate" unit in the global geologic map. The dark vermicular and dark furrowed units also share a similar definition and should therefore also be combined into a single unit. Given the more common use of dark furrowed material as a unit, we prefer its use for the combined unit in this image.

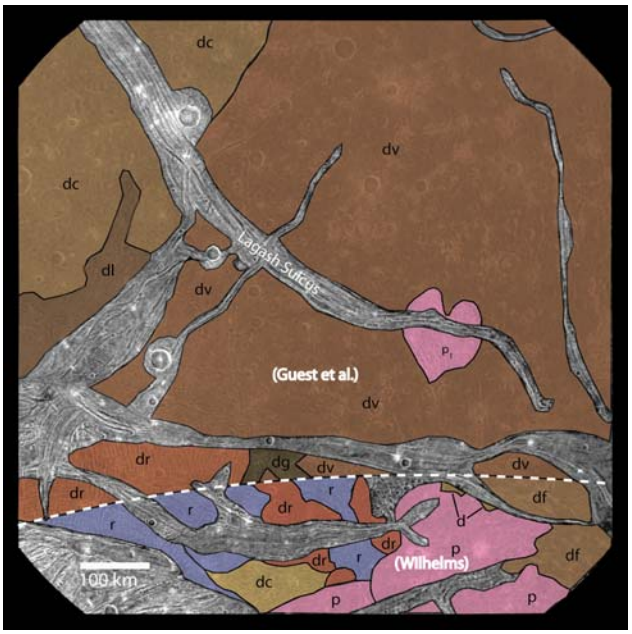

Fig. 1 Voyager 2 image C20637.29 found in the Jg-8 Uruk Sulcus quadrangle. Dark terrain geologic units (as defined by *Guest et al.* [7] and *Wilhelms* [10]) have been superimposed. Dashed line indicates approximate boundary between Jg-8 and Jg-12 quadrangles.

Beyond variations in mapped units between quadrangles, verifying the distinguishing characteristics between previously mapped units with high resolution Galileo images is an important step in defining the units that will comprise the global map of Ganymede. Figure 2 includes two high resolution images in the Uruk Sulcus quadrangle [7] that encompass three dark terrain geologic units: scabrous material, furrowed material, and lineated material. The images indicate no discernable difference between any of the three units at high resolution. This implies that they should be represented by a single unit and again we prefer the more commonly used furrowed material unit.

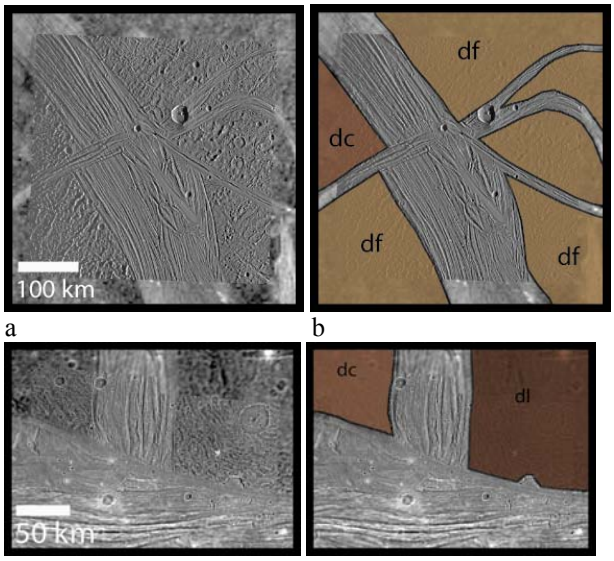

Fig. 2 High resolution Galileo images found in the Jg-8 Uruk Sulcus region; a) Tiamat Sulcus; b) superimposed dark terrain units as indicated by *Guest et al*. [7]; c) Erech Sulcus; d) superimposed dark terrain units as indicated by *Guest et al*. [7]

Another important consideration is whether or not the distinguishing characteristics of various material units would be visible at the 1:15M scale. While the preceding argument indicated that many of the previously mapped dark material units may actually comprise a single unit, high resolution images of Ganymede do indicate regional differences in the texture of dark terrain (Fig. 3). These differences however, are not visible at the kilometer scale represented by the global map being prepared. This, coupled with incomplete high resolution spatial coverage of the surface of Ganymede, implies that these differences cannot be effectively mapped at this time.

Conclusions: Taking into account the issues outlined above, we propose dividing dark terrain on Ganymede into four material units: 1) dark material, 2) lineated material, 3) reticulate material, and 4) undivided material. Dark material will encompass units previously mapped as cratered material, furrowed material, vermicular material, scabrous material, smooth material, and hummocky material. Lineated material will encompass all previously mapped lineated material and some materials previously mapped as grooved material. Reticulate material will combine all reticulate material units mapped in various quadrangles and some materials previously mapped as grooved material. Undivided material will comprise all materials of sufficiently low resolution that its material properties cannot be determined.

All structural properties distinguishable at the 1:15M scale will be superimposed on the material units described above. The text of the map will reflect the fact that, while indistinguishable at the scale mapped, regional textural differences in dark terrain do exist. This will be accomplished by including specific examples of these "subunits" at Voyager and Galileo resolution as sketch map and image examples in figures within the text.

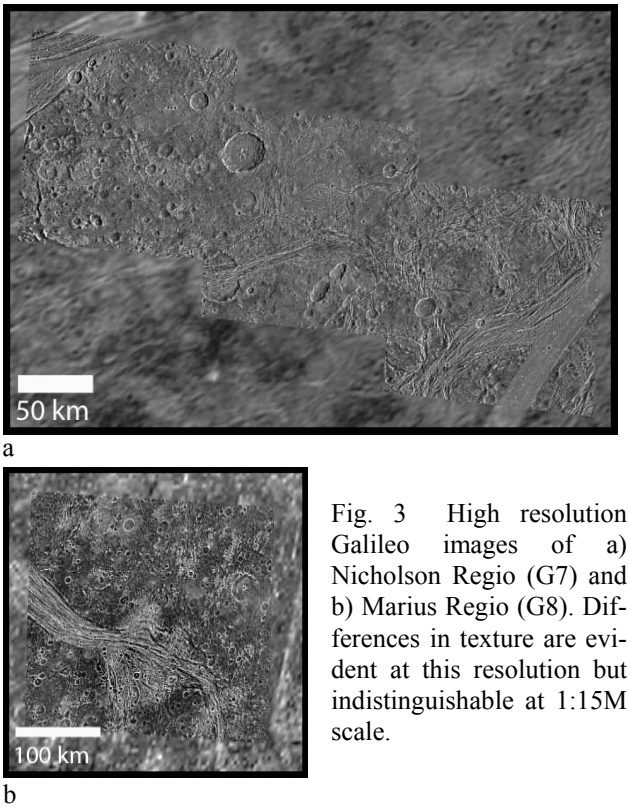

Fig. 3 High resolution Galileo images of a) Nicholson Regio (G7) and b) Marius Regio (G8). Differences in texture are evident at this resolution but indistinguishable at 1:15M scale.

References: [1] G. Collins et al., Icarus, 135, 345, 1998; [2] G. Neukum et al., LPSC XXIX, #1742, 1998; [3] K. Zahnle et al., Icarus, 136, 202, 1998; [4] E. Shoemaker et al., Sats. of Jupiter, 435, 1982; [5] L. Prockter et al, Icarus, 135, 317, 1998; [6] L. Prockter et al., JGR, 105, 22,519, 2000; [7] J. Guest et al., USGS Map I-1934, 1988; [8] B. Lucchitta et al., USGS Map I-2289, 1992; [9] R. Wagner et al., USGS Map I-2497, 1995; [10] D. Wilhelms, USGS Map I-2242, 1997.

REGIONAL GEOLOGIC MAPPING OF IO USING *GALILEO* SPACECRAFT DATA. D.A. Williams[1], L.P. Keszthelyi[2], E.P. Turtle[3], J. Radebaugh[3], W.L. Jaeger[3], M.P. Milazzo[3], A.S. McEwen[3], J.M. Moore[4], P.M. Schenk[5], R.M.C. Lopes[6], and R. Greeley[1], [1]Department of Geological Sciences, Arizona State University, Box 871404, Tempe, Arizona, 85287 (David.Williams@asu.edu); [2]Astrogeology Branch, U.S. Geological Survey, Flagstaff, Arizona; [3]Lunar and Planetary Laboratory, University of Arizona, Tucson, Arizona; [4]NASA Ames Research Center, Moffett Field, California; [5]Lunar and Planetary Institute, Houston, Texas; [6]NASA Jet Propulsion Laboratory, Pasadena, California.

Introduction: NASA's *Galileo* spacecraft has successfully completed its Mission at Jupiter, which included 5 close flybys of the volcanic moon Io (I24: October 1999, I25: November 1999, I27: February 2000, I31: August 2001, I32: October 2001). A wide range of global, regional, and local-resolution color and grayscale images were obtained during these flybys [1], mostly of the antijovian hemisphere that was poorly imaged by the 1979 Voyager flybys. These new images provide an excellent resource for new geologic mapping of Io. We have been funded by the NASA Planetary Geology and Geophysics program (grants to R. Greeley and A. McEwen) to study Io using planetary mapping techniques. Some of the goals we hope to accomplish through our mapping include: 1) identifying the styles and diversity of explosive and effusive volcanic materials erupted on Io; 2) defining the volcanic histories of specific regions of Io; and 3) developing guidelines that can be extended to both future local-scale and global-scale mapping to better understand the geologic evolution of Io. Here we outline our initial approach to mapping Io using *Galileo* spacecraft data, present our results from mapping two regional mosaics, and state our plans for future work.

Approach: Our initial approach to mapping Io using *Galileo* data has been to start with regional-resolution (150-300 m/pixel) mosaics that cover a variety of surface features in regions of the antijovian hemisphere. Our primary basemaps are Solid-State Imaging (SSI) grayscale images, along with versions that have been merged with lower-resolution global color data from orbit C21 (July 1999). Because active eruptions can cause surface changes in our map regions since the color data were obtained, we restrict our use of the merged images to color interpretations of features that appear unchanged from orbit to orbit. We also utilize Near-Infrared Mapping Spectrometer (NIMS) data where possible to note the locations of active hotspots, any changes in activity, and estimates of SO_2 abundance. As of this writing (June 2003) we have completed two regional maps of Io: the Chaac-Camaxtli region, and the Culann-Tohil region (**Fig. 1**). The Chaac-Camaxtli map was published in the September 2002 issue of *JGR-Planets* [2] (because of an error in the color page in the journals mailed to subscribers, a corrected color map was published in the March 2003 issue of *JGR-Planets*). The Culann-Tohil map was submitted to the *Icarus* Io Special Issue; it has been reviewed and is currently in revision.

Mapping Results: The following paragraphs summarize some of the key insights that have been learned from mapping of the Chaac-Camaxtli region and the Culann-Tohil region. For the the Chaac-Camaxtli region (see page 4 of abstract), key insights include: (a) the close proximity of dark and bright lava flows and diffuse deposits suggests that there is an intimate interaction between silicate magmas and sulfur-bearing volatile materials that produced a variety of explosive and effusive deposits in the recent geologic past; (b) the paterae in this region are volcanic centers analogous in morphology to terrestrial calderas but larger in size, in which most active paterae occur in apparent topographic lows, whereas less active or inactive paterae occur on higher mesas, suggesting that crustal thickness variations may influence magma access to the surface; (c) the relatively regular spacing of paterae (~100-150 km) along a line in this region may indicate there are multiple interlacing fractures in the crust that serve as magma conduits; and (d) some inactive patera floors may be evolving into bright plains material, suggesting that if the crust is composed of silicates (covered in a mantle of bright sulfurous materials), then it should have sufficient strength to support the steep patera walls in Chaac Patera (2.8 km deep, 70° slope) and the high mountains seen elsewhere on Io.

For the Culann-Tohil region (see page 5 of abstract), key insights include: (a) a new shield volcano has been discovered with an adjacent bright lava flow field, Tsũi Goab Fluctus, that is the center of a low-temperature NIMS hotspot that could represent the best case for active effusive sulfur volcanism detected by *Galileo*; (b) irregularly-shaped green diffuse deposits in Culann Patera and Tohil Patera suggest that they are a coating produced by the interaction of warm, silicate lava flows with ballistically-emplaced contaminants from Culann's sulfurous plumes; (c) Culann Patera has produced a range of explosive and effusive deposits, including: (i) an outer yellowish ring of enhanced sulfur dioxide (SO_2), (ii) an inner red ring of SO_2 with short-chain sulfur (S_3-S_4) contaminants, (iii) fresh black lava flows west of the Culann vent, and (iv) unusual red-brown flows east of the vent; (d) Tohil Mons is composed of an older unit of tectonically-disrupted crustal material and a younger unit of mottled crustal materials that was displaced by mass wasting; and (e) from 0°-15°S the hummocky bright plains contains scarps, grooves, pits, graben, and channel-like features

which are indicative of erosional processes. Discrete volcanic events can be identified through stratigraphic correlation of map units.

Future Work: We are currently funded to produce one additional regional geologic map, the Zamama-Thor* region (Fig. 1, orange boundary). Figure 1 shows several other well-imaged regions of Io (outlined in red) that would benefit from geologic mapping. We also intend to publish a paper that outlines our suggested guidelines for further geologic mapping of Io using *Galileo* data, similar to the paper published by Greeley et al. (2000) for Europa [3]. For example, based on our previous geologic mapping of Io, there are five primary types of geologic material units that can be defined and characterized: plains, patera floors, flows, mountains, and diffuse deposits. These are essentially the same types found from *Voyager* analyses. The plains materials have various degrees of layering and texturing, resulting from a complex history of deposition and erosion of sulfurous [4] and silicate explosive and effusive volcanic deposits, volcanic vent and mountain formation, and perhaps other as yet unidentified processes. Patera floor materials have a wide range of colors, albedos, and textures that depend upon the composition and eruption styles of the volcanic materials that cover them. Lava flow materials also have a range of colors and albedos from dark to bright; dark flows are thought to be mafic or ultramafic silicate lavas and bright flows are thought to be sulfur and/or sulfur dioxide (SO_2) flows [5, 6]. Mountain materials resulted from uplift of crustal blocks [7, 8, 9], mantling by plume deposits, and erosion by mass movement [10]. Diffuse deposits, which *Galileo* images show exist in five basic colors (white, black, yellow, red, and green), are produced when material ejected in explosive plume eruptions settles on the surface. These deposits likely consist of both pyroclastic fragments and frozen gases.

References: [1] Keszthelyi et al., *J. Geophys. Res. 106*, 33,025-33,052, 2001; Turtle et al., *Icarus*, in review; [2] Williams, D.A., et al., *J. Geophys. Res. 107*(E9), 5068, doi:10.1029/2001JE001821, 2002; [3] Greeley, R. et al., *J. Geophys. Res., 105*, 22,559-22,578, 2000; [4] Douté, S., et al., *Icarus 149*, 107-132, 2001; Douté, S., et al., *Icarus, 158*, 460-482, 2002; [5] McEwen et al., *Science 288*, 1193-1198, 2000; [6] Williams, D.A., et al., *J. Geophys. Res. 106*, 33,105-33,119, 2001a; Williams, D.A., et al., *J. Geophys. Res., 106*, 33,161-33,174, 2001b; [7] Carr, M.H., et al., *Icarus 135*, 146-165, 1998; [8] Schenk, P.M. and M.H. Bulmer, *Science, 279*, 1514-1517, 1998; Schenk, P., et al., *J. Geophys. Res. 106*, 33,201-33,222, 2001; [9] Turtle, E.P., et al., *J. Geophys. Res. 106,* 33,175-33,200, 2001; [10] Moore, J.M., et al., *J. Geophys. Res. 106*, 33,223-33,240, 2001.

Figure 1 (page 3). Current geologic mapping coverage of the antijovian hemisphere of Io using *Galileo* imaging data. Green represents regions where mapping has been completed; orange represents regions where mapping is in progress under currently funded PG&G proposal; red represents well-imaged regions that remain unmapped. Basemap is SSI observation C21ISCOLOR01, a "true" color image obtained in June, 1999. North is up. Processing by the University of Arizona. Modified from NASA Photojournal PIA02308.

*Proposed name for the I31 Plume site (source of the largest plume ever observed on Io).

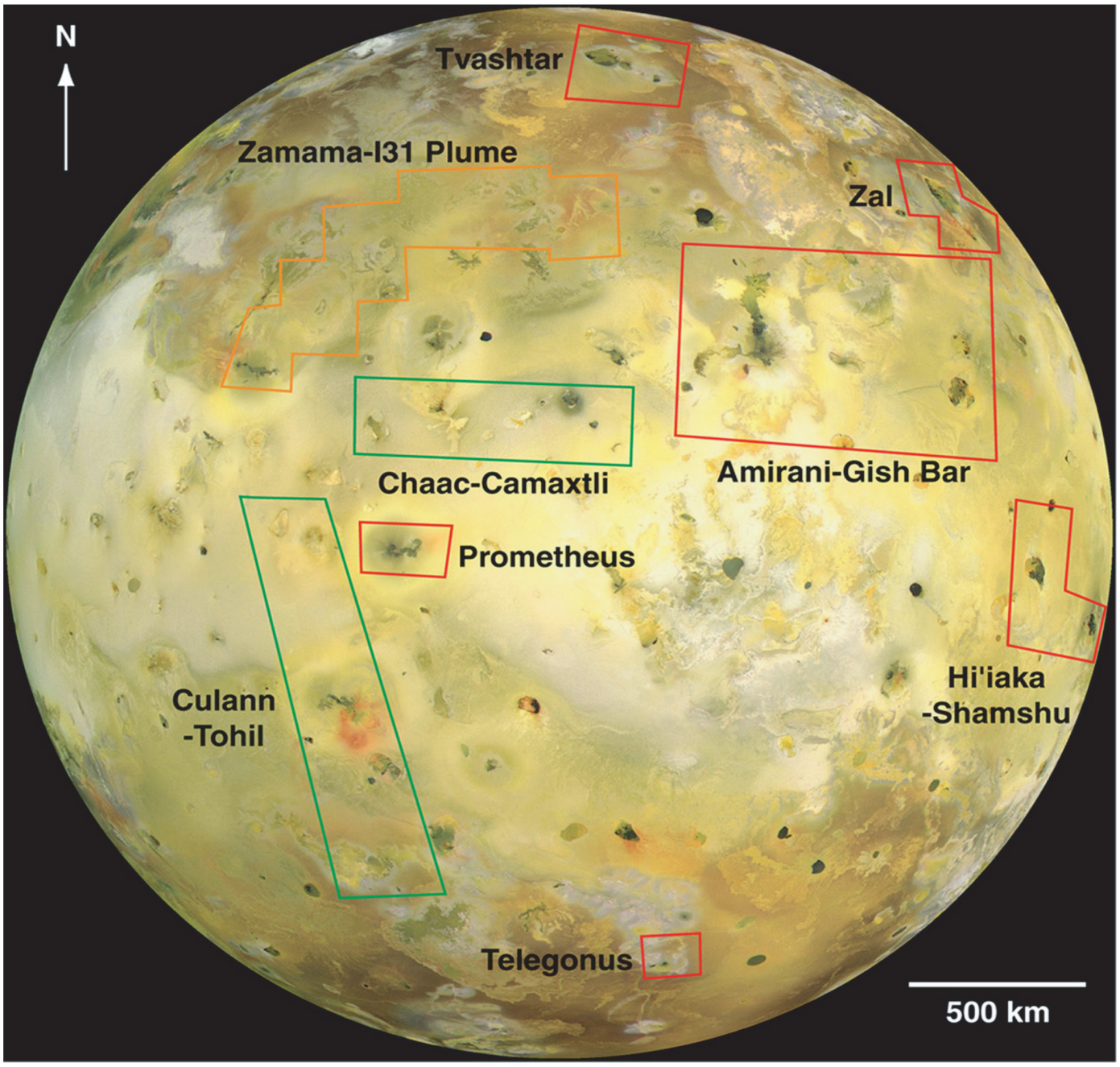
N
Tvashtar
Zamama-I31 Plume
Zal
Amirani-Gish Bar
Chaac-Camaxtli
Prometheus
Culann
-Tohil
Hi'iaka
-Shamshu
Telegonus
500 km

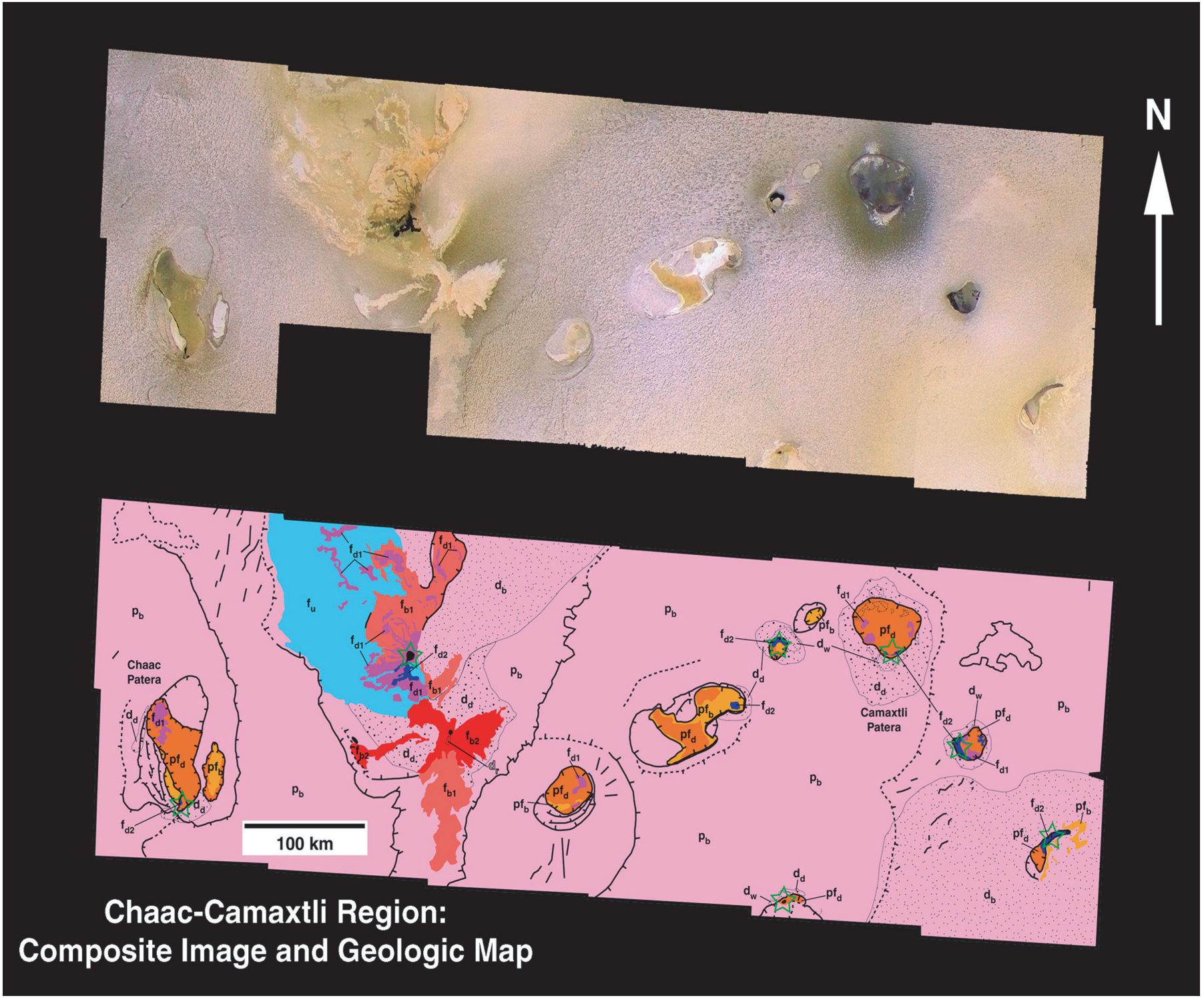

Chaac-Camaxtli Region:
Composite Image and Geologic Map

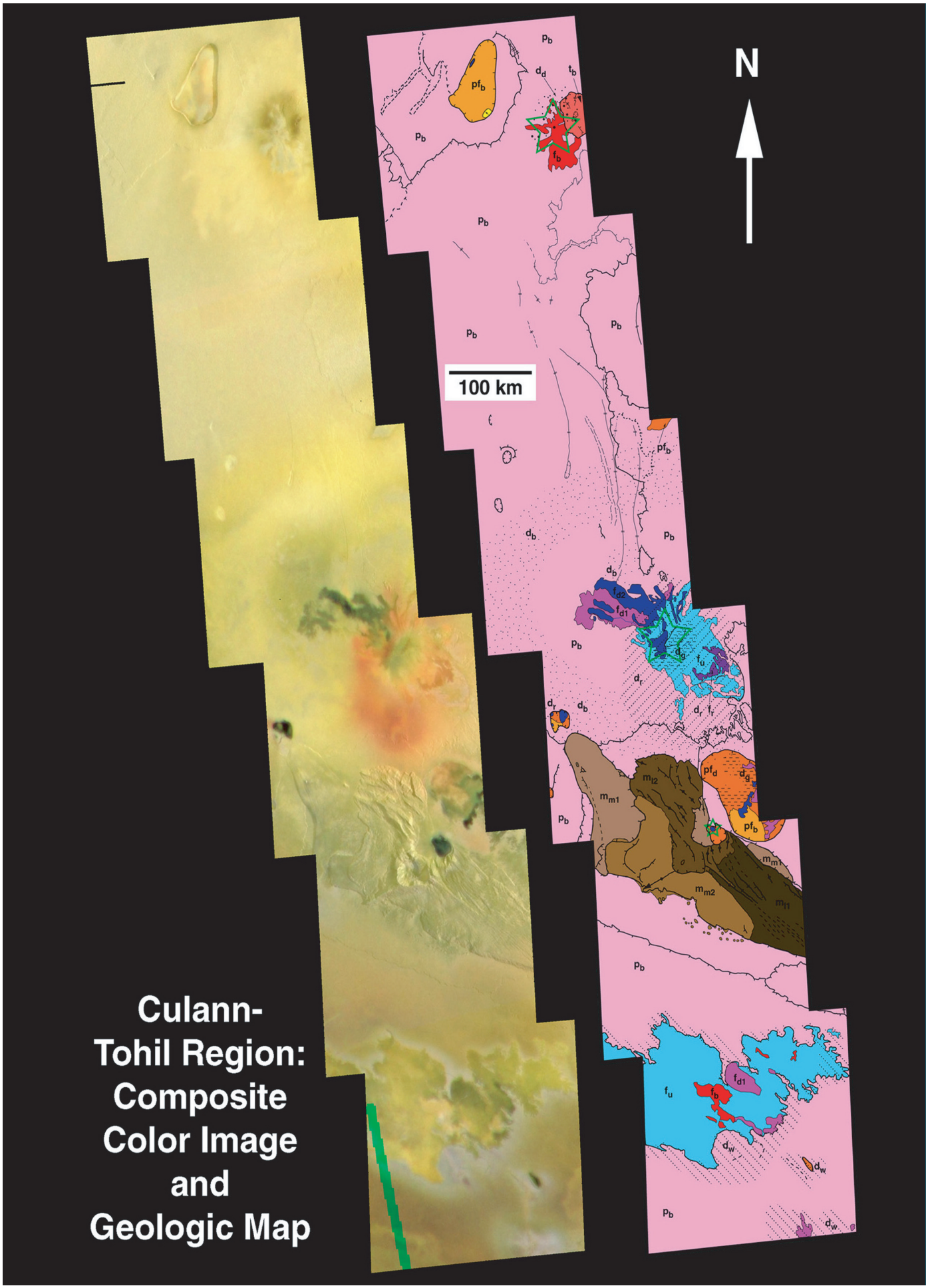
N
100 km
Culann-
Tohil Region:
Composite
Color Image
and
Geologic Map

MAPPING TECTONOMAGMATIC PLANETS. Vicki L. Hansen, Department of Geological Sciences, University of Minnesota-Duluth, Duluth, MN, 55812 (vhansen@d.umn.edu)

Introduction. Geologists create geological maps of planet surfaces in order to understand the processes of planet evolution. The method through which geological maps are created can bias resulting maps and thus influence interpreted geological histories. It is critical that methodology does not pre-determine a geologic map, and hence limit the range of possible viable geological histories. This thesis, highlighted by Gilbert [1], is discussed in terms of remote data sets focused on tectonomagmatic dominated planets.

Background. Methods of geologic mapping have receive much critical attention throughout the history of the geosciences, and important concepts and strategies have evolved, including such important concepts as uniformitarianism, stratigraphic superposition, cross-cutting relations, inclusions, index fossils and biostratigraphic correlation (quite different from lithologic correlation), radiometric dating, sequence stratigraphy, and facies analysis (with facies ranging from sedimentary facies to igneous facies, metamorphic facies and even tectonic or structural facies), and seismic and time series analysis. Consideration of time, and related concepts of unit correlation are critical to geologic mapping and to interpretation of geohistory and processes, as highlighted by the classic (and long) debate spurred by W. Smith's 1815 'index fossil' biostratigraphic correlation. That debate ultimately led to the downfall of A.G. Werner's 'Standard Stratigraphic Column' with its underlying paradigm of a unique terrestrial global stratigraphy. Construction of geologic maps forms a critical step to understanding geological processes [e.g., 1, 2]. Although a geological map is itself an interpretation, it should allow users to test a wide range of geologic histories, and processes that may have led to the possible recorded histories. Geologic mapping is an iterative process and although mapping should not be model driven one must have a model in mind during the mapping process [1]. That is, an understanding of basic physical processes/environment/operative conditions that affected a specific field area is extremely useful in selecting an approach to geologic mapping. For example, some approaches to, or critical aspects of, mapping terrestrial volcanic terrain vary from that of mapping high-grade metamorphic terrain, or mapping of sedimentary-dominated supracrustal terrain. Regardless of the approach, however, the mapping method must not predetermine the geological relations. Attention to mapping methodology with the express concern that map method does not predetermine 'documented' geologic relations, and hence unduly influence interpreted geohistories is critical for all geologic maps, but it is particularly critical for mapping planet surfaces that can only be accessed remotely.

Discussion. Geologic mapping is iterative and interpretive; hence it is critical to determine levels of confidence in geologic mapping. In mapping using remote data sets it is important to understand what surface features can be recognized with the most confidence in the particular data set and begin mapping such features. Using Venus as an example: given the tectonomagmatic nature of Venus, and the nature of Magellan SAR data, surface topographic features are most easily delineated and interpreted. Such features typically represent both primary and secondary structures. Primary structures form as a result of unit emplacement whereas secondary, or tectonic, structures represent strain and form as a result of material rheology and stresses imposed on a rock body after emplacement. Primary structures include lava channels or levees, lobate flow fronts, shield edifices; secondary structures include folds, faults, wrinkle ridges, ribbons, graben. Some features are transitional, or could be considered either primary or secondary depending on the question at hand. For example, pit chains cut preexisting units (and thus are secondary relative to the material they cut), yet pit chains represent primary structures formed during the emplacement of dike magma at depth. To further complicate the issue, pit chains might follow preexisting weakness (early formed tectonic structures such as fractures or faults), or they might form as a result of crack propagation across homogenous isotopic material driven by magma emplacement along newly formed dikes. Regardless of how individual pit chains form, however, their location, distribution, and orientations are easily recognized and noted on a Venus geological map, and as such they provide an example of map data with high geological confidence. Thus mappers should delineate the location, orientation, spacing, etc. of primary and secondary features on their geologic map. The patterns of these structures that emerge will assist the mapper (and other map users) in determining how these features might have formed, as well as if the original interpretation as primary or secondary is consistent with other relations that emerge through the mapping process, or future discoveries.

In contrast to primary and secondary structures, material units, or more precisely, individual geologic units, can be extremely difficult to uniquely identify in SAR data. Radar backscatter is a function of surface orientation, surface roughness, material composition,

and weathering. Given each of these separate, but possibly related variables, it can be extremely difficult to deconvolve a radar signal or backscatter value as uniquely representative of a specific material, much less a specific geologic unit. Material (or lithologic) units differ from geologic units in that geologic units should be temporally equivalent. Different geologic units could have similar compositions (e.g. basaltic) yet they could have been emplaced at different times. Basalt has a limited range of compositions that make it basalt, but individual basaltic units cans be widely different in age. Thus delineating the extent of individual geologic units using SAR data can be extremely difficult, and in a robust sense, impossible because correlation must be based on time, and not character alone.

Compton [2, p. 85] outlines what is required for correlation of map units. "Correlation consists of working out the equivalence of rock units from one area to another, based on one or more of these criteria: age, stratigraphic position, lithologic characteristics, and fossil content. Correlations are generally made when a field study has reached the stage that local rock units have become well enough known to be compared with units established elsewhere." He goes on to clarify. "Fossil collections and isotopic data are typically the surest means of correlating units by age; they can be in error, however, so that equivalence should be checked by as many of the following as possible: 1) specific thin units that can be identified with certainty, such as a tuff bed, a limestone bed, a phosphate-rich bed, a claystone, or a layer rich in unusual detrital minerals; 2) geomagnetic polarity; 3) climatic markers such as glacial deposits, specific kinds of paleosols, or fossils indicative of changes in ocean temperature; 4) duration of time expressed by varves or other annual layers in sediments or fossils; 5) intrusive or extrusive igneous rocks recording unique igneous events; 6) evidence of rapid marine transgression or regression, such as sequences of primary structures; 7) major unconformities; 8) unique sequences of lithologic units; 9) tectonic events, as indicated by deformed rocks or by rapidly accumulated coarse sediments; and 10) age relations among deposition, deformation, metamorphism, and igneous activity. Although all of these means of correlation can be fallible, certain ones may work well in a given area." Two important points emerge from Compton's criteria for correlation. Fist, virtually none of these kinds of data are available for Venus. Second, implicit in Compton's discussion of correlation is that a marker bed, or marker unit, the tool of correlation, have both unique characteristic(s) (within the operative map data) and formed over a limited time range; in addition the unit must extend spatially across the region of interest for correlation.

To date no such marker units or marker beds have been identified on Venus, and thus we have no means of robust global correlation on Venus (or Io, Europa, Ganymede [although individual cycloids on Europa might provide local 'timelines' of sorts]). Map unit correlation requires a unique and distinctive unit, one that can be uniquely identified in the remote data set employed. Furthermore, we must be able to propose with great confidence and independently from models that the unit formed over a short time period. I propose that until such units are identified and robustly accepted as having formed in a geological instant, we have no means to uniquely correlate units across Venus, and that any models that propose such correlation should be highly suspect and can lead to circular geologic interpretations or models of geohistory.

Just as one considers the type of geologic environment for terrestrial mapping methods, we should consider the general environment on Venus. Given that Venus processes can be characterized as dominated by tectonomagmatic processes, and given that such processes impart changes to a surface from below (as opposed to from above as in the case of, for example, planets with strong hydrologic cycles, such as Earth or perhaps early Mars), it is critical that we think about the formation of tectonic structures and the emplacement of geologic units and consider emplacement and deformation mechanisms (including considerations of rheology) in our mapping prowess. I present an example from Venus that illustrates maps constructed following two different methods. The first method begins with identification of primary and secondary structures, including specific contact relations, and follows with geologic unit or material unit identification only after this exercise. I compare this with a map constructed (apparently) with a focus on geologic/material unit identification, with structures highlighted locally. Each methods results in different possible views and potential geohistories of the map area. The possible geohistories that result from the later method are extremely limited, and in fact mutually exclude histories that might be proposed through study of the map created by the former method. Furthermore, the history that results from the later method cannot be independently tested within the context of that mapping method, and thus it is scientifically and geologically circular.

Summary. Geologic maps are constructed to present data in a manner that promotes understanding of the geohistory of an area, but geologic maps need to aim to transcend the views of individual geologists given that maps will likely become part of the public 'data' record and influence further geologists long past the lifetimes of the map creators. Geologic maps that limit the questions that can be asked of the map, or that *a priori* discount possible geohistory models are not

useful scientific documents, and in fact they can be harmful to the goal of planetary exploration, which is to understand the processes that contributed to planet evolution. Mapping methods that begin with identification of the most obviously and least controversial features and work toward *discovery* of the less obvious relations should best serve the goals of scientific investigation and planetary exploration.

References: [1] Gilbert, G.K., (1886) Inculcation of the scientific method, Am. J. Sci. 31, 284-299; [2] Compton, R.R. (1985) Geology in the Field; John Wiley & Sons, 398 pp.